Universidade do Minho
Escola de Ciências

Rafaela Alves de Oliveira

Expression and internalization analysis of nutrient transporters in mammalian cells

Janeiro 2022

Expression and internalization analysis of nutrient transporters in mammalian cells

Rafaela Alves de Oliveira

UMINHO | 2021

Universidade do Minho
Escola de Ciências

Rafaela Alves de Oliveira

Expression and internalization analysis of nutrient transporters in mammalian cells

Dissertação de Mestrado
Mestrado Genética Molecular

Trabalho efetuado sob a orientação do(a)
Professora Doutora Sandra Cristina Almeida Paiva
Professor Doutor Carlos Pedro Fontes Oliveira

Janeiro 2022

AGRADECIMENTOS

A realização desta etapa contou com vários e importantes apoios e incentivos. Como tal, não poderia deixar de agradecer a todos aqueles que direta ou indiretamente foram essenciais para esta jornada.

À minha orientadora Professora Doutora Sandra Paiva pelo conhecimento científico, disponibilidade, motivação e dedicação prestada ao longo deste percurso.

Ao meu orientador Professor Doutor Pedro Oliveira pela disponibilidade e predisposição a ajudar, bem como pela competência científica que me ajudou a melhorar e elevar o nível deste trabalho.

Queria a agradecer a ambos os orientadores também pelas críticas construtivas e sugestões que contribuíram para a realização deste trabalho. Sem a orientação de ambos este trabalho não seria possível.

A todos os meus colegas de laboratório, tanto aos da UM do laboratório de Genética Molecular, como aos colegas do grupo Sertoli Cell and Gamete Biology Group, do ICBAS, onde desenvolvi a maior parte do trabalho apresentado.

À Rita, à Du e à Lecas o meu enorme obrigada, por todo o incentivo, os desabafos, as correções e sugestões, e acima de tudo pelo apoio e amizade.

Ao meu namorado, Filipe, que por tantos dias e noites me ouviu, ajudou e incentivou a dar sempre o melhor de mim, obrigada! Com o teu apoio foi mais fácil ultrapassar os momentos menos bons.

Aos meus pais, por acreditarem em mim e me permitem realizar mais uma jornada. Pelo apoio incondicional, paciência e ajuda durante todo este percurso.

STATEMENT OF INTEGRITY

I hereby declare having conducted this academic work with integrity. I confirm that I have not used plagiarism or any form of undue use of information or falsification of results along the process leading to its elaboration.

I further declare that I have fully acknowledged the Code of Ethical Conduct of the University of Minho.

Análise da expressão e internalização de transportadores de nutrientes em células de mamífero

RESUMO

Vários são os transportadores de nutrientes cruciais para o correto desenvolvimento e adequada manutenção do organismo. Neste estudo focamo-nos em dois grupos, os transportadores de ácidos monocarboxílicos (MCTs) e os transportadores de cobre (CTRs). Os primeiros – MCTs - são responsáveis pelo influxo e / ou efluxo de ácidos monocarboxílicos das células, como o lactato. Uma elevada percentagem de tumores produz energia via glicólise, um processo denominado efeito Warburg, que resulta na elevada produção de lactato, e exportação deste por meio dos MCTs. Por sua vez, o lactato exportado fornece-lhes a capacidade de proliferar e aumentar a malignidade do tumor. As células de Sertoli também mantêm uma elevada taxa glicolítica e de exportação de lactato, que é posteriormente importado pelas células germinativas masculinas. Contudo, estas células não demonstram os fenótipos cancerígenos associados a este metabolismo semelhante ao efeito Warburg. O MCT4 é um dos dois MCTs cuja sobre expressão está presente numa grande variedade de cancros, para além de ser um elemento-chave no exporte de lactato das células de Sertoli. Assim, um dos objetivos deste trabalho consistiu na comparação da expressão e do tráfego do MCT4 em células cancerígenas versus células de Sertoli. E assim, detetamos que após tratamentos de hipoglicemia ou na ausência total de glicose, o MCT4 é internalizado na linha celular PC-3, e em resposta a tratamentos de concentração fisiológica de glucose ou hiperglicémicos a sua localização na membrana plasmática é mantida. No entanto, na linha celular de Sertoli TM4, o MCT4 não parece ser internalizado. Para além disso, a expressão proteica do MCT4 não varia significativamente quer entre tratamentos, quer entre linhas celulares. No entanto, são necessários estudos adicionais para melhor caracterizar o tráfego do MCT4 nestas linhas celulares.

O cobre (Cu) é um ião metálico que desempenha um papel crucial em todos os seres vivos, atuando como cofator de várias enzimas fundamentais. No entanto, o estudo do Cu ganha importância quando se considera o seu envolvimento nos fenómenos de progressão do cancro, tais como, angiogénese e metastização. A importação celular de Cu ocorre via dois transportadores principais, CTR1 e CTR2. Com isso em mente, geramos um conjunto de valiosas ferramentas biomoleculares que serão utilizadas no futuro para estudar a expressão e o tráfego dos transportadores de cobre CTR1 e CTR2.

Palavras-chave: Cancro, células de Sertoli, cobre, lactato, transportadores de ácidos monocarboxílicos, transportadores de cobre.

Expression and internalization analysis of nutrient transporters in mammalian cells

ABSTRACT

There are several crucial nutrient transporters needed for proper organismal Development and maintenance. In this study we focused on two groups of transmembrane transporters, the monocarboxylate transporters (MCTs) and copper transporters (CTRs) some of these key players. MCTs are responsible for the influx and/or efflux of monocarboxylic acids, as lactate. A high percentage of solid tumors produce energy through glycolysis, a process named the Warburg effect, which results in high production of lactate, and export via MCTs, providing them the ability to proliferate and increase tumor malignancy. Sertoli cells also maintain a high glycolytic production of lactate, to be imported by developing germ cells, without the cancerous-like phenotypes. MCT4 is one of the two MCTs which overexpression is present in a more variety of cancer types, and is also a key player in lactate export from Sertoli cells. Hence, one of the main objectives of this work was to compare the expression and trafficking of MCT4 in cancer versus Sertoli cells, as there are few studies on this matter. We detected that upon hypoglycemic or zero glucose treatments, MCT4 is internalized in the PC-3 Prostate cancer cell line, and in physiological or hyperglycemic treatments its plasma membrane location is maintained. However, in the TM4 Sertoli cell line, MCT4 does not seem to be internalized. Furthermore, MCT4 protein expression levels do not change significatively in either of the cell lines nor between them, in all of the glucose treatments. Nevertheless, more studies and diverse techniques are needed to better characterize MCT4 trafficking in these cell types.

Copper (Cu) is an essential metal ion with a crucial role in the biochemistry of every living organism, acting as a cofactor for several enzymes. Moreover, the study of Cu gains importance when considering its involvement in cancer progression phenomena, namely angiogenesis, and metastasis. The cellular Cu uptake occurs through two major copper transporters, CTR1 and CTR2. With that in mind, we generated a set of valuable biomolecular tools that will be used in the future to study the expression and trafficking of copper transporters CTR1 and CTR2.

Keywords: Cancer, copper, copper transporters, lactate, monocarboxylate transporters, Sertoli cells.

TABLE OF CONTENTS

LIST OF ABBREVIATIONS AND ACRONYMS

CD147	Cluster of differentiation 147
cKO	Conditional knockout
CMV IE Promoter	Cytomegalovirus-immediate early promoter
CTR(s)	Copper transporter(s)
DMEM	Dulbecco's Modified Eagle Medium
FACS	Fluorescence-activated Cell Sorting
FAK1	Focal adhesion kinase 1
FBS	Fetal Bovine Serum
FRET	Fluorescence Resonance Energy Transfer
GFP	Green fluorescent protein
GLUT	Glucose transporter
HBSS	Hank's Balanced Salt solution
HIF-1α	Hypoxia-inducible factor 1α
HRE	Hypoxia response elements
IMiDs	Immunomodulatory Drugs
ITS	Insulin-transferrin sodium selenite
LB	Luria-Bertani broth
LDH	Lactate dehydrogenase
LOX	Lysyl oxidase enzymes
MAPK	Mitogen-activated protein kinase
MCS	Multiple cloning site
MCT(s)	Monocarboxylate Transporter(s)
NAD	Nicotinamide Adenine Dinucleotide
PBS	Phosphate buffered saline
PC-3 cell line	Prostate Cancer cell line
PD-1	Programmed death receptor 1
PD-L1	Programmed death-ligand 1
PFA	Paraformaldehyde
PM	Plasma Membrane

RIPA	Radio-Immune Precipitation Assay
RPMI	Roswell Park Memorial Institute
SC	Sertoli cell
SOB	Super Optimum Broth
SOC	Super Optimal broth with Catabolite repression
Sp1	Specificity protein 1
TAE	Tris-Acetate-EDTA
TB	Transformation Buffer
TM4 cell line	Mouse Sertoli cell line
TMD	Transmembrane domain
WND	Wilson's disease

LIST OF FIGURES

LIST OF TABLES

CHAPTER I

INTRODUCTION

I. INTRODUCTION

I.1. The Warburg effect

In the 20's, Otto Warburg realized that cancer and normal cells display different pathways regarding the metabolism of glucose. His work demonstrated that cancer cells switch from mitochondrial phosphorylation to a glycolytic metabolism that "ferments" glucose into lactate, a process known as aerobic glycolysis. This change in metabolism occurs regardless of the presence or absence of oxygen (Warburg et al., 1924). This phenomenon was later described as the "Warburg effect", by Efraim Racker in 1972 (Racker, 1972) (see Figure 1).

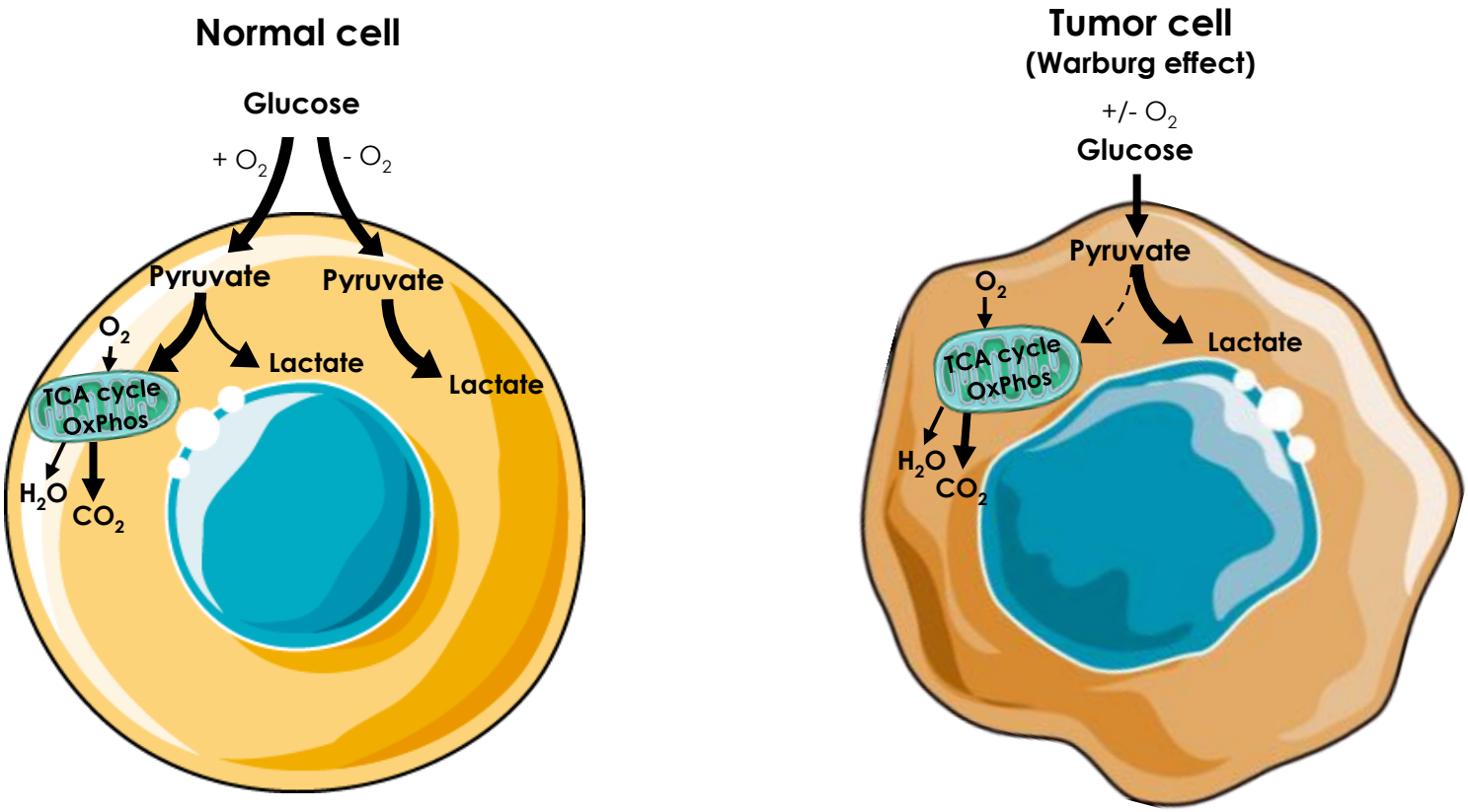

Figure 1: Schematic representation of Warburg's postulate. Warburg observed that cancer cells display high rates of glucose uptake and a preference for lactate production, through glycolysis, regardless of the presence or absence of oxygen. Cancer cells need to maintain energy homeostasis, which leads to a much lower rate of mitochondrial oxidative phosphorylation in comparison with lactate production through glycolysis. In contrast, normal cells in the presence of oxygen metabolize glucose into pyruvate through glycolysis and complete its final oxidation in the mitochondria via oxidative phosphorylation. In oxygen limiting conditions, normal cells can redirect

pyruvate to be converted into lactate. TCA: tricarboxylic acid; OxPhos: oxidative phosphorylation. Some components of the figure were drawn using pictures from Servier Medical Art (http://smart.servier.com/).

Moreover, Otto Warburg's discoveries showed that cancer cells have an exacerbated glucose uptake, leading to an increase in lactate production (Warburg et al., 1927). At first glance, this metabolic switch does not seem viable, considering the amount of adenosine triphosphate (ATP) produced through glycolysis versus the amount produced by the mitochondrial phosphorylation pathway. As reviewed in Vander Heiden et al., 2009, cancer cells may prefer to convert pyruvate, derived from glycolysis, into lactate, to achieve a higher cell division rate, since the effectiveness in disposing excess carbons allows for faster incorporation and metabolization of carbons into biomass (Vander Heiden et al., 2009). The hypothesis that tumor hypoxia induces this change was also brought up, by Gatenby & Gillies (Gatenby & Gillies, 2004), and even though tumor hypoxia occurs, and is one of the main features in cancer biology, it happens in a late state of the tumor, suggesting that it may not be a major contributor to the metabolic switch. Furthermore, leukemia cells and even lung tumor cells exhibit the Warburg effect (Christofk et al., 2008; Elstrom et al., 2004; Gottschalk et al., 2004; Nolop et al., 1987), although both cell types have high oxygen concentrations in their surroundings, highlighting even more the importance of studying this phenomenon.

Interestingly, Sertoli cells (SCs) are normal cells that display a Warburg-like metabolism. These cells have the metabolic capability of maintaining high glycolytic rates, metabolizing glucose into lactate, without the main physiological consequence inherent to this metabolism, an uncontrolled proliferation (Oliveira et al., 2015; Vander Heiden et al., 2009).

I.1.1. Lactate: the main product of the Warburg effect

The main product of the Warburg effect, lactate, must not be forgotten nor its importance diminished. Lactate has been implicated in several of the main characteristics of carcinogenesis. This substrate acts as a promoter of angiogenesis, cell migration, metastasis, acidosis of tumor

microenvironment, contributing to cancer cells immune escape, and even to cancer relapse (San-Millán & Brooks, 2017), as schematized in Figure 2.

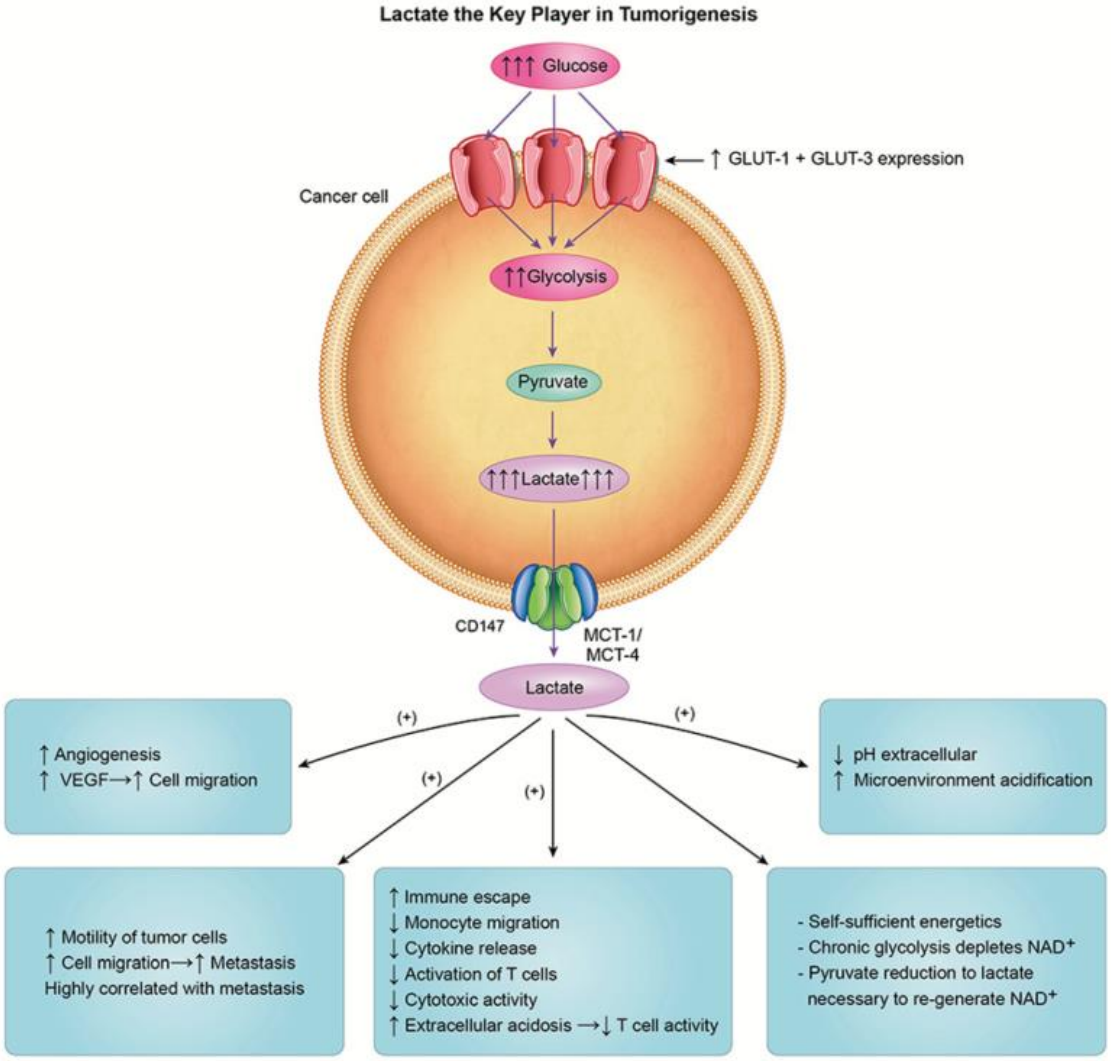

Figure 2: Lactate, the key player in carcinogenesis. Lactate is fundamental for the key steps of tumor development and progression. This substrate is involved in angiogenesis, by increasing the expression of vascular endothelial growth factor. Lactate also decreases activation of T-cells and monocyte migration, plus it causes a decrease in cytokine release and consequent cytotoxic activity, favoring cancer "immune escape". Lactate export causes a decrease in the extracellular pH, impairing the ability of T-cells to export lactate, therefore decreasing its immune activity. Furthermore, pyruvate conversion to lactate re-generates the levels of nicotinamide adenine dinucleotide (NAD^+), which is vital for the energy autonomy of cancer cells, and for the equilibrium of the intracellular redox pair ($NADH/NAD^+$), allowing for the continuity of glycolysis (San-Millán & Brooks, 2017). CD147: Cluster of differentiation 147; GLUT-1 and -3: Glucose transporter 1 and 3; MCT-1: Monocarboxylate transporter 1; MCT-4: Monocarboxylate transporter 4; VEGF: Vascular endothelial growth factor.

Hence, the continuous release of lactate from tumor cells to the extracellular milieu promotes carcinogenesis in susceptible cells and tissues. Additionally, lactate induces overexpression of the Monocarboxylate transporter (MCT) 4 (protein that will be further described in the next section), which in consequence leads to its further release into the extracellular environment promoting tumor growth and carcinogenesis.

However, the roles of lactate are not limited to this type of glycolytic cells – cancer cells. Sertoli cells (SCs), present in the testis, which display a glycolytic metabolism similar to cancer cells, produce and export high levels of lactate for nutritional support of germ cells. Therefore, the roles of lactate are not only limited to cancer progression, but also extend to spermatogenesis (Boussouar & Benahmed, 2004; Oliveira et al., 2015), which will be further discussed.

I.2. Monocarboxylate Transporters

Monocarboxylic acids, such as lactate, pyruvate, and ketone bodies are major sources of energy to all cells of the human body, being indispensable for cellular metabolism (Halestrap & Price, 1999).The import and/or export of these substrates to and/or from cells is mediated by a specific family of transmembrane transporters - the monocarboxylate transporters (Halestrap, 2013; Morris & Felmlee, 2008).

Monocarboxylate transporters are plasma membrane (PM) transporters encoded by the SLC16 gene family. This family of transporters has a total of fourteen members, from which only MCT1, MCT2, MCT3, and MCT4 were demonstrated to display proton-linked monocarboxylate transport, meaning that a proton is used to catalyze the facilitated diffusion of monocarboxylates (Halestrap & Meredith, 2004; Halestrap & Price, 1999). These transmembrane transporters can perform the efflux and/or influx of such substrates depending on H^+ and substrate concentration gradients (Figure 3) (Fisel et al., 2018; Halestrap, 2013). MCT1-4 differ from the rest of the monocarboxylate transporters in the amino acid sequences, which corroborates an evolutionary divergence, coupled with their functional role (Pinheiro et al., 2012). Among these four members, MCT3 is the least characterized transporter likely due to its restricted distribution in the human body, namely the basal membrane of the retinal pigment epithelium (Felmlee et al., 2020; Halestrap & Meredith, 2004). On the other hand, MCT1, with an extended range of functions in the human body, is undoubtedly the foremost characterized MCT (Felmlee et al., 2020), followed by MCT2 and MCT4.

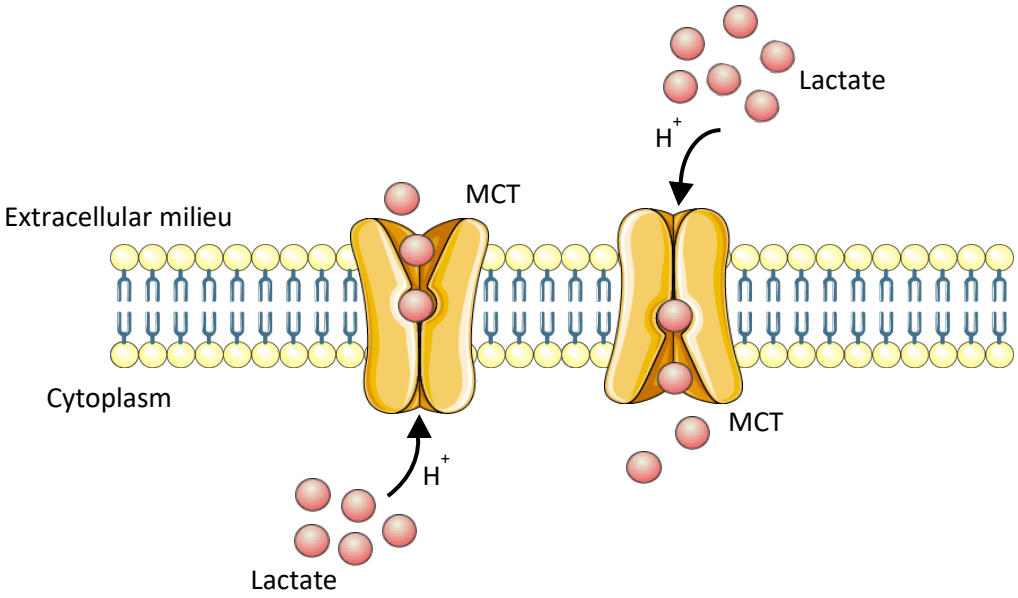

Figure 3: Schematic representation of cellular import and export of lactate through Monocarboxylic acid transporters. Monocarboxylic acid transporters catalyze the proton-linked facilitated diffusion of metabolically relevant monocarboxylates, as lactate. Some components of the figure were drawn using pictures from Servier Medical Art (http://smart.servier.com/).

MCT4 has lower affinity for monocarboxylates than MCT1 and MCT2, being the latter the one with the highest affinity for monocarboxylates (Felmlee et al., 2020; Halestrap & Meredith, 2004). MCT1 and MCT2 have been extensively described as importers of monocarboxylates, due to their kinetic properties (Bonen, 2001; Halestrap, 2009; Halestrap & Wilson, 2012). However, the role of MCT1 as an importer or exporter depends on tissue and intra/extracellular conditions (Fisel et al., 2018; Kirk et al., 2000). For instance, in glycolytic astrocytes, MCT1's function seems to be restricted to the supply of lactate for oxidative neurons' energy production (Pellerin & Magistretti, 2012), instead of displaying its typical role as an importer of monocarboxylic acids.

Regarding MCT2, it is predominantly expressed in organs with a metabolic cooperation between their own cells via lactate shuttling, as are the testis, brain, muscle, and even eyes, allowing for a sufficient lactate uptake (Fisel et al., 2018; Halestrap & Wilson, 2012). MCT4 is also expressed in the organs mentioned above, in the lactate supplying cells. This transporter is mainly responsible for maintaining the lactate export necessary for a lactate shuttling cooperation between highly glycolytic cells, and oxidative cells (Bonen, 2001; Felmlee et al., 2020; Halestrap & Wilson, 2012). Therefore, MCTs' roles are widely extended throughout the human body.

Hence, the transport of lactic acid across the PM is of special interest. MCTs have the essential role of either performing the removal of lactate after being produced by glycolysis or allowing its influx into liver and kidney cells, and even heart and red muscle cells. Lactate will then be used as a substrate to perform gluconeogenesis, or as a respiratory fuel (Halestrap, 2013; Halestrap & Meredith, 2004). Thus, MCTs have an important function in a variety of metabolic diseases. In fact, MCT4 was reported to be overexpressed, in cases of obesity, in muscle cells (Fisel et al., 2018). In addition, MCT1's deficiency has already been associated with recurrent ketoacidosis in children, due to a reduction in the uptake of ketone bodies, which contributes to an acid-base imbalance (Fisel et al., 2018). Furthermore, a greater percentage of solid tumors produces energy through glycolysis, which consequently results in high production of lactate (Pinheiro et al., 2012; San-Millán & Brooks, 2017). MCTs are mandatory for the export of the produced lactate into the extracellular milieu, which in turn will acidify the tumor microenvironment, and give cancer cells the ability to proliferate and increase tumor malignancy (San-Millán & Brooks, 2017; Vander Heiden et al., 2009).

MCT1 and MCT4 are the two main MCT overexpressed in a wide variety of cancer cell types (Felmlee et al., 2020; Pinheiro et al., 2012). In these cells, MCT4 is responsible for the export of the produced monocarboxylates, namely lactate, and, although MCT1 is generally involved in their uptake (Fisel et al., 2018). This main role of MCT1 as importer is consolidated by the fact that MCT4 is present in highly glycolytic muscle fibers, whereas fibers of the soleus muscle - that present a highly oxidative metabolism - express higher levels of MCT1, as they do not have the role of exporting lactate (Bonen, 2001; Halestrap & Meredith, 2004). However, MCT1 can act as importer or exporter (Felmlee et al., 2020; Halestrap & Meredith, 2004).

Cluster of differentiation 147 (CD147), a PM glycoprotein, has already been shown to interact specifically and directly with MCT1 and MCT4 (Kirk et al., 2000). CD147 was identified as a chaperone to these two specific MCTs, facilitating their proper expression and function at the PM. Furthermore, this transmembrane protein was also implicated in the chaperoning of MCTs to the PM, in tumors such as multiple myeloma, breast and lung cancers (Kirk et al., 2000; Pinheiro et al., 2010; Walters et al., 2013). More specifically, CD147 expression was linked to MCT1 expression in ovarian cancer, and to MCT4 expression in both lung and breast cancers (Pinheiro et al., 2010).

Since MCT4 is one of the main focus points of this MSc project, its functions, as well as the specific regulation that it is subjected to, will be further detailed in the following sections.

I.2.1. Monocarboxylate transporter 4: role and regulation

MCT4 is widely expressed in the human body, but its highest expression occurs in tissues/cells with high glycolytic rates, such as white blood cells, SCs, and white skeletal muscle fibers (Bonen, 2001; Halestrap, 2013). Therefore, MCT4's main role relies on the export of the principal substrate resultant from glycolysis – lactate (Bonen, 2001; Pinheiro et al., 2012).

Given that MCT4 acts as the main lactate exporter, it is plausible to hypothesize there is an increase in the mRNA and protein levels in response to hypoxia, since glycolytic rates will also increase. In fact, hypoxia-inducible factor 1α (HIF-1α), a transcription factor present in higher levels under hypoxia, stimulates MCT4 gene expression, through the interaction with two hypoxia response elements (HRE) present in the MCT4 promoter region (Ullah et al., 2006). The study performed by Lim et al., 2014, in glioblastoma cells, came to solidify this interaction by demonstrating that HIF-1α transcriptional activity is inhibited through MCT4 knockdown (Lim et al., 2014). Furthermore, HIF-1α is incapable of upregulating MCT1 in a hypoxic environment due to the absence of any likely HRE sequences in the MCT1 promoter region (Ullah et al., 2006).

I.3. Sertoli cells and MCTs

Since the late 80's Sertoli cells have been characterized as the prime "nurse" cells for the developing germ line. For instance, it was reported that when SCs isolated from immature rats are incubated in anaerobic conditions, mimicking the natural oxygen-deprived ambiance experienced in the testis (Wenger & Katschinski, 2005), and with glucose-containing medium, they metabolize glucose into pyruvate and lactate (Grootegoed & Den Boer, 1989). The produced lactate is used by germ cells for energy production (Oliveira et al., 2015).

In fact, throughout spermatogenesis, a metabolic cooperation is formed between testicular cells, namely SCs and germ cells (Oliveira et al., 2015), SCs are responsible for giving physical and nutritional support for germ cells. Moreover, various diseases such as *diabetes mellitus*, that affect this specific metabolic cooperation, lead to an impairment in the male reproductive function (Alves, Martins, Cavaco, et al., 2013), highlighting the importance of its study.

In resume, SCs metabolize glucose into lactate and provide this substrate for proper germ cell development and male fertility performance. The high-level production of lactate in these cells is achieved

through the metabolism of glucose (Dias et al., 2013), displaying a "Warburg-like" metabolism. SCs aim at obtaining high levels of lactate production and export, similarly to cancer cells, without the malignant phenotypical shift since this metabolism naturally occurs in SCs.

In the seminiferous tubules, SCs uptake glucose specifically through two glucose transporters, GLUT 1 and GLUT3 (Dias et al., 2013), where it is metabolized into pyruvate. A greater amount of the obtained pyruvate is converted into lactate, so that it can be made available extracellularly for germ cells (Oliveira et al., 2015). This conversion process is mediated by the action of lactate dehydrogenase (LDH), an isoenzyme system able to reversibly convert pyruvate to lactate (Boussouar & Benahmed, 2004; Oliveira et al., 2015). The produced lactate is then exported via specific monocarboxylic transporters, namely MCT4 and MCT1 (Halestrap, 2013; Oliveira et al., 2015). Once lactate leaves SCs it is imported by germ cells to fulfill its major role as their main energy fuel, being MCT1 and MCT2 the proteins in charge of that import (Boussouar & Benahmed, 2004; Halestrap, 2013).

I.3.1. Lactate transport: Sertoli cells to germ cells

The first step undergone by lactate during spermatogenesis relies on its release from the cytoplasm of SCs, into the intratubular fluid. This process is mainly mediated by MCT4 (Galardo et al., 2007), even though it is a lower affinity transporter of lactate (Bonen, 2001; Brauchi et al., 2005; Galardo et al., 2007; Rato et al., 2012). Such notion is highly supported by the differences of MCT1 and MCT4 K_m values for pyruvate. Whereas the K_m value of MCT1 for this substrate is about 1.0 mM, the K_m of MCT4 exceeds 150 mM (Halestrap, 2013; Halestrap & Meredith, 2004). This unique feature prevents the efflux of pyruvate from SCs, allowing its conversion to lactate, for further release. Nevertheless, it has been already described MCT1 expression in SCs (Bernardino et al., 2019; Boussouar & Benahmed, 2004), notwithstanding MCT4 as the key player in SCs for lactate's disposal (Galardo et al., 2007).

Furthermore, in a study involving *MCT1* conditional knockout (cKO) mice was suggested that the absence of MCT1 compromises lactate's availability for germ cells (Bernardino et al., 2019), having already been considered the prime exporter in SCs for the glycolytically produced lactate (Boussouar & Benahmed, 2004). The knockout of *MCT1* culminated in a depletion of germ cells and subsequent absence of spermatozoa, in *MCT1* cKO mice (Bernardino et al., 2019). The spermatogenic arrest that follows *MCT1* knockout is likely due to the lack of capacity from germ cells to uptake lactate provided by SCs, and not by MCT1's action in SCs. Therefore, without diminishing MCT1's significance throughout

spermatogenesis, MCT4 has been widely characterized and considered the prime lactate exporter from the glycolytic metabolism of SCs (Alves, Martins, Rato, et al., 2013; Dias et al., 2013; Oliveira et al., 2015).

Male fertility is reliant on the activity of these proteins, as for import or export of lactate. Such roles turn MCTs into targets for male contraception, as well as a mean to optimize *in vitro* assisted reproduction treatments, two objectives, that although distinguishable, rely on the same metabolic basis, MCTs' activity in the male reproductive system.

Even though there is a growing body of work towards the understanding of MCTs in SCs and throughout spermatogenesis in humans, we are still far from unveiling the complete roles and regulation of these transporters.

I.4. Role and regulation of MCTs in cancer

Having in mind the importance of lactate in major steps of carcinogenesis, as schematized in Figure 2, it becomes essential to take a closer look at MCT4 - the transporter playing a major role in its export from tumor cells (Halestrap & Price, 1999). In particular, as said, MCT1 and MCT4 were proven to have an overexpression in a variety of cancers (Kim et al., 2015; Pinheiro et al., 2012; Walters et al., 2013). Their higher rates of expression in cancer cells result from the need to export the large amounts of lactate produced by these cells, as a result of their high glycolytic rates. Through the mediation of the co-transport of lactate with protons, MCTs allow not only for the maintenance of cancer cells' elevated glycolytic rates, but also help in the counterattack of acid-induced apoptosis, through stabilization of alkaline values inside tumor cells (Pinheiro et al., 2008, 2012).

An example of this overexpression is found in colon tumor cells, that present increased levels of MCT1 and MCT4 when compared to cells of the normal epithelium (Koukourakis et al., 2006; Pinheiro et al., 2008). The upregulation of MCT1 in these tissues revealed an association with angiogenesis (Pinheiro et al., 2012). Furthermore, the increased levels of these two monocarboxylate transporters were found in a wide range of tumor cell types, such as lung, breast, and even ovarian cancer cells, in comparison to what was found in the normal epithelium of each tissue (Pinheiro et al., 2012).

As aforementioned, MCT4 expression is stimulated by HIF-1α, which in turn is upregulated under hypoxia, a subliminal condition to many cancers, resulting in an increase of mRNA levels in cancer cells comparing to normal cells (Ullah et al., 2006). This increase in MCT4 gene transcription was shown to

occur in bladder cancer, favoring the extrusion of large amounts of lactate resultant from the enhanced glycolytic metabolism (Ord et al., 2005). On the other hand, HIF-1α does not interact with MCT1, therefore it is not responsible for regulating its expression under hypoxia. This control is attributed to the tumor suppressor protein p53, whose correspondent wild type was already shown to have a repressor activity regarding MCT1 transcription and to decrease its mRNA stability in colon cancer cells (Boidot et al., 2012). Therefore, p53 deficiency upon hypoxic conditions, promotes MCT1 expression, facilitating the export of large amounts of lactate. Upon glucose deprivation, and under moderate hypoxia conditions, in p53 null cells, the upregulated MCT1 has shown to work in reverse of its initial action, mediating lactate import to be used in mitochondrial respiration, promoting cell proliferation (Boidot et al., 2012).

I.4.1. MCTs as therapeutic targets in cancer

As aforementioned, MCTs have a wide tissue distribution and a broad range of substrates, adding their potential to affect the pharmacokinetics of compounds. MCT1 and MCT4 have been explored as targets in cancer therapy. One of the main goals in this area of research aims at inhibiting these transporters, which might result in a chemotherapeutic strategy (Felmlee et al., 2020).

Many studies have been conducted following this line of thought, like the one published by Lim et al., 2014. The authors used short-hairpin RNAs to suppress MCT4 expression, which led to a growth inhibition of 50-80% in two of the glioblastoma cell lines tested, under hypoxic conditions (Lim et al., 2014). These results suggest that cancer cell lines' growth impairment can be acquired through the inhibition of MCT4. In a more recent study, the researchers focused on MCT1, and the use of a potent MCT1's inhibitor - AZD3965 - as a novel therapeutic compound. It is already on Phase I of clinical trials in the United Kingdom for the treatment of Burkitt lymphoma and diffuse large B cell lymphoma (Noble et al., 2017).

Another study revealed that exposure of immunomodulatory drugs (IMiDs), such as thalidomide or pomalidomide, in IMiDs-sensitive multiple myeloma cells, causes destabilization of the CD147-MCT1 complex. Consequently, in these cells a variety of cellular functions are put to an end, including proliferation, invasion and angiogenesis (Eichner et al., 2016).

I.5. Glycolysis and oxidative phosphorylation involvement in cancer

The activity of cytochrome c oxidase is essential for oxidative phosphorylation and is affected by copper (Cu) levels in tumors (Ishida et al., 2013). Additional copper bioavailable facilitates the increase of ATP production, which is consumed for the rapid proliferation of cancer cells (Ishida et al., 2013). Nevertheless, copper does not initiate the initial transformation of cancer cells but may contribute to its proliferation by providing the energy needed for cell-cycle progression.

Glycolysis is usually used by normal cells as an adaptive mechanism in response to low levels of oxygen, or even in its total absence. However, tumors yield increased amounts of lactate even in the presence of oxygen (Warburg et al., 1927). Ishida et al*.,* 2013, suggest that the increased glycolysis in tumors may reflect a lack of bioavailable copper in the tumor microenvironment (Ishida et al., 2013). Moreover, they show copper levels' ability to modulate oxidative phosphorylation in tumors (Ishida et al., 2013). Interestingly, and reinforcing the previous idea, in chinese hamster ovary cells was already demonstrated that an increase of 20-fold in initial copper concentration enabled these cell cultures to start consuming lactate instead of producing it (Luo et al., 2012; Qian et al., 2011). Weinhouse, S., 1956, reported that oxygen consumption is not quantitatively reduced in a variety of tumors despite increased glycolysis (Weinhouse, 1956), and in fact, in the majority of cancer cells, 70-90 % of total ATP produced is generated by oxidative phosphorylation, being glycolysis responsible for the remaining percentage (Ishida et al., 2013).

Thus, cancer cells reveal to have a complex and tightly regulated metabolism, dependent on several factors, such as copper and oxygen bioavailability (Denoyer et al., 2015; Gatenby & Gillies, 2004), initial transformation stage, or proliferation stage (Ishida et al., 2013; Vander Heiden et al., 2009), as well as glucose levels in the surroundings.

Through the balance of oxidative phosphorylation and aerobic glycolysis cancer cells can achieve the best metabolic combination for their increased proliferation and malignancy. Hence, copper and lactate levels are connected, and their transporters are key regulators of cancer proliferation, turning them into excellent targets for anticancer treatments.

I.6. The biological importance of copper

Copper is an essential metal ion required for all cells in the human body to fulfill their metabolic needs. Being so, copper has a crucial role in the biochemistry of every living organism, acting as a co-factor for several enzymes. As discovered in the late '50s by Wende and Wainio, copper is needed for the proper function of cytochrome c oxidase, in mitochondria (Vander Wende & Wainio, 1960). Later, McCord and Fridovich found that Cu acts as an essential co-factor for superoxide dismutase (McCord & Fridovich, 1969). These two roles render Cu a key player in cellular respiration and in the detoxification of oxygen radicals, respectively. Furthermore, copper is involved in a series of physiological events, as hemoglobin formation, carbohydrate metabolism, or even in the antioxidant defense mechanism (Iakovidis et al., 2011). Copper deficiency diminishes the activity of its associated enzymes, thus affecting their physiological functions (Gupta & Lutsenko, 2009). However, excess copper is also harmful to cellular metabolism, affecting tissues and organs, as is the example of the brain, whose structure and function are affected by copper toxicosis (Erfanizadeh et al., 2021; Smolinski et al., 2019).

Therefore, tight and extremely well-coordinated regulation of copper levels in cells and tissues is mandatory for proper cellular homeostasis. To properly play its biological role, Cu has the ability to shuttle between different oxidation states, Cu^{2+} (oxidized) and Cu^{+} (reduced). In turn, it interferes with its acquisition regarding bioavailability and uptake's specificity (Öhrvik & Thiele, 2014), and even increasing the risk for toxicity if mis regulated (Grubman & White, 2014). This toxicity is associated with excessive levels of copper, or even with its redox cycling, where Cu may generate reactive oxygen species, resulting in oxidative damage to tissues (Pham et al., 2013). Therefore, through evolved protein-based systems that tightly regulate/modulate copper trafficking it is possible to maintain copper homeostasis in both cells and tissues across the human body.

I.7. Cellular transport of copper

Throughout the years, several key proteins involved in the influx, distribution, and efflux of copper from cells have been identified. Among those, in humans, there are the copper-transporting ATPases - ATP7A and ATP7B (Gupta & Lutsenko, 2009). These proteins, through the efflux of copper, demonstrate to be key players in the prevention of excess copper levels, a condition that has been described to lead

to hepatic abnormalities and/or neurological impairment in patients with Wilson's disease (WND), which is caused by a mutation in the *ATP7B* gene (Das & Ray, 2006; Smolinski et al., 2019).

Copper transporter 1 (CTR1) (encoded by *SLC31A1*) and copper transporter 2 (CTR2) (encoded by *SLC31A2*) are the two copper importers known to exist in mammals (Mandal et al., 2020) (see Figure 4). CTR1 is the high-affinity transporter of Cu, responsible for both influx of Cu across the PM and endomembranes, located mostly at the PM (Mandal et al., 2020). CTR2 locates mostly in the endosomal system (Öhrvik et al., 2013; Van Den Berghe et al., 2007). However, there is already evidence that CTR2 might be connected, to some extent, with copper influx (Van Den Berghe et al., 2007). These CTR proteins and their roles and regulation will be further described in the following section.

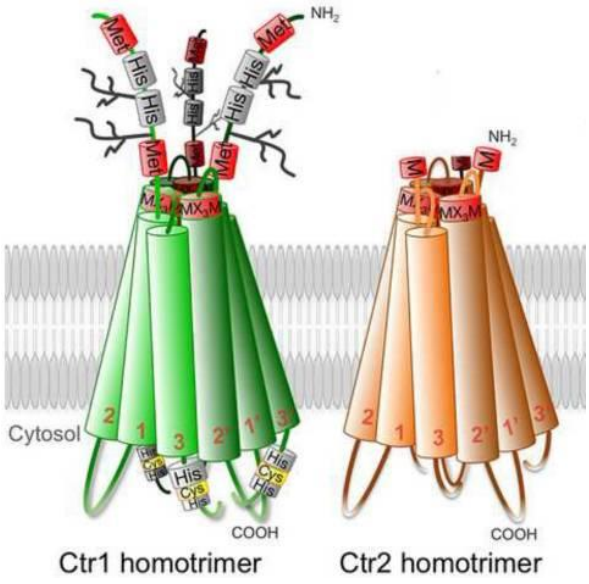

Figure 4: Schematic representation of copper transporter 1 and copper transporter 2 homotrimers. Cys, cysteine; His, histidine; Met, methionine; CTR1: Copper transporter 1; CTR2: Copper transporter 2; MX3M, crucial motif for Cu transport; TMD1-3, CTR1/CTR2 monomer number 1; TMD1′-3′, CTR1/CTR2 monomer number 2 (Öhrvik & Thiele, 2015).

I.7.1. Copper transporter 1

Through genetic studies in baker's yeast, *Saccharomyces cerevisiae*, the CTR1 encoding gene was the first eukaryotic gene encoding a specific copper importer ever discovered (Dancis et al., 1994). The resultant protein is a member of the family of copper uptake transporters identified as high-affinity copper

transporters in insects, fungi, plants, mammals, such as hCTR1 for humans (Puig et al., 2002). Furthermore, through a knockout study of the *Ctr1* gene in mice, was demonstrated that it its critical role in the uptake of dietary Cu *in vivo*, since its absence resulted in cardiac hypertrophy, iron accumulation in the liver, among several other life-threatening consequences (Nose et al., 2006).

But how does this metal ion enter the cell? Considering the two distinct forms that copper appears in nature, it is important to notice that only the reduced form can be imported via hCTR1. Therefore, extracellular Cu^{2+} suffers a metal-reduction carried out by Cu^{2+} cell-surface reductases (Hassett & Kosman, 1995), before its uptake through hCTR1 (Öhrvik & Thiele, 2014).

Regarding the physical process involved in copper import into human cells, through its high-affinity transporter hCTR1 (Dancis et al., 1994), urges the need to look closely at the structure of this protein. This transmembrane transporter is composed of three transmembrane domains (TMD), with an extracellular amino-terminal metal-binding domain rich in methionine residues, responsible for the mediation of high-affinity Cu^{+} intake from the extracellular milieu (Brady et al., 2014; Eisses & Kaplan, 2002; Y. Guo, Smith, Lee, et al., 2004).

Cu's transport through CTR1 is unidirectional and passive, from the extracellular milieu to the cellular interior. The study of Tsigelny et al., from 2012, suggests that the negative charge of the amino terminus of hCTR1 attracts Cu^{+} from the extracellular environment, directing it to the center of the hCTR1 pore, where it has a neutral passage. Regarding its liberation into the cytoplasm, it is conducted by the dipole formed in the carboxyl-terminal tail of this transporter, due to the duality of charges present. This tail displays a positive charge in the proximal parts of the center of the channel and a negative charge in the sides, further from the center, which in turn repels Cu^{+} and directs its way into the cell (Tsigelny et al., 2012). Other works have suggested that conformational changes may also contribute to force the passage of Cu^{+} through the pore, being these, induced by ligand exchange reactions occurring in different binding sites of the pore (De Feo et al., 2009; Puig et al., 2002; Rubino et al., 2010). Overall, changes in the electrostatic field and in hCTR1 conformation, allied to concentration gradients of copper, are the driving forces of copper cell intake through hCTR1 (Öhrvik & Thiele, 2014).

Even though CTR1 is the main copper importer in mammalian cells, its cellular location varies between the PM and intracellular vesicles, as previously described (Van Den Berghe & Klomp, 2010). Being, however, well known that its principal cellular location resides in the cell membrane (Mandal et al., 2020; Puig et al., 2002).

hCTR1 is broadly expressed, being found in every organ and/or tissue examined, with the highest expression found in liver, heart, and pancreas (Zhou & Gitschier, 1997). In mice, CTR1's highest expression levels were detected in liver, heart, small intestine, and kidneys (Y. Kuo et al., 2006; J. Lee et al., 2001). Regarding *hCTR1*'s regulation, it has been described that at the genomic level, that both *hCTR1* and *hCTR2* respond to cellular copper requirements and variations of microenvironmental copper levels (Wee et al., 2013). Moreover, it was discovered that the specificity protein 1 (Sp1) binds to *hCTR1*'s promoter and its own promoter, under copper-depleted conditions, favoring the expression of both proteins, and consequently copper import. On the other hand, excess copper levels prevent the binding of Sp1 to *Sp1* and *hCTR1* promoters, diminishing their expression, and in turn controlling copper homeostasis (Liang et al., 2012).

The regulation of hCTR1 in response to copper levels does not stop there, in fact, its location is reactive to extracellular copper concentrations. In response to a high extracellular copper concentration, hCTR1 is internalized and degraded (Wee et al., 2013). Other post-translational regulatory actions regulate hCTR1's function. For example, with the cleavage of the N-linked glycosylation of hCTR1 at residue 15, its copper transport activity is significantly reduced, when compared to the full-length hCTR1 protein (Maryon et al., 2007). However, its O-linked glycosylation at Thr27 protects hCTR1 from proteolytic cleavage (Maryon et al., 2007; Wee et al., 2013).

I.7.2. Copper transporter 2

CTR2 is the second transporter of the copper transporter family – CTRs – known as the low-affinity transporter of copper. It was first discovered through the screening of cDNA libraries, which culminated in the determination of the hCTR2 full-length coding region (Zhou & Gitschier, 1997). Even though structural and biochemical studies focused on hCTR2 are lacking, it is known that it has structural homology with the second TM of hCTR1, which is fundamental for the transport of copper (Zhou & Gitschier, 1997). Regarding its structural organization, CTR2 is very similar to CTR1, with three putative TMs but without an extended N-terminal domain, and functioning as an oligomeric protein (Schweigel-Röntgen, 2014) (see Figure 4).

In mammals, CTR2 mainly locates in the membranes of intracellular organelles, as endosomes and lysosomes (Van Den Berghe et al., 2007). However, it is estimated that 5 % of total CTR2 present is localized in the PM and mediates copper transport into the cytoplasm (Bertinato et al., 2008; Van Den

Berghe et al., 2007). Furthermore, CTR2 might display a role in recycling copper from intracellular stores as hypothesized in Gupta and Lutsenko, 2009 (Gupta & Lutsenko, 2009). These researchers theorized that if CTR2 is localized in lysosomes and exports copper from there, it might be retrieving copper from cuproenzymes that were degraded in these lysosomes.

In rat, the highest levels of CTR2 were found in the heart and placenta (Bertinato et al., 2008), in contrast to the broad expression detected for CTR1. However, the first study on hCTR2, by Zhou and Gitschier, 1997, revealed a wider expression at the transcript level, however much weaker in comparison to hCTR1. CTR2 highest expression levels were found in the placenta, spleen, heart, and brain (Zhou & Gitschier, 1997) Further expression analyses are required to determine the exact expression profile of hCTR2, at both transcript and protein levels.

In humans, *hCTR2* regulation, at the genomic level, is similar to the expression regulation of *hCTR1*. *hCTR2* responds to changes of microenvironmental copper levels, as well as to cellular copper requirements (Bertinato et al., 2008; Wee et al., 2013) Nonetheless, little to nothing is known about hCTR2 expression regulation, from the transcriptional to the post-translational level.

I.8. Copper importers in Sertoli cells

Even though in the last 30 years our knowledge regarding copper metabolism and regulation at a molecular level has significantly increased, there is still much to understand when it comes to the male reproductive system. What is already known is the deleterious effect of high copper concentrations in both the testis structure and the spermatogenic process, reported in both humans and animals (Akinloye et al., 2011; Aydemir et al., 2006; Y. Li et al., 2021; Liu et al., 2016). Copper deficiency has also shown to display consequences in male fertility (Tvrda et al., 2015; Van Niekerk & Van Niekerk, 1989).

However, there was a contradictory study conducted by Ghaffari et al., in 2019, where they generated mice with a SC-specific disruption of the *Ctr1* gene. Even though there was a decrease of copper concentration in the testicles by about 30 %, this reduction did not affect the fertility of these animals, that when mated with virgin WT females sired a comparable number of pups as to WT males (Ghaffari & Richburg, 2019). The discrepancy of these results might be related with the cell and tissue specificity of copper deficiency, instead of the systemic deficiency of Cu reported in some studies (Lyubimov et al., 2004; Van Niekerk & Van Niekerk, 1989). However, the loss of CTR1's function in germ cells leads to a progressive failure of spermatogenesis in adult mice (Ghaffari & Richburg, 2019). There

is still much to investigate regarding CTR2 expression in Sertoli cells or even its involvement in the spermatogenic process.

I.9. Copper and cancer

In recent years, it has been increasingly documented that copper levels are significantly elevated in both serum and tumor in cancer patients when compared to healthy individuals (Gupte & Mumper, 2009). These high levels were described in a wide variety of tumors, including lung (Diez et al., 1989), breast (H. W. Kuo et al., 2002), prostate (Habbib et al., 1980), ovarian (Chan et al., 1993), among others. Due to Cu's involvement in several physiological phenomena and interaction with numerous enzymes (Iakovidis et al., 2011), it is only plausible that Cu is involved in this pathological condition – cancer.

I.9.1. The importance of CTRs in cancer progression

The excessive levels of Cu have been linked with phenomena involved in cancer progression, such as cancer cell proliferation, metastasis, immune evasion, and angiogenesis (Denoyer et al., 2015; Grubman & White, 2014; Gupta & Lutsenko, 2009; Y. Li, 2020; Shanbhag et al., 2021). Furthermore, increased expression of the high-affinity transporter of copper – CTR1 – in several tumors (Denoyer et al., 2015; Grubman & White, 2014; Gupte & Mumper, 2009; Y. Li, 2020; Shanbhag et al., 2021) reinforces Cu determinant roles in cancer progression.

The programmed death-ligand 1 (PD-L1) is a transmembrane protein that allows evasion of the immune system (Voli et al., 2020) through binding to its receptor, programmed death receptor 1 (PD-1), present on the extracellular side of lymphocytes' PM, which in turn suppresses cytotoxic T-cells from killing cancer cells (Xu et al., 2020). Increased copper accumulation, due to increased expression of CTR1, was found to upregulate two signaling pathways that lead to elevated expression levels of PD-L1, demonstrating that copper has an, although indirect, effect on tumor immune evasion (Shanbhag et al., 2021; Voli et al., 2020).

Copper has also been demonstrated to be involved in oncogenic signaling, where its uptake via CTR1 stimulates the mitogen-activated protein kinase (MAPK) pathway (Turski et al., 2012). In more detail, MAPK kinase Mek1, the penultimate kinase in the MAPK pathway, has a high-affinity copper-binding site, that stimulates Mek1-dependent phosphorylation of the following kinase, and potentiate gene

expression, promoting cell survival and proliferation. Therefore, copper allosterically activates Mek1 and potentiates oncogenic signaling via the MAPK pathway (Brady et al., 2014; Shanbhag et al., 2021).

Cancer cell migration and metastasis are also influenced by copper through its binding to the family of copper-dependent lysyl oxidase enzymes (LOX and LOXL1–4). In resume, copper import via CTR1 enables its delivery by ATOX1 to the ATP7A copper pump, which transports copper to the LOX family of enzymes. Subsequently, the LOX family catalyzes the cross-linking of collagen fibers, generating H_2O_2, which enables the activation of the focal adhesion kinase (FAK1), and consequently promote cancer cell migration and metastasis (Baker et al., 2013; Shanbhag et al., 2021; Su et al., 2016).

Considering all of copper's roles in cancer progression, it is only plausible to target its high-affinity cellular importer – CTR1 - for anticancer treatments. Cisplatin is an anticancer platinum-based DNA crosslinking drug used in a high percentage of cancer patients that undergo chemotherapy (Shanbhag et al., 2021). However, there has been a growing biological resistance towards cisplatin treatment, including a mechanism that reduces its accumulation or even allows its sequestration by endogenous nucleophiles (Shanbhag et al., 2021). It was found that cisplatin seemed to bind with high affinity with domains and Cu-binding residues of CTR1 (Y. Guo, Smith, & Petris, 2004). Hence, allowing the cellular uptake of cisplatin by cancer cells, without however existing a fully understood mechanism of how cisplatin influx occurs (Shanbhag et al., 2021). Furthermore, hCTR1 silencing reduces cellular cisplatin levels compared to control in some cancer types (Holzer et al., 2004; Ishida et al., 2002), having high levels of hCTR1 already been associated with a good prognosis and chemotherapy response (Chen et al., 2012; Ishida et al., 2002; Y. Y. Lee et al., 2011). On the other hand, CTR2 expression is linked with cisplatin insensitivity. Lee et al., 2011, demonstrated that concomitant loss of hCTR1 expression and hCTR2 up-regulation are indicators of poorer cancer patient outcomes in breast and ovarian cancer (Y. Y. Lee et al., 2011). Therefore, the assessment of the hCTR1/hCTR2 ratio in cancer patients allows whether platinum-based drug therapies, like cisplatin, are the right treatment.

However, far more knowledge regarding CTR1 and CTR2 expression regulation and interplay is still to acquire. This work aims at facilitating this area of research through the future use of the biomolecular tools developed.

CHAPTER II

OUTLINE OF THE THESIS

II. OUTLINE OF THE THESIS

This work was focused on two groups of nutrient transporters: MCT4 monocarboxylate transporter and Copper transporters 1 and 2, whose interplay has never been investigated in carcinogenesis or spermatogenesis. As aforementioned, both MCT4 lactate transporter and CTRs play important roles in major steps of these biological processes. On the other hand, copper levels influence cellular metabolism, namely mitochondrial respiration and glycolysis, justifying its impact on the two glycolytic cell types mentioned above – Sertoli and cancer cells.

One of the main objectives of this work was to compare the expression and trafficking of MCT4 in cancer versus Sertoli cells, as there are few studies on this matter. In the first part of this thesis, a previously developed construct harboring MCT4 fused with mCherry was transfected to PC-3 and TM4 cell lines to study the expression and trafficking of pMCT4-mCherry by fluorescence microscopy and western blot, upon distinct glucose treatments.

In the second part of this thesis, we aimed at generating several biomolecular tools that will be used in the future to study the expression and trafficking of copper transporters CTR1 and CTR2, both in the PC-3 Prostate cancer cell line and in the TM4 Sertoli cell line.

CHAPTER III

MATERIALS AND METHODS

III. MATERIALS AND METHODS

III.1. Chemicals

Fetal Bovine Serum (FBS) was purchased from Biochrom AG (Berlin, Germany). Insulin-transferrin sodium selenite supplement (ITS supplement) was obtained from Life Technologies (Gaithersburg, MD, USA). Radio-Immune Precipitation Assay (RIPA) and BCA Protein Assay Kit were purchased from Life Technologies. WesternBright™ ECL substrate was obtained from Bio-Rad (Hemel Hempstead, UK). Dulbecco's Modified Eagle Medium: Ham's Nutrient Mixture F12 (DMEM: Ham's F12), DMEM without glucose, Roswell Park Memorial Institute (RPMI) 1640, Bovine Serum Albumin (BSA), EDTA, trypsin-EDTA and other chemicals were purchased from Sigma-Aldrich (St. Louis, MO, USA), unless stated otherwise.

III.2. Cell line culture

Mouse Sertoli cells (TM4 cell line) were purchased from ATCC (Manassas, VA, USA), and the Human Prostate Cancer cell line (PC-3 cell line) (neoplastic cell line) was kindly provided by Dr. [a] Margarida Fardilha (University of Aveiro, Portugal). In brief, TM4 and PC-3 cells were cultured in 75 cm^2 flasks (VWR collection, Amadora, Portugal) at 37°C, 5 % CO_2, with specific Sertoli culture medium – DMEM: Ham's F12 1:1 – or RPMI medium, respectively, supplemented with 50 µg/mL gentamicin, 50 U/mL penicillin, 50 mg/mL streptomycin sulfate, 0.5 mg/mL fungizone and 10 % heat inactivated FBS at pH 7.4. TM4 is a Sertoli cell line derived from the testis of immature BALB/c mouse selected by morphology and hormonal response (Mather, 1980) that express specific Sertoli cell markers (Wang et al., 2016). Every "n" corresponds to a cell passage.

III.3. Transfection

The previously generated plasmid pMCT4-mCherry (see Appendix A Figure 30), was transiently transfect in PC-3 cells using Lipofectamine™ 3000 Transfection Reagent (Invitrogen™, Waltham, Massachusetts, USA).

Initially, the plasmid was extracted using the NZYTech Midiprep Kit, according to manufactorer's protocol, to obtain a high plasmid concentration for the transfection protocol. Briefly, PC-3 cells were

plated in a 96-well glass-bottom plate, for low fluorescence emission, and cultured for 24 h at 37°C, 5 % CO_2. The plasmid construction component was prepared through the addition of 5 µL Opti-MEM per well and 1 µL/500 ng DNA of P3000 reagent (complementary reagent of the Lipofectamine™ 3000 purchased). Lipofectamine was also prepared by the addition of 5 µL Opti-MEM per well. Both components were mixed for the determined incubation time. Afterward, the mix was added to each well, and cells were left in the optimal growing conditions.

Prior to the use of transfection for MCT4 localization studies, a transfection optimization was recquired. For that, the following conditions were tested (per well of a 96-well plate):

- number of initially plated cells: 1.24×10^4 versus 2.48×10^4 cells;
- volume of Lipofectamine 3000 reagent (which results in a different lipid: DNA ratio): 0.15 µL versus 0.3 µL;
- quantity of DNA: 25 ng versus 50 ng versus 100 ng;
- time of incubation prior to transfection (to allow the establishment of lipid-DNA complexes for transfection): 8 versus 12 min.

Cells were stained using Hoechst dye, for nuclei count. Concisely, the culture medium was exchanged to a medium containing an optimized Hoechst dye concentration of 0.5 µg/mL at 37 °C, for 30 min. Afterwards, medium containing Hoechst was removed and replaced with Hank's Balanced Salt solution (HBSS), for image acquisition purposes after 24 h and 48 h post-transfection, using Zoe Fluorescent Cell Imager (Bio-Rad). Trough the ratio from transfected/total cells was possible to access transfection efficiency.

III.4. *In vitro* Treatments

When TM4 and PC-3 cultures reached the optimal time post-transfection, or, for protein expression studies (without transfection), after they reached 90-95 % confluence, cells were washed thoroughly and the culture medium replaced by serum free DMEM without glucose (with ITS supplement: insulin 10 mg/L; sodium selenite 6.7 µg/L; transferrin 5.5 mg/L, pH 7.4). In order to evaluate the effect of glucose on TM4 and PC-3 cells we defined four experimental groups, the first group was glucose-free, and the three following groups were supplemented with glucose in increasing concentrations of 2 mM, 5.5 mM and 20 mM. The 5.5 mM concentration was selected in accordance with the physiological blood glucose concentration (World Health Organization, 2021), hence being the control group. The 20 mM of glucose,

was chosen given that it is already a hyperglycemic value, presented by an individual with diabetes (World Health Organization, 2021). We also considered pertinent to evaluate the effects of a hypoglycemic value of 2 mM (World Health Organization, 2021), and 0 mM. Treatments were performed for 24 h, at 37 °C in an atmosphere of 5 % CO_2.

III.5. Immunofluorescence and internalization analysis

For the localization analysis, cells were seeded in 48-well plates containing glass coverslips, and transfection was performed using an adequate proportion for the optimal transfection values determined previously. 48 h later, cells were treated with the glucose concentrations mentioned in the previous section, for 24 h. After the treatments, cells were fixed with paraformaldehyde (PFA) 4 % for 20 min. After rinsing with phosphate buffer saline (PBS) 1x, cells were permeabilized with PBS-Triton 0.1 % for 15 min, and rinsed again with PBS 1x. Cells were then blocked in PBS-Gelatin 0.1 % for 15 min and washed with PBS 1x. Subsequently, cells were incubated with the primary antibody rabbit anti-β-catenin (1:50, Abcam, Cambridge, MA, ab68183), in PBS-Gelatin 0.1 % at 4 °C overnight in a humidified chamber. Afterwards, cells were washed with PBS-Gelatin 0.1 % and then labelled with goat anti-rabbit Alexa fluor 488 (1:1500, Invitrogen™, Waltham, Massachusetts, USA) for 1 h in a humidified chamber. Cell were then washed with PBS 1x, and the coverslips mounted into a lamina using *Vectashield* Mounting Medium with DAPI. Samples were maintained at -20 °C until visualization. The results were visualized in a Nikon Eclipse E400 microscope equipped with a Y-FL epi-fluorescence attachment and HB-10103AF Super high-pressure mercury lamp power supply (Nikon, Shinagawa, Tokyo, Japan), coupled with a Nikon NIS Elements Image Software.

III.6. Total protein extraction

After the 24 h treatments, TM4 and PC-3 cells were detached from the culture dishes with the use of a trypsin-EDTA solution. Once detached, the total cell number was determined with the use of a Neubauer chamber. Following, cells were washed in PBS and collected with a centrifugation of 3000 g for 5 min.

Cells were lysed with an appropriate volume of RIPA buffer (1x PBS, 1 % NP-40, 0,5 % sodium deoxycholate, 0,1 % SDS, 1 mM PMSF) supplemented with 1% protease inhibitor cocktail, aprotinin and

100 mM sodium orthovanadate, and left at 4 °C for 40 min. Finally, the suspension was centrifuged at 14000 g, at 4 °C for 20 min. Subsequently, the pellet was discarded. Finally, the total protein concentration was determined with the use of the Pierce™ BCA Protein Assay Kit according to manufacturer's instructions, where different known concentrations of BCA are used as standards for calibration, and the optical densities measured at 595 nm.

III.7. Western blot

Western blot was performed to analyze protein levels of MCT4 following treatments in TM4 and PC-3 cells. Briefly, protein samples (20 μg) were mixed with sample buffer (10 % glycerol, 2 % SDS, 60 mM Tris.HCl, 5 % β-mercaptoethanol, 0.01 % bromophenol blue, pH 6.8) and denatured at 70 °C for 10 min. The protein samples were fractionated in 12 % polyacrylamide gels from the Kit TGX Stain Free 12 % at 90 V for 90 min. Subsequently, proteins were transferred to previously activated polyvinylidene difluoride membranes (Bio-Rad) in a Mini Trans-Blot® cell (Bio-Rad), and the total transferred protein was read with the Bio-Rad ChemiDoc XR (Bio-Rad). Afterwards, the membrane was blocked for 3 hours in a 5 % BSA solution at room temperature. The membranes were then washed and incubated overnight at 4 °C with rabbit anti-Slc16a3 (1:5000, Abcam, Cambridge, MA, Ab 74109) for the PC-3 protein extracts and with rabbit anti-Slc16a3 (1:1000, Alomone Labs, Jerusalem, Israel, AMT014) for the TM4 protein extracts. The immune-reactive protein was detected using mouse anti-rabbit IgG-HRP (1:5000, Santa Cruz Biotechnology Heidelberg, Germany, SC-2357). Membranes were reacted with WesternBright™ ECL and read in the Bio-Rad ChemiDoc XR (Bio-Rad). The densities from each band were obtained according to standard methods with the Image Lab Software (Bio-Rad). Each band density was divided by the respective total protein density and then normalized with the control group value.

III.8. Proton Nuclear Magnetic Resonance (^{1}H-NMR) spectroscopy

The post-treatment media was analyzed for the presence of certain metabolites by proton nuclear magnetic resonance (^{1}H-NMR) and spectra analysis. 1D ^{1}H-NMR spectra were acquired on a 500 MHz Bruker Avance III HD spectrometer equipped with a 5-mm TXI probe, at 298 K. 120 μL of sodium fumarate 10 mM were added to each 480 μL of post-treatment medium, for a final volume of 600 μL.

Sodium fumarate was used as the internal reference for metabolite quantification in the media. The following metabolites were quantified (multiplicity, chemical shift (ppm)): alanine (doublet, 1.46); acetate (singlet, 1.90); pyruvate (singlet, 2.35); glutamine (multiple, 2.45); lactate (quartet, 4.09); glucose (doublet, 5.22). The baseline was corrected, and the spectra manually phased. NUTS-Pro NMR software (Acorn NMR, Inc, Fremont, CA, USA) was used to process and integrate the peaks of the chosen metabolites. The concentration of the chosen metabolites is expressed in nmol/10^6 cells.

III.9. Strains and cell culture media

During this study, *Escherichia coli* strain XL1 Blue (Table 1) was used. The protocol for making competent cells is described in Appendix B. The transformation of these cells was carried out following the protocol described in section III.12.6.

Table 1: Description of *Escherichia coli* strain XL1 Blue.

Strain	Genotype	Source
XL1 Blue	*recA1 endA1 gyrA96 thi-1 hsdR17 supE44 relA1 lac [F' proAB + lac LqZ* ΔM15 Tn 10 (Tet^R)]	This study / laboratory collection

Luria-Bertani broth (LB) medium was used to grow the *E. coli* cultures. This medium is composed of 5g/L yeast extract, 5 g/L NaCl, 10 g/L tryptone ad 18 g/L Agar*. For optimal growth conditions, cells were incubated at 37 °C, 200 rpm in an orbital agitator. Furthermore, kanamycin was added to the medium, at the final concentration of 50 μg/mL, as the selection marker for the bacteria that were successfully transformed with the plasmids.

*Used only in solid media

III.10. Plasmids

The plasmids used in this study are described in Table 2. For more detailed information, such as the predicted nucleotide sequences and the horizontal map of the constructed plasmids see Appendix C Figure 31, Figure 32, Figure 33, Figure 34 and Figure 35.

Table 2: List of plasmids used in this study.

Plasmids	Selectable markers	Promoter	Source
pAcGFP1-C1	Kanamycin/Neomycin	CMV	Takara Bio Group
pAcGFP1-N1	Kanamycin/Neomycin	CMV	Takara Bio Group
pmCherry-C1	Kanamycin/Neomycin	CMV	Takara Bio Group
pmCherry-N1	Kanamycin/Neomycin	CMV	Takara Bio Group
pEYFP-CTR1	Kanamycin/Neomycin	CMV	Laboratory collection
pEYFP-CTR2	Kanamycin/Neomycin	CMV	Laboratory collection
pCTR1-mCherry	Kanamycin/Neomycin	CMV	This study
pmCherry-CTR1	Kanamycin/Neomycin	CMV	This study
pCTR2-mCherry	Kanamycin/Neomycin	CMV	This study
pCTR2-AcGFP	Kanamycin/Neomycin	CMV	This study
pAcGFP-CTR2	Kanamycin/Neomycin	CMV	This study
pMCT4-mCherry	Kanamycin/Neomycin	CMV	Laboratory collection

Abbreviations: CMV: cytomegalovirus.

IIII.11. Primer design

The primers used in this study are described in the following table (Table 3), the ones used to amplify *hCTR1* and *hCTR2* genes, and the primers for the confirmation of the plasmid constructions obtained, through sequencing.

Table 3: List of primers used in this study. The enzymes' restriction sites in the primers are marked in bold.

Primers	Sequence (5'- 3')	Source
FW_CTR1	GA**AGATCT**ATGGATCATTCCCACCATATGGGGATG	This study
RV_mCherry_CTR1	GA**AAGCTT**TCAATGGCAATGCTCTGTGATATCCAC	This study
RV_CTR1_mCherry	GA**AAGCTT**ATGGCAATGCTCTGTGATATCCACTAC	This study
FW_CTR2	GA**AGATCT**ATGGCGATGCATTTCATCTTCTCAGAT	This study
RV_CTR2_mCherry/AcGFP	GA**AAGCTT**AGCTGTGCTGAGAAGTGGGTAAGCTAG	This study
RV_AcGFP_CTR2	GA**AAGCTT**CTAAGCTGTGCTGAGAAGTGGGTAAGC	This study
Seq_FW_CMV	CGCAAATGGGCGGTAGGCGTG	Laboratory collection
Seq_RV_CTR_GFP	CTCACGCTGAACTTGTGGCCATTCACATCGCCATT	Laboratory collection
Seq_FW_mCherry_CTR	GGACATCACCTCCCACAACGAGGAC	Laboratory collection
Seq_RV_CTR_mCherry	CCGTTCACGGAGCCCTCCATGTGCACCTTGAAGCG	Laboratory collection
Seq_FW_GFP_CTR	AAGCGCGATCACATGATCTACTTCG	Laboratory collection
Seq_RV_TAG_CTR	TGTTTCAGGTTCAGGGGGAGGTGTGGGAGGTTTTT	Laboratory collection

The first group of primers includes specific restriction sites flanking the target genes, present in the Multiple Cloning Site (MCS), but absent in any other part of the vector, and a GA tail needed to prevent the exclusion of the nucleotides that follow. These components are required for the insertions of the genes into different expression vectors, through the sticky-ends created.

All the primers were designed using the ApE program 2.0.55 (created by Wayne Davis from the University of Utah), and synthetized by Eurofins Genomics.

III.12. Cloning strategy

Using the classical cloning method, we designed and construct 5 plasmid constructions harboring *hCTR1* or *hCTR2* genes, fused with the Green Fluorescent Protein (GFP) or the fluorescent protein m-Cherry, giving rise to the following biomolecular tools: pmCherry-CTR1, pCTR1-mCherry, pCTR2-mCherry, pCTR2-AcGFP and pAcGFP-CTR2.

As it is well known, this traditional cloning method relies on five main steps, starting by the insert preparation, which includes insert amplification and digestion with specific restriction enzymes, followed by vector preparation, meaning the digestion of the vector, the ligation of the digested fragments, and, finally, transformation with the plasmid constructions created and colony screening, as schematically shown in Figure 5.

In more detail, genes *hCTR1* and *hCTR2* were amplified by Polymerase Chain Reaction (PCR), with the following combination of primers. To fuse *mCherry* to the 3' end terminal of *hCTR1*, the *hCTR1* gene was amplified from the pEYFP-CTR1 plasmid, using primers FW-CTR1 and RV_CTR1_mCherry. Whereas for the fusion of *mCherry* to the 5' end terminal of *hCTR1*, the *hCTR1* gene was amplified from the pEYFP-CTR1 plasmid, using primers FW-CTR1 and RV_mCherry_CTR1. For the fusion of *GFP* or *mCherry* to the 3' end terminal of *hCTR2*, the *hCTR2* gene was amplified from the pEYFP-CTR2, using primers FW-CTR2 and RV_CTR2_mCherry/AcGFP. At last, for the fusion of *GFP* gene to the 5' end terminal of *hCTR2*, the *hCTR2* gene was amplified from the plasmid pEYFP-CTR2, using primers FW-CTR2 and RV_AcGFP_CTR2. For the fusion of *mCherry* or *GFP* genes at the 5' end terminal of the *CTRs* genes, we used pmCherry-N1 and pAcGFP-N1 as backbones, respectively. To fuse *mCherry* or *GFP* genes at the 3' end terminal of the *CTRs* genes, plasmids pmCherry-C1 and pAcGFP-C1 were used as backbone, respectively. After the amplification, both inserts and plasmids were digested with *Bgl*II and *Hind*III (Thermo Scientific™, Waltham, Massachusetts, USA) restriction enzymes. The digested inserts were then purified using the NZYTech Gelpure Kit (NZYTech, Portugal). Regarding the digested plasmids, they were run in an agarose gel (1 % TAE agarose) and extracted from the gel following the manufacturer's protocol, also from the NZYTech Gelpure Kit (NZYTech, Portugal).

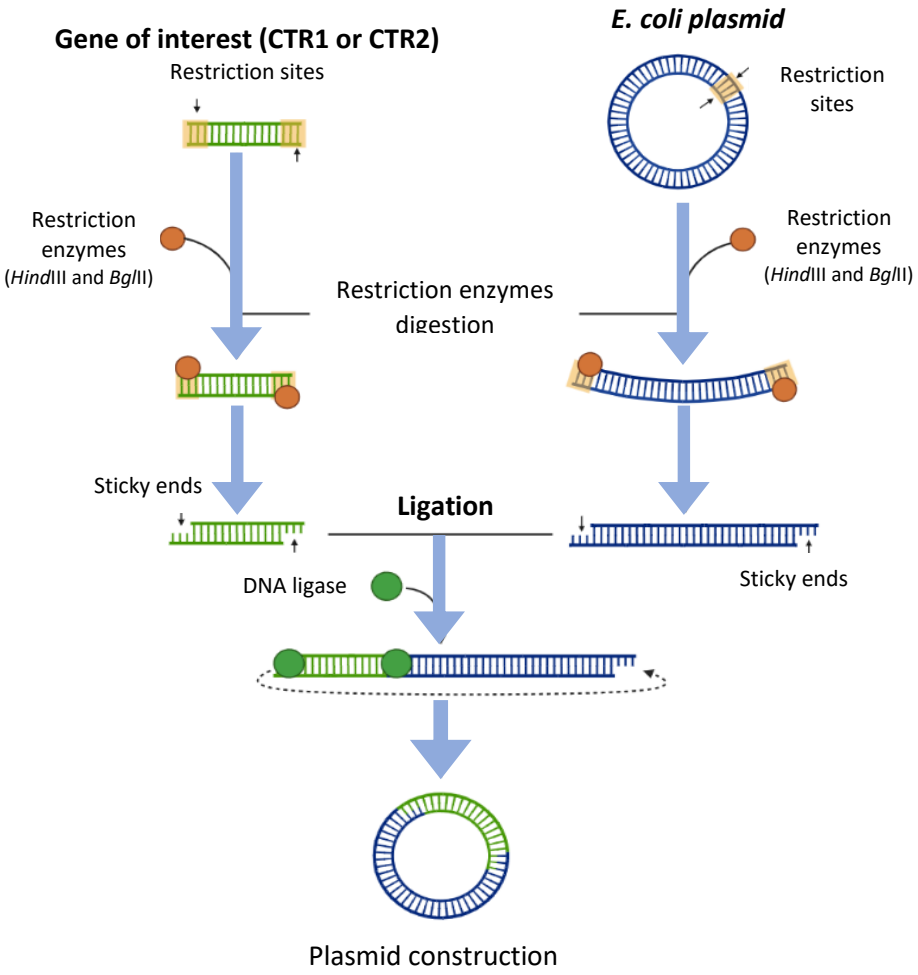

Figure 5: Schematic representation of the classical cloning strategy. Firstly, the classical cloning strategy relies on the digestion of both insert and vector, with specific restriction enzymes, namely *Hind*III and *Bgl*II. The action of these enzymes creates sticky ends in the digested fragments. Following, insert and vector suffer ligation through the action of DNA ligase, giving rise to the plasmid construction (created with Biorender.com). CTR1: Copper transporter 1; CTR2: Copper transporter 2. Some components were drawn using Biorender (https://biorender.com/).

The ligation between the plasmids and the respective insert was made and then transformed in *E. coli* XL1 Blue competent cells, in LB medium, supplemented with kanamycin 50 µg/mL, so that the positive transformants could be selected. After the first confirmation by colony PCR, there was another confirmation where the plasmid from 1/2 positive colonies was extracted following the manufacturer's protocol from the NZYTech Miniprep Kit (NZYTech, Portugal). Finally, all the constructions made were confirmed by sequencing (see section III.12.9.), using the previously extracted plasmids.

III.12.1. Insert Amplification by PCR

PCR is an *in vitro* method that allows the amplification of a single and specific region of a DNA molecule, into millions of identical copies. Following that, genes *hCTR1* and *hCTR2* were amplified by PCR using Supreme NZYProof DNA Polymerase (NZYTech, Portugal), from pEYFP-CTR1 and pEYFP-CTR2, respectively, using the primers stated in section III.11.

The reaction mixture was composed by the following components: Reaction Buffer 1 x (NZYTech); dNTPs 0.2 mM (NZYTech); Supreme NZYProof DNA Polymerase 0.025 U/μL (NZYTech); Primer Forward 0.5 μM; Primer Reverse 0.5 μM; Ultrapure Water to final volume of 20 μL; Template 0.05 ng/μL. After the preparation, the reaction mixture was gently mixed, and the PCR tubes placed in the T100TM Thermal Cycler (Bio-Rad) for amplification. Regarding the PCR cycling conditions of each amplification, they are described in Table 4 and Table 5. Finally, to confirm amplification, the samples were run on an 1 % (w/v) Tris-Acetate-EDTA (TAE) agarose gel electrophoresis at 180 V, and their quantity and quality assessed using the NanoDrop® ND-1000 system.

Table 4: PCR cycling parameters for *hCTR1* amplification from pEYFP-CTR1 using Supreme NYZPROOF.

Step	Temperature (ºC)	Time	Cycles
Initial denaturation	96	4 min	1
Denaturation	96	30 s	30
Annealing	57	30 s	30
Extension	72	45 s	30
Final	72	10 min	1

Table 5: PCR cycling parameters for *hCTR2* amplification from pEYFP-CTR2 using Supreme NYZPROOF.

Step	Temperature (ºC)	Time	Cycles
Initial denaturation	96	4 min	1
Denaturation	96	30 s	30
Annealing	58	30 s	30
Extension	72	45 s	30
Final	72	10 min	1

III.12.2. Agarose gel electrophoresis of DNA

So that the PCR products could be analyzed, agarose gels were prepared by mixing Agarose (Grisp) with TAE buffer, for the final concentration of 1 % (w/v). To dissolve the agarose, the mixture was heated using a microwave. The solution was left at room temperature until it cooled down, and finally, poured in a specific gel tray and left to solidify.

The NZYDNA Ladder III (NZYTech) was used as the DNA molecular weight marker. DNA samples were then prepared through mixing with the loading buffer 12 % (w/v) FICOLL 400 (100 %); 0,0075 % (w/v) Xylene Cyanole FF (1 mg/mL); 1,8 % (v/v) VAHINE yellow; 0,144 % (v/v) Orange G (1 % w/v). Subsequently, the samples were run on a 1 % (w/v) TAE agarose gel electrophoresis at 180 V. For proper visualization of DNA bands, the gel was post-stained with Midori green (Nippon genetics), and their images acquired at 610 nm in a UV transilluminator (VWR Genosmart, VWR).

III.12.3. DNA purification

After the *hCTR* genes' amplification, the PCR products were purified for the removal of primer dimers, enzymes, proteins, nucleotides and other impurities, using the NZYTech Gelpure Kit (NZYTech) by following manufacturer's protocol. Finally, the concentration and quality of the DNA samples were determined using the NanoDrop® ND-1000 system. The purified DNA was stored at -20 °C.

III.12.4. Plasmids and inserts' digestion

Before the ligation step, both inserts and plasmids (pAcGFP-N1, pAcGFP-C1, pmCherry-N1 and pmCherry-C1) were digested using *Bgl*II (ThermoFisher) and *Hind*III (ThermoFisher) enzymes. The reaction mixture was composed by the following components: Buffer Fast Digest 1 x; *Bgl*II restriction enzyme 0.33 mM; *Hind*III restriction enzyme 0.33 mM; DNA 50 ng/μL. After gently mixing all the components, they were kept at 37 °C, for 1 h. Sequentially, the digested plasmids were stained with loading buffer (previously described) and run on a 1 % (w/v) TAE agarose gel electrophoresis at 180 V, alongside with the NZYDNA Ladder III. For the visualization of DNA, the gel was once again post-stained with Midori green (Nippon genetics), and the gel observation performed at 610 nm in a UV transilluminator

(VWR). At last, the linearized plasmids were directly extracted from the gel and purified using the NZYTech Gelpure Kit (NZYTech), following manufacturer's protocol.

III.12.5. Ligation

After both inserts (PCR amplified fragments) and vectors (digested plasmids) were prepared, they undergone the process of ligation using the T4 DNA Ligase (ThermoFisher). The ligation reactions were performed for two molar ratios of vector: insert, namely 1:1 and 1:5. To calculate the amount of insert added to the mixture, the concentration of the vector and the sizes of both vector and insert were considered, applying the following equation (Figure 6):

$$\frac{\text{ng of vector x kb size of insert}}{\text{kb size of vector}} \text{ x molar ratio of } \frac{\text{insert}}{\text{vector}} = \text{ng of insert}$$

Figure 6: Equation for the determination of the optimal quantity of DNA insert in a ligation reaction.

These calculations were performed using an online tool, found at: https://worldwide.promega.com/resources/tools/biomath/?calc=ratio&fbclid=IwAR0NOMXJDk13NGC96rUSm3xOB3nfijhTRVGhE-kMznmzlgPyKwco5Hylkio

Therefore, the ligation mixture was composed by the following components: T4 DNA Ligase 0.25 U/ µL; T4 DNA Ligase buffer 1 x; vector (1 µL); insert (variable volume); Ultrapure water. Afterwards, the reaction mixture was incubated at room temperature (22 °C) for 1 h.

III.12.6. *E. coli* transformation

The transformation of competent *E. coli* XL1 Blue cells, with the fully constructed designed plasmids, was done by heat-shock. Firstly, cells were transferred from the deep-freezer (-80 °C) to ice, where they stayed for 10 to 15 min. For each transformation, 100 µL of competent cells were used. Afterwards, the ligation mixture was added to the cell suspension, by the flame, which were put back on ice for more 30 min. Immediately after, the heat-shock was performed at 42 °C for 45 s, and cells return

to ice for 10 min. After the heat-shock strategy, 800 µL of Super Optimal broth with Catabolite repression (SOC) antibiotics free were added to the cell suspension, for recovery purposes, and incubated for at 37 °C, 200 rpm, for 1 h. Cells were then centrifuged for 1 min at 5000 rpm, and 750 µL of the supernatant is removed. A small volume of media remains to facilitate the pellet's gently resuspension. After this step, the entire remaining volume was spread on the previously made plates of LB with kanamycin 50 µg/mL, and incubated overnight at 37 °C. After 18-24 h, some of the positive colonies were collected and streaked onto a new LB plate and incubated at 37 °C for another 18-24 h.

NOTE: There were performed 3 controls, under the exact conditions described above, for the transformation of each plasmid construction made. The controls were: negative control with only cells (no DNA); control with the digested vector (without the insert); positive control with the vector without the insert.

III.12.7. Colony PCR

After *E. coli* transformation, some of the positive colonies were picked, and grown overnight at 37 °C. In the following day, the grown colonies were tested by PCR (colony PCR), to confirm the presence of the desired plasmid. To verify the constructs, the same primers used in section III.12.1. to amplify *hCTR1* and *hCTR2* from pEYFP-CTR1 and pEYFP-CTR2, respectively, were used.

The reaction consisted in the amplification of gene *hCTR1* or *hCTR2*, from the supposedly positive colonies. For the template, a small amount of each colony was suspended in 100 µL of Ultrapure water, and only 3 µL of that suspension was used.

The reaction mixture was composed by the following components: Master mix 1 x (PCR buffer 5 x; $MgCl_2$ 25 mM; dNTPs 5 mM; Taq Polymerase (0.025 U/µL); Ultrapure water); Primer Forward 1 µM; Primer Reverse 1 µM; Template (3 µL); Ultrapure water. Regarding the PCR cycling conditions of each amplification, they are described in Table 6 and Table 7. It is important to notice that the initial denaturation lasted 10 min so that cell lysis occurs, and DNA could be exposed to the PCR reaction.

At the end of the PCR reaction, the amplification products were run on an 1 % (w/v) TAE agarose gel electrophoresis at 180 V, and their quantity and quality determined using the NanoDrop® ND-1000 system.

Table 6: PCR cycling parameters for *hCTR1* amplification from pmCherry-CTR1/pCTR1-mCherry using *Taq* DNA Polymerase.

Step	Temperature (ºC)	Time	Cycles
Initial denaturation	94	10 min	1
Denaturation	94	30 s	30
Annealing	59	30 s	30
Extension	72	1 min 30 s	30
Final	72	10 min	1

Table 7: PCR cycling parameters for *hCTR2* amplification from pCTR2-mCherry/ pCTR2-AcGFP/ pAcGFP-CTR2 using *Taq* DNA Polymerase.

Step	Temperature (ºC)	Time	Cycles
Initial denaturation	94	10 min	1
Denaturation	94	30 s	30
Annealing	60	30 s	30
Extension	72	1 min 30 s	30
Final	72	10 min	1

III.12.8. Confirmation PCR

After the colony PCR, 1/2 positive colonies were inoculated in 5 mL LB, supplemented with kanamycin 50 μg/mL, overnight at 37 °C, under 200 rpm. On the following day, it was performed a plasmid extraction using the NZYTech Miniprep Kit, following manufacturer's protocol. The plasmid concentration was determined using the NanoDrop® ND-1000 system, and then the microcentrifuge tube with the extracted plasmid were stored at -20 °C.

The extracted plasmids were then used as template for a final PCR confirmation of the positive colonies, using once again the primers mentioned in section III.12.1. The reaction mixture was composed by the following components (and respective final concentrations): Master mix 1 x (PCR buffer 5 x; $MgCl_2$ 25 mM; dNTPs 5 mM; *Taq* DNA Polymerase (0.025 U/μL); Ultrapure water); Primer Forward 1 μM; Primer Reverse 1 μM; Template (3 μL); Ultrapure water. Regarding the PCR cycling conditions of each amplification, they are described in Table 6 and Table 7, only varying at the duration of the initial denaturation step, which is changed for only 4 min. Finally, the amplification products were run on an 1 % TAE agarose gel electrophoresis.

III.12.9. Sequencing

To properly confirm that the plasmids constructed did not had any errors introduced during the cloning strategy, their sequence was confirmed by DNA sequencing (Eurofins Genomics).

The primers used for sequencing pCTR1-mCherry and pCTR2-mCherry were Seq_FW_CMV and Seq_RV_CTR_mCherry. Whereas for sequencing pCTR2-AcGFP the primers used were Seq_FW_CMV and Seq_RV_CTR_GFP. Primers Seq_FW_GFP_CTR and Seq_RV_TAG_CTR were the ones used for sequencing pAcGFP-CTR2. Finally, for the sequencing of pmCherry-CTR1, the used primers were Seq_FW_mCherry_CTR and Seq_RV_TAG_CTR.

III.12.10. Glycerol stocks

After validation of the plasmid constructions by sequencing, glycerol stocks were prepared to preserve the sequences for further extraction to future studies.

In more detail, one day before the preparation of the stocks, cells were incubated in 5 mL of LB medium with kanamycin 50 µg/mL, at 37 °C with 200 rpm. In the following day, cell suspension was centrifuged for 2 min at 5000 rpm, and the pellet resuspended in a 40 % glycerol solution. The stocks were then kept in the deep freezer (-80 °C).

III.13. Statistical Analysis

The statistical significance among the experimental groups was assessed by ANOVA multiple comparisons. In some experimental results, the control sample is represented by 1, and results are presented by relative comparison with control group. The experimental data are shown as Mean ± SEM. Possible outliers were removed using Grubbs' method, alpha=0.2. Statistical analysis was performed using GraphPad Prism 8 (GraphPad software, San Diego, CA, USA). $p < 0.05$ was considered significant.

CHAPTER IV

RESULTS

IV. RESULTS

IV.1. MCT4 Expression and Intracellular Trafficking analysis in response to distinct glucose concentrations: a comparison between PC-3 Prostate Cancer cell line and TM4 Sertoli cell line

For many years, research on MCT4 has been separately focused on cancer cells and Sertoli cells. However, the urge of a comparative study rises, for better understanding their phenotypical differences upon the same Warburg-like metabolism. For that we studied the trafficking and expression of MCT4 in a comparative manner between the PC-3 cell line and the TM4 cell line, upon different glucose treatments, ranging from zero to hyperglycemic levels. For that we used the previously described plasmid construction harboring Human *MCT4* fused with the *mCherry* gene, which results in a MCT4 protein fused with mCherry after transfection. Further concluded with an analysis of glucose and glutamine consumption, and lactate, pyruvate, alanine and acetate export, in response to the same glucose treatments.

IV.1.1. Transfection optimization of pMCT4-mCherry in PC-3 cells

Prior to the expression and trafficking analysis of MCT4 fused with mCherry fluorescent protein we developed an optimized protocol using Lipofectamine™ 3000 for the transfection of pMCT4-mCherry into both PC-3 and TM4 cell lines. Several conditions were tested in a 96-well glass-bottom plate, for low fluorescence emission, allowing to test several conditions in one single experiment, such as the number of plated cells, the volume of Lipofectamine™ 3000, DNA amount, and optimal time after transfection for the highest transfection efficiency in PC-3 cells. Transfection efficiency was determined by the count of at least 500 cells in several microscopic fields and through the calculation of the percentage of red fluorescent cells relative to total cells (with nuclei stained in blue with Hoechst dye). For control purposes, the plasmid carrying only the mCherry gene was also transfected into the PC-3 cell line. It is important to notice that the values of each condition tested are indicated per well of the 96-well plate.

As depicted in Figure 7, there were no significant differences between 50 or 100 ng of DNA used when 1.24×10^4 cells were plated. Therefore, we selected 50 ng as the optimal amount of DNA for transfection. However, there was a significant statistical difference in transfection efficiency between 24

h (14.47 ± 2.807 %) and 48 h (33.93 ± 3.580 %) after transfection, using 50 ng of DNA. On the other hand, when 2.48 x 10^4 cells were plated, there was no significant difference in the transfection efficiency, as presented in Figure 8, either between DNA amounts or time post-transfection. Finally, considering only the values of 48 h post-transfection with 50 ng of DNA, it is possible to determine that 1.24 x 10^4 plated cells is the most adequate number to reach the highest transfection efficiency (33.93 ± 3.580 %) when compared to the values reached by plating 2.48 x 104 (16.13 ± 1.524 %), as seen in Figure 9.

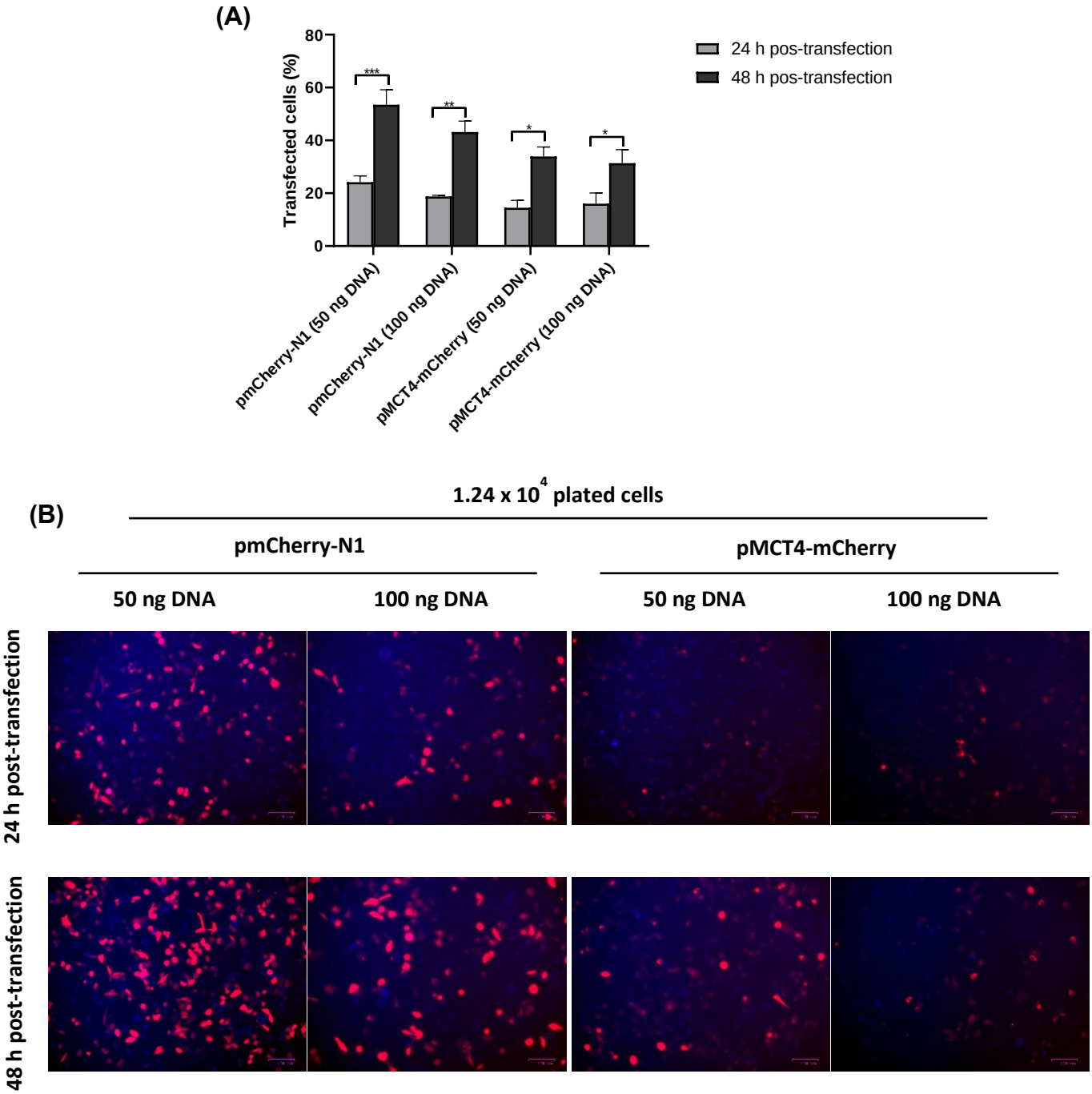

Figure 7: Transfection efficiency in the PC-3 cell line at 24 and 48 h after transfection with pmCherry-N1 or pMCT4-mCherry, using the Lipofectamine™ 3000 reagent, with 1.24 x 10^4 plated cells. (A) Percentage of

transiently transfected cells with pmCherry-N1 or pMCT4-mCherry. Results are expressed as Means ± SEM (n=3). * $p < 0.05$: ** $p < 0.01$; *** $p < 0.001$. The horizontal bar corresponds to the statistical significance between 24 h and 48 h post-transfection. (B) Analysis of transiently transfected cells with pmCherry-N1 or pMCT4-mCherry. Representative images of PC-3 cells 24 h and 48 h after transfection. Staining of cell nuclei with Hoechst (blue) of transiently transfected cells with the pmCherry-N1 or pMCT4-mCherry to determine the transfected cells (red).

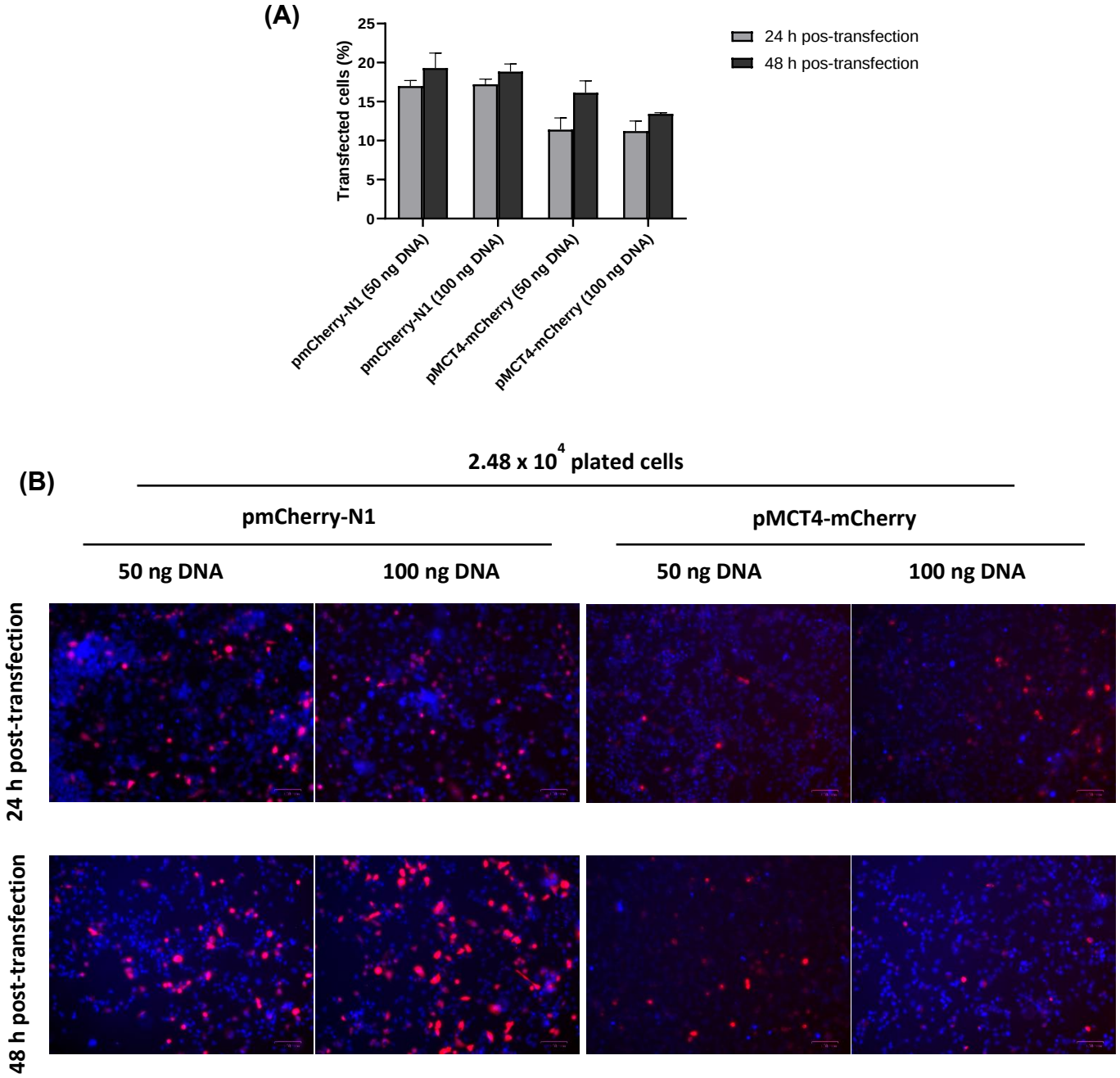

Figure 8: Transfection efficiency in the PC-3 cell line at 24 and 48 h after transfection with pmCherry-N1 or pMCT4-mCherry, using the Lipofectamine™ 3000 reagent, with 2.48 x 10^4 plated cells. (A) Percentage of transiently transfected cells with pmCherry-N1 or pMCT4-mCherry. Results are expressed as Means ± SEM (n=3). (B) Analysis of transiently transfected cells with pmCherry-N1 or pMCT4-mCherry. Representative images of PC-3

cells 24 h and 48 h after transfection. Staining of cell nuclei with Hoechst (blue) of transiently transfected cells with the pmCherry-N1 or pMCT4-mCherry to determine the transfected cells (red).

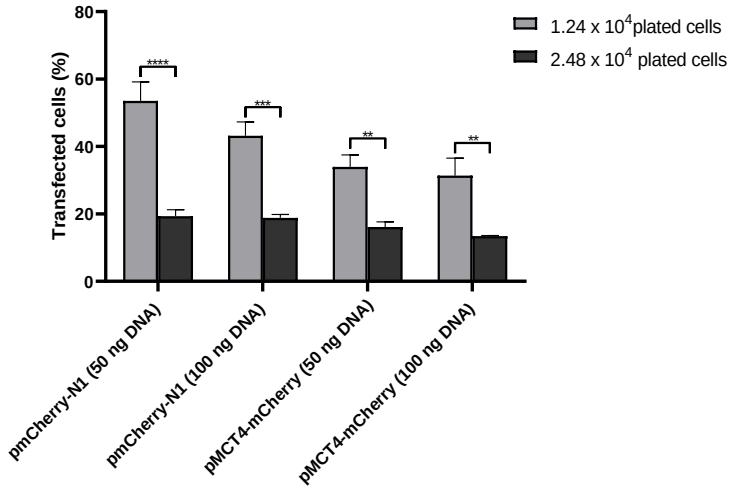

Figure 9: Transfection efficiency in the PC-3 cell line at 48 h after transfection with pMCT4-mCherry, using the Lipofectamine™ 3000 reagent, comparing 1.24 x 10^4 with 2.48 x 10^4 plated cells. Results are expressed as Means ± SEM (n=3). ** $p < 0.01$; *** $p < 0.001$; **** $p < 0.0001$. The horizontal bar corresponds to the statistical significance between 1.24 x 10^4 and 2.48 x 10^4 plated cells.

Therefore, we discovered that the best conditions (per well of a 96-well plate) to achieve the highest transfection efficiency of pMCT4-mCherry into PC-3 cells include the use of 50 ng of DNA, 1.24 x 10^4 plated cells, and 48 h post-transfection. These conditions were then adapted in subsequent immunofluorescence experiments, for the use of a 48-well plate.

IV.1.2 MCT4 trafficking is altered in PC-3 cell line, but not in TM4 cell line, in response to distinct glucose treatments

After the determination of the optimal transfection conditions, both PC-3 and TM4 cell lines were transiently transfected with the pMCT4-mCherry plasmid and submitted to four different glucose treatments (in mM: 0, 2, 5.5 and 20).

MCT4 is a transmembrane protein (Halestrap & Meredith, 2004), therefore, to study its subcellular trafficking and possible internalization, we used β-catenin, that is expressed at the PM (Ozawa et al., 1989), as a PM marker.

In the absence of glucose (0 mM) and in the presence of 2 mM glucose there was an increase of the MCT4-mCherry fluorescent signal in the cytoplasm of PC-3 cells when comparing to the other 5.5 and 20 mM treatments, (arrowheads in Figure 10 Panel A). Whereas in the presence of 5.5 and 20 mM of glucose MCT4 co-localizes with β-catenin in the PM (Figure 10 Panel A). On the other hand, treatments with distinct glucose concentrations in TM4 cell line did not affect MCT4 localization at the PM (Figure 10 Panel B).

(A)

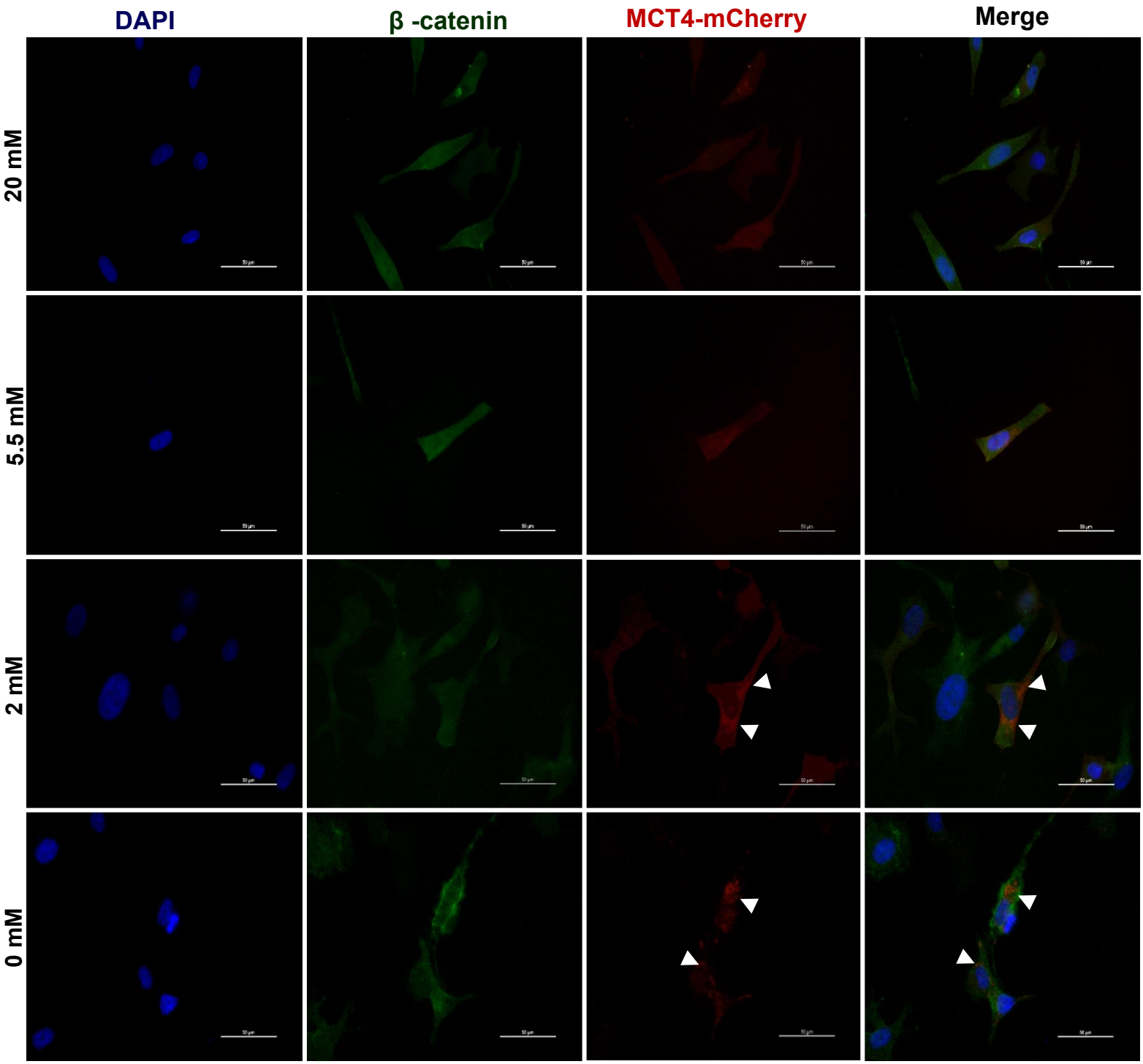

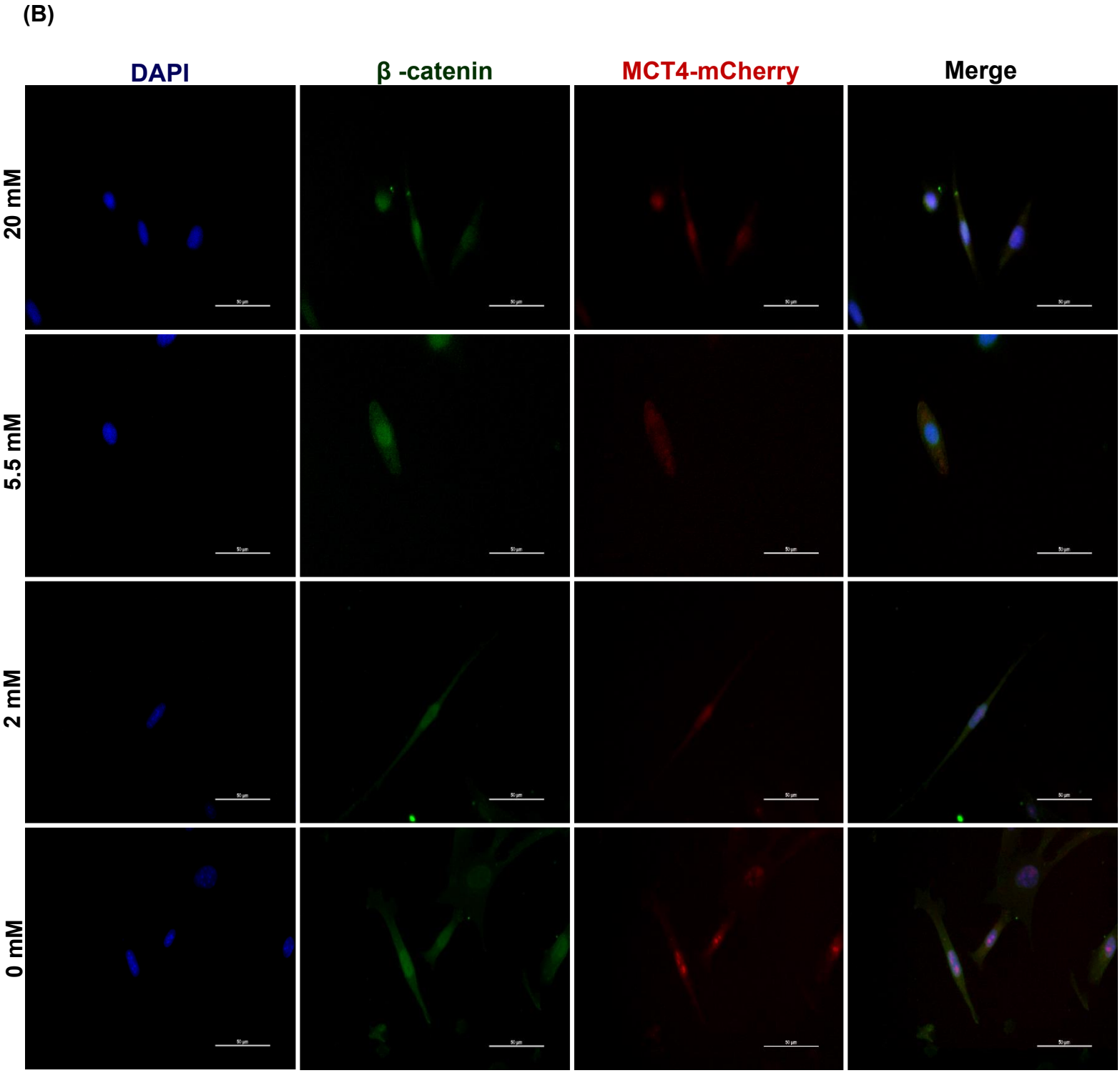

Figure 10: MCT4 cellular trafficking in response to distinct glucose concentrations in the PC-3 cell line versus the TM4 cell line. (A) Cellular localization of MCT4 in the PC-3 cell line in response to a 24 h treatment of DMEM-without glucose non-supplemented, supplemented with 2 mM, supplemented with 5.5 mM and supplemented with 20 mM of glucose. Immunostaining for β-catenin (green) and DAPI (blue) of cells transiently

transfected with the pMCT4-mCherry to determine the cellular trafficking of MCT4 (red). Arrow heads: cell with cytoplasmic localization of MCT4. (B) Cellular localization of MCT4 in the TM4 cell line in response to a 24 h treatment of DMEM-without glucose non-supplemented, supplemented with 2 mM, supplemented with 5.5 mM and supplemented with 20 mM of glucose. Immunostaining for β-catenin (green) and DAPI (blue) of cells transiently transfected with the pMCT4-mCherry to determine the cellular trafficking of MCT4 (red). Shown are representative images of 2 independent experiments.

IV.1.3. MCT4 protein expression does not alter in response to different glucose concentrations, on PC-3 and TM4 cells

After observing the differences regarding MCT4 internalization between PC-3 and TM4 cells, we analyzed the protein expression levels of MCT4 in both cell lines, by Western-blot. The protein levels of MCT4 were not significantly different in the PC-3 cell line upon glucose treatments when compared with the group of the physiological concentration – 5.5 mM of glucose – nor the unphosphorylated protein, the phosphorylated protein, and the total MCT4 protein expression (Figure 11 Panel B, C, and D). These results were normalized to the total transferred protein present in the previously activated polyvinylidene difluoride membranes (see Appendix D Figure 42), read with the Bio-Rad ChemiDoc XR, and calculated using the Image Lab Software.

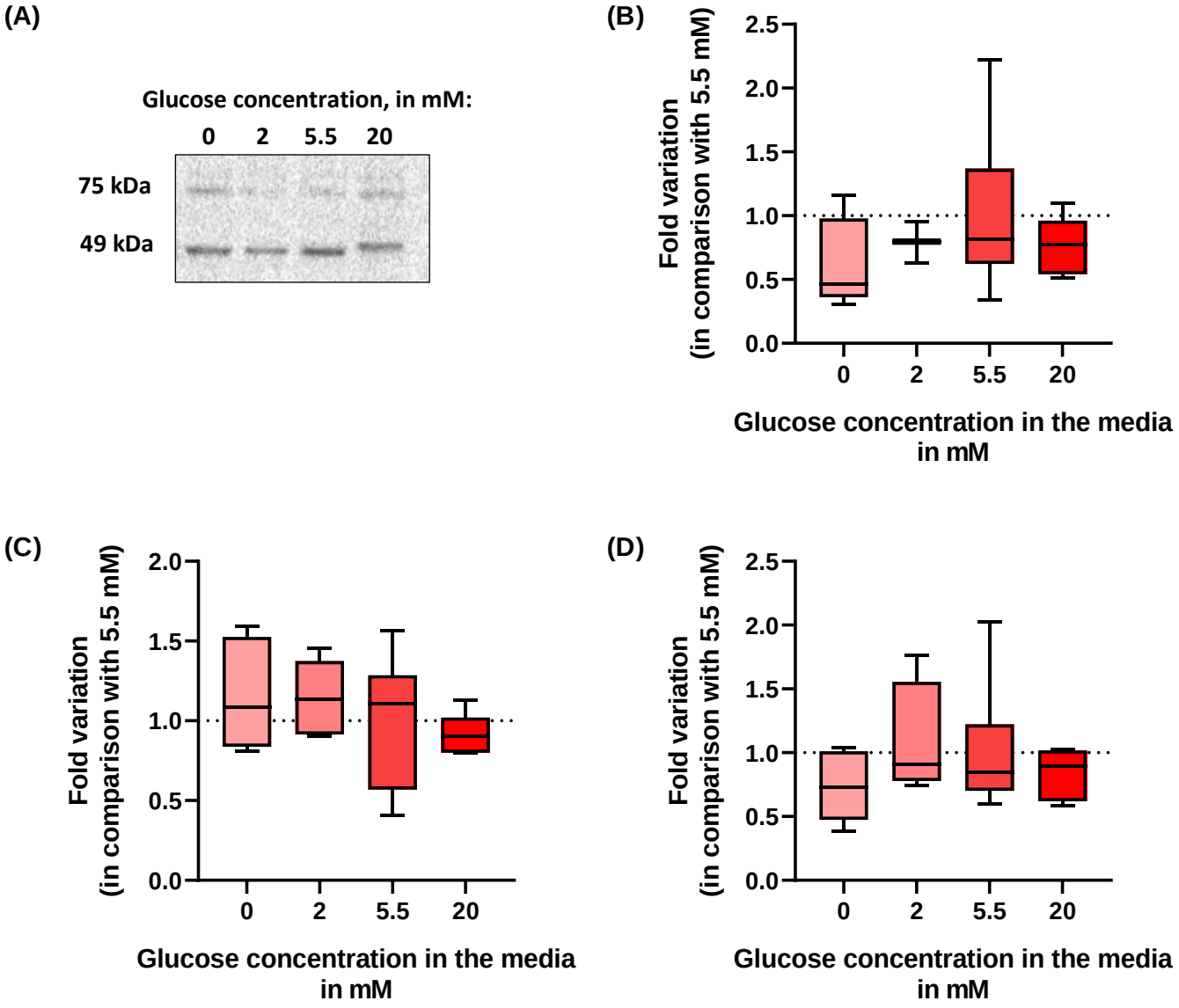

Figure 11: Effect of increasing glucose concentrations in the media on MCT4 protein levels in PC-3 cells. Panel A shows a representative western-blot experiment. Panels B, C and D show pooled data of independent experiments. Panel B indicates the fold variation of the 49 kDa unphosphorylated MCT4 protein levels found in PC-3 cells when compared to the 5.5 mM group treatment (physiological level). Panel C indicates the fold variation of the 75 kDa phosphorylated MCT4 protein levels found in PC-3 cells when compared to the 5.5 mM group treatment (physiological level). Panel D indicates the fold variation of the total MCT4 protein levels found in PC-3 cells when compared to the 5.5 mM group treatment (physiological level). The results are presented as Tukey's whisker boxes (median, 25^{th} to 75^{th} percentiles ± 5^{th} to 95^{th} percentile values) (n=6).

Likewise, in the TM4 cell line, there were no statistical differences detected for the protein levels of MCT4 upon the glucose treatments when compared with the group of the physiological concentration – 5.5 mM of glucose – nor the unphosphorylated protein, the phosphorylated protein, and the total MCT4 protein expression (Figure 12 Panel B, C, and D).

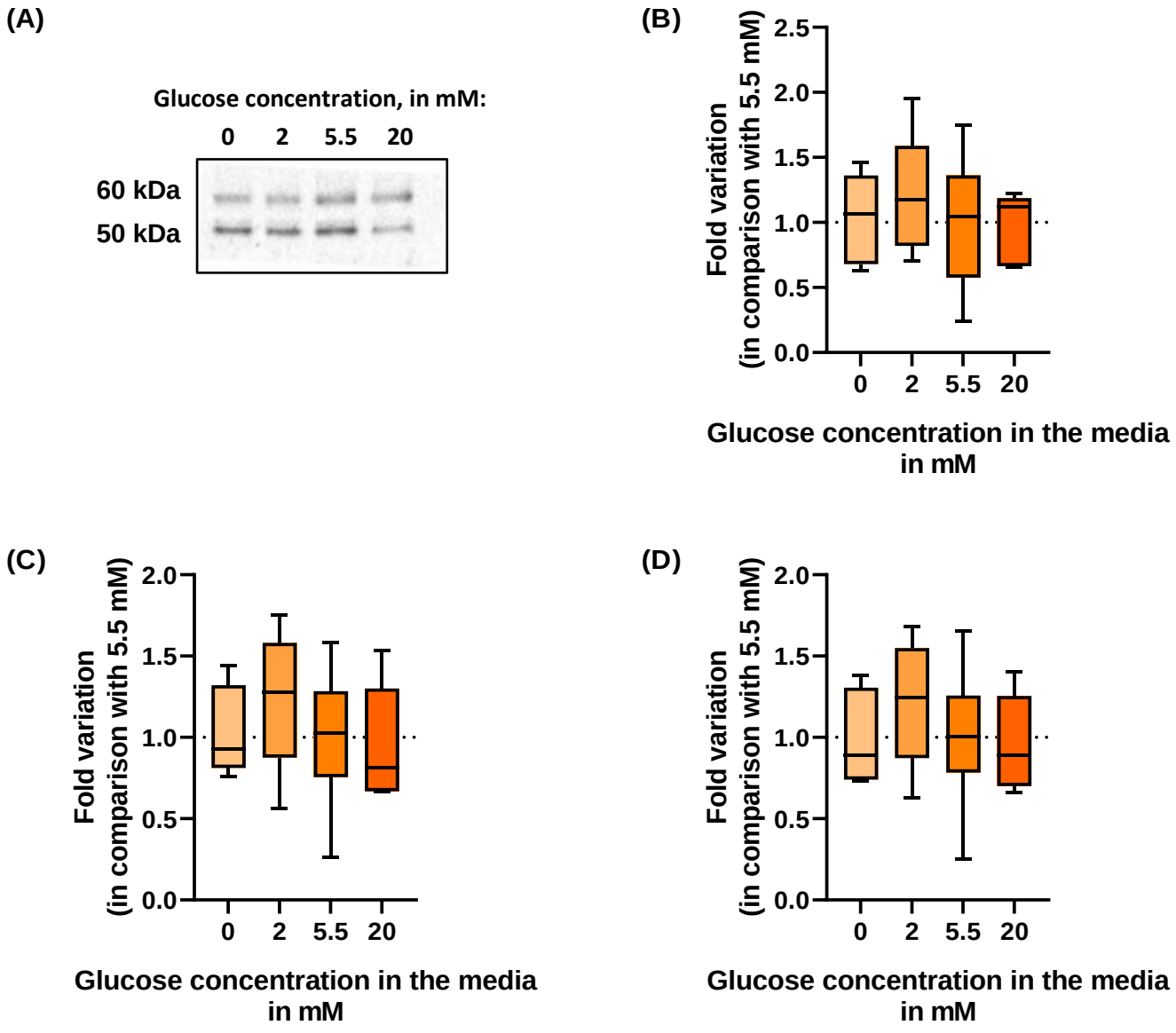

Figure 12: Effect of increasing glucose concentrations in the media on MCT4 protein levels in TM4 cells. Panel A shows a representative western-blot experiment. Panels B, C and D show pooled data of independent experiments (n=6). Panel B indicates the fold variation of the 50 kDa unphosphorylated MCT4 protein levels found in TM4 cells when compared to the 5.5 mM group treatment (physiological level). Panel C indicates the fold variation of the 60 kDa phosphorylated MCT4 protein levels found in TM4 cells when compared to the 5.5 mM group treatment (physiological level). Panel D indicates the fold variation of the total MCT4 protein levels found in

TM4 cells when compared to the 5.5 mM group treatment (physiological level). The results are presented as Tukey's whisker boxes (median, 25th to 75th percentiles ± 5th to 95th percentile values) (n=6).

Finally, total MCT4 protein expression levels in response to the glucose treatments were compared, between the PC-3 and TM4 cell lines (Figure 13). However, there was any significant statistically difference found.

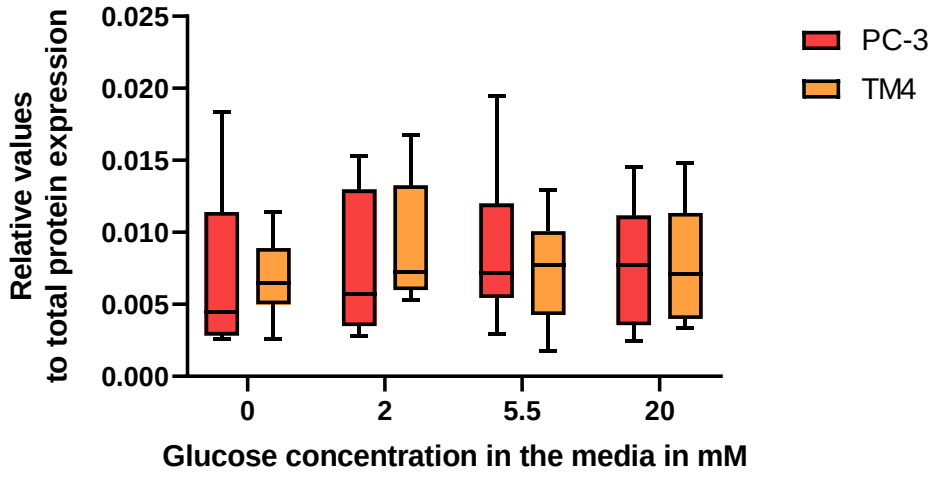

Figure 13: Comparison of the effects of increasing glucose concentrations in the media on MCT4 protein levels in PC-3 versus TM4 cells. The results are presented as Tukey's whisker boxes (median, 25th to 75th percentiles ± 5th to 95th percentile values) (n=6).

IV.1.4. Glucose consumption and lactate export are augmented in response to increasing glucose concentrations, whereas pyruvate and alanine export, and glutamine consumption levels are not significantly altered

Glucose is the main substrate for cancer cells, as well as Sertoli cells, for their main purpose of producing and exporting lactate (Oliveira et al., 2015). Therefore, to disclose the effects of the different glucose concentrations at test on the metabolism of PC-3 and TM4 cells, we performed a ^{1}H-NMR analysis, for determining glucose consumption, lactate, pyruvate, and alanine production, and glutamine consumption.

As we can see in Figure 14 Panel A, regarding glucose consumption of PC-3 cells, there were significant differences detected when comparing the treatments of 0 mM (0 ± 0 nmol/10^{6} cells) and 2 mM (2.653 ± 0.4435 nmol/10^{6} cells) with both 5.5 mM (7.472 ± 1.442 nmol/10^{6} cells) and 20 mM

(10.70 ± 1.225 nmol/10^6 cells). TM4 cells showed significant statistical differences between the 20 mM treatment (6.759 ± 1.523 nmol/10^6 cells) and the 0 mM treatment (0 ± 0 nmol/10^6 cells), as well as 2 mM (0.8143 ± 0.2850 nmol/10^6 cells) and 5.5 mM (2.002 ± 0.1080 nmol/10^6 cells). The comparison of glucose consumption between the two cell lines, revealed a significant increase in TM4 cells relatively to PC-3 cells, both in the 5.5 mM (2.002 ± 0.1080 and 7.472 ± 1.442, respectively, in nmol/10^6 cells) and the 20 mM (6.759 ± 1.523 and 10.70 ± 1.225, respectively, in nmol/10^6 cells) treatments.

Regarding lactate production (see Figure 14 Panel B), it is null in the treatment without glucose in both cell lines. However, the treatment of 20 mM (6.759 ± 1.523 nmol/10^6 cells) of glucose in the TM4 cell line originated significant increases in lactate production when comparing to 0 mM, 2 mM and 5.5 mM treatments (0 ± 0, 0.8143 ± 0.2850 and 2.002 ± 0.1080, respectively, in nmol/10^6 cells), which was also detected regarding the 20 mM (10.70 ± 1.225 nmol/10^6 cells) treatment in the PC-3 cell line (0 ± 0, 2.653 ± 0.4435 and 7.472 ± 1.442, respectively to each treatment, in nmol/10^6 cells). There was also reported a significant increase in lactate production in PC-3 cells when comparing the 5.5 mM treatment (7.472 ± 1.442 nmol/10^6 cells) with 0 mM and 2 mM (0 ± 0 and 2.653 ± 0.4435, respectively, in nmol/10^6 cells), as well as when comparing the 2 mM treatment (2.653 ± 0.4435 nmol/10^6 cells) with the non-glucose treatment (0 ± 0 nmol/10^6 cells). Furthermore, there is a significant difference between the PC-3 and the TM4 cell line, in both 5.5 mM (7.472 ± 1.442 and 2.002 ± 0.1080, respectively, in nmol/10^6 cells) and 20 mM treatments (10.70 ± 1.225 and 6.759 ± 1.523, respectively, in nmol/10^6 cells).

Pyruvate and alanine production did not display significant differences between the two cell lines, in every glucose treatment (Figure 14 Panel C and D). However, the TM4 cell line exhibited statistically different values for pyruvate production in the treatment of 5.5 mM (0.4604 ± 0.08018 nmol/10^6 cells) and 20 mM (0.4752 ± 0.1085 nmol/10^6 cells), when compared to the non-glucose treatment (0.05196 ± 0.03745 nmol/10^6 cells). Regarding alanine production, only the treatments of 0 mM (0.4053 ± 0.09650 nmol/10^6 cells) and 5.5 mM (1.061 ± 0.1941 nmol/10^6 cells) in the PC-3 cell line displayed significant differences.

At last, glutamine consumption did not exhibit statistically different results in any comparison made (Figure 14 Panel E). Furthermore, acetate export was only assessed for TM4 cells, since it was not quantifiable for PC-3 cells, and did not report significant statistical differences (Appendix E Figure 43).

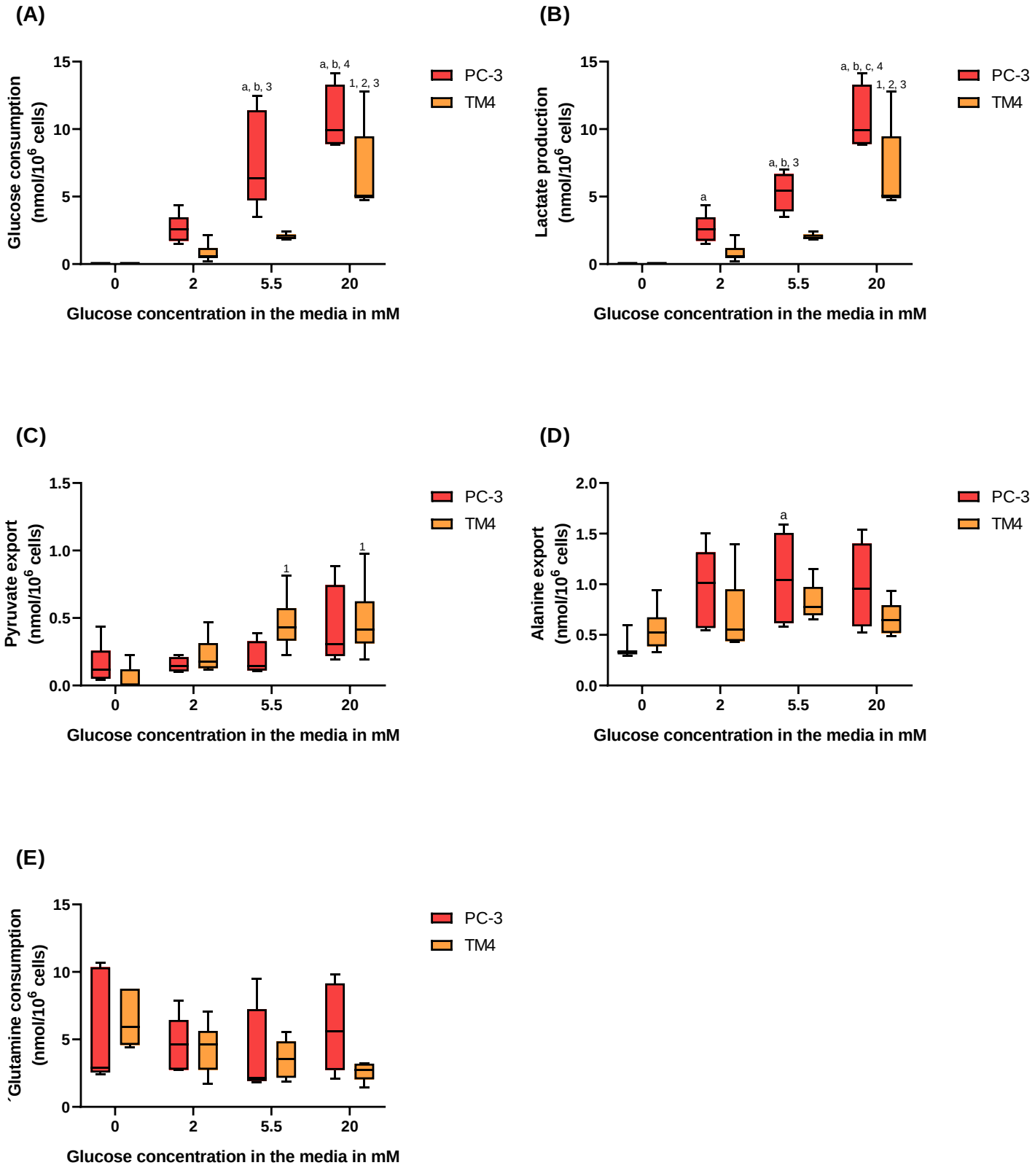

Figure 14: Measurement of glucose (A), lactate (B), pyruvate (C), alanine (D), and glutamine (E) concentrations in the extracellular medium after a 24 h of treatment with distinct glucose concentrations in TM4

and PC-3 cells. These graphics represent the consumption or export of the mentioned metabolites found in the media after a 24 h treatment with DMEM-without glucose, non-supplemented, supplemented with 2 mM of glucose, 5.5 mM of glucose and 20 mM of glucose (n=6). The results are presented as Tukey's whisker boxes (median, 25^{th} to 75^{th} percentiles ± 5^{th} to 95^{th} percentile values). The significantly different results ($p < 0.05$) are indicated as (a) relative to 0 mM group in PC-3; (b) relative to 2 mM group in PC-3; (c) relative to 5.5 mM group in PC-3 cells; (d) relative to 20 mM group in PC-3 cells; (1) relative to 0 mM group in TM4 cells; (2) relative to 2 mM group in TM4 cells; (3) relative to 5.5 mM group in TM4 cells; (4) relative to 20 mM group in TM4 cells.

IV.2. Design and construction of fluorescent tagged human CTRs

IV.2.1. Construction of pCTR1-mCherry and pmCherry-CTR1

Firstly, to generate the pCTR1-mCherry and pmCherry-CTR1 constructs, the sequence of *hCTR1* gene was amplified from pEYFP-CTR1. The *hCTR1* (573 bp) gene was amplified from pEYFP-CTR1 with primers FW_CTR1 and RV_CTR1_mCherry, or with FW_CTR1 and RV_mCherry_CTR1, for the insertion in pmCherry-N1 and pmCherry-C1, respectively. The size of the PCR products was analyzed by DNA gel electrophoresis, and images were acquired using a UV transilluminator (VWR) (Figure 15 and Figure 16). After confirmation of the size of the PCR products, both inserts and vectors were digested with *Bgl*II and *Hind*III and subsequently ligated. The plasmid generated by ligation was transformed in competent *E. coli* XL1 Blue competent cells were transformed with the resulting construct and plated in of LB medium with kanamycin 50 μg/mL. The cloning strategy followed is schematized in Figure 17.

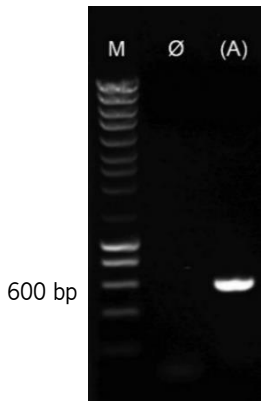

Figure 15: DNA agarose gel of the amplified *hCTR1* fragment obtained by PCR amplification from pEYFP-CTR1, using specific primers to clone in pmCherry-N1. "M" lane: molecular weight marker (NZYDNA Ladder III).

"Ø" lane: negative control (PCR reaction without template). (A) lane: *hCTR1* gene amplified (573 bp + 16 bp from primers) from pEYFP-CTR1, using primers FW_CTR1 and RV_CTR1_mCherry, specific for cloning in pmCherry-N1.

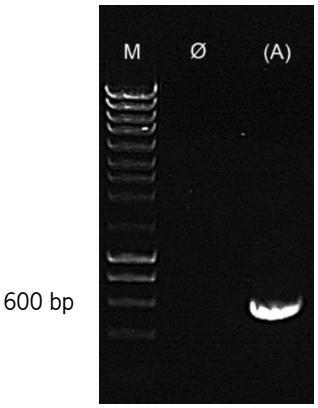

Figure 16: DNA agarose gel of the amplified hCTR1 fragment obtained by PCR amplification from pEYFP-CTR1, using specific primers to clone in pmCherry-C1. "M" lane: molecular weight marker (NZYDNA Ladder III). "Ø" lane: negative control (PCR reaction without template). (A) lane: *hCTR1* gene amplified (573 bp + 16 bp from primers) from pEYFP-CTR1, using primers FW_CTR1 and RV_mCherry_CTR1, specific for cloning in pmCherry-C1.

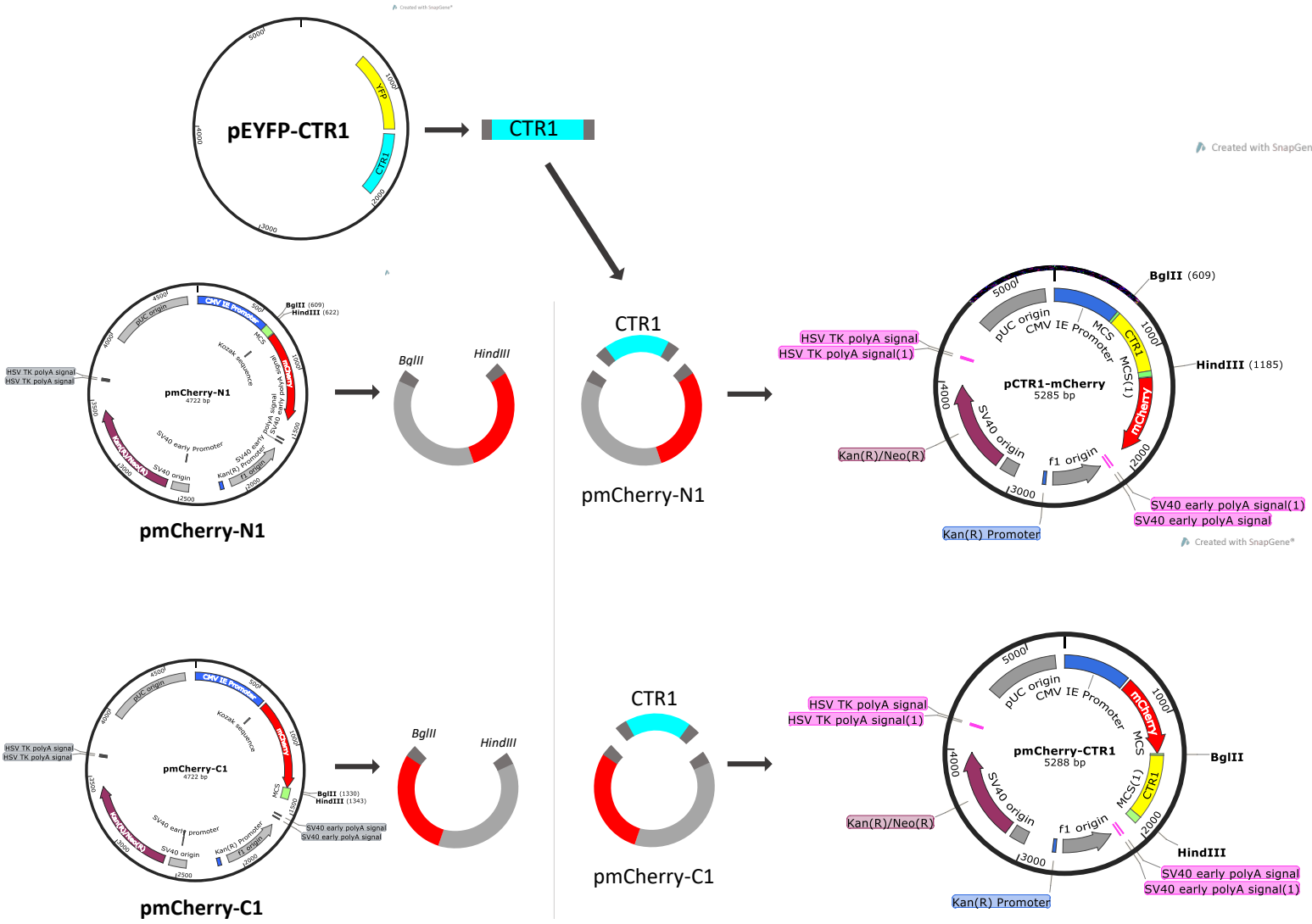

Figure 17: Schematic representation of the cloning strategy followed for the construction of the pCTR1-mCherry and pmCherry-CTR1. CTR1 was amplified from pEYFP-CTR1, and digested, as pmCherry-N1 and pmCherry-C1, with *Bgl*II and *Hind*III. pmCherry-N1 or pmCherry-C1 were ligated with CTR1, giving rise to pCTR1-mCherry or pmCherry-CTR1, respectively. CTR1: Copper transporter 1.

To confirm that the grown colonies were positive transformants, containing the desired plasmid constructions, a PCR colony was performed, through the amplification of *hCTR1* (573 bp). As seen in Figure 18, fourteen possible positive transformants of pCTR1-mCherry were tested, and only three tested positive for the presence of *hCTR1* (Cl 2, 9 and 12).

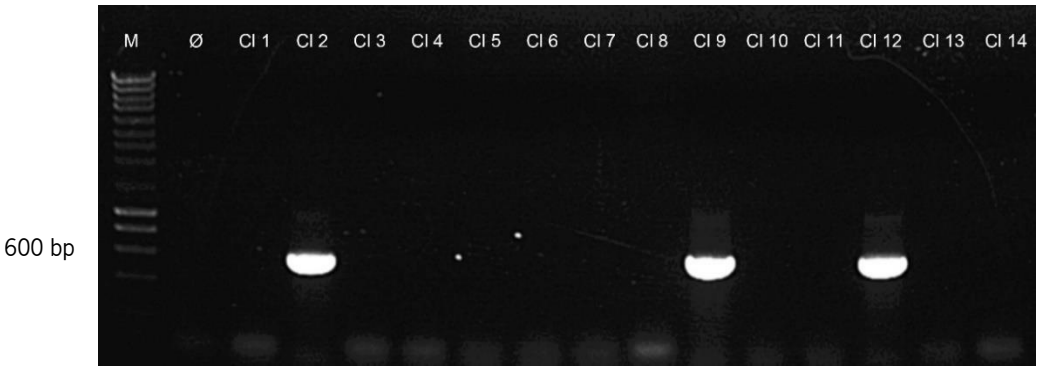

Figure 18: DNA agarose gel of the amplified *hCTR1* fragment obtained by PCR colony from pCTR1-mCherry. "M" lane: molecular weight marker (NZYDNA Ladder III). "Ø" lane: negative control (PCR reaction without template). Lanes Cl 1 to Cl 14: *hCTR1* amplification (573 bp + 16 bp from primers) using primers FW_CTR1 and RV_CTR1_mCherry. With this methodology, it came to conclusion that the positive transformants with pCTR1-mCherry were Cl 2, Cl 9 and Cl 12. Cl: clone.

For the pmCherry-CTR1 construction also fourteen potentially positive transformants were tested by colony PCR, from which thirteen of tested positive by *hCTR1* (573 bp) amplification (Cl 1, 2, 4, 5, 6, 7, 8, 9, 10, 11, 12, 13 and 14) (Figure 19).

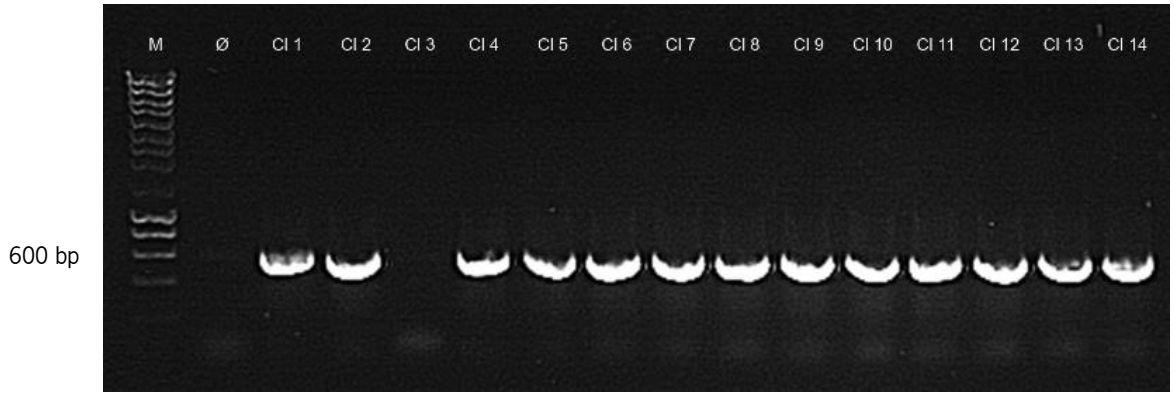

Figure 19: DNA agarose gel of the amplified *hCTR1* fragment obtained by PCR colony from pmCherry-CTR1. "M" lane: molecular weight marker (NZYDNA Ladder III). "Ø" lane: negative control (PCR reaction without template). Lanes Cl 1 to Cl 14: *hCTR1* amplification (573 bp + 16 bp from primers) using primers FW_CTR1 and RV_mCherry_CTR1. With this methodology, it came to conclusion that the positive transformants with pmCherry-CTR1 were Cl 1, Cl 2, Cl 4, Cl 5, Cl 6, Cl 7, Cl 8, Cl 9, Cl 10, Cl 11, Cl 12, Cl 13 and Cl 14. Cl: clone.

For further confirmation of the effectiveness of the cloning strategy, 1 or 2 positive colonies were selected, and their plasmid extracted. Finally, a confirmation PCR was performed, using specific primers to amplify *hCTR1* (573 bp) and the PCR products analyzed by DNA gel electrophoresis. All of the tested clones were positive for the respective construction (Figure 20 and Figure 21).

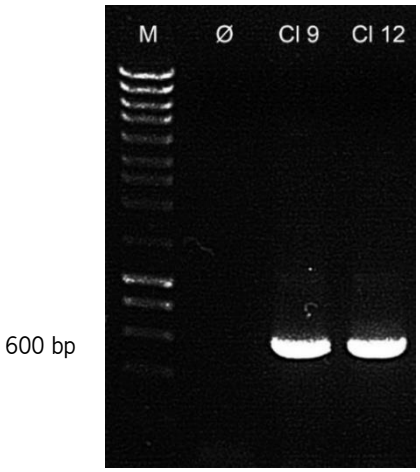

Figure 20: DNA agarose gel of the amplified *hCTR1* gene obtained by a confirmation PCR, from the pCTR1-mCherry extracted from positive transformants. "M" lane: molecular weight marker (NZYDNA Ladder III). "Ø" lane: negative control (PCR reaction without template). Lanes Cl 9 and Cl 12: *hCTR1* amplification (573 bp + 16 bp from primers) using primers FW_CTR1 and RV_CTR1_mCherry. Cl: clone. With this methodology, it came to conclusion that clones 9 and 12 are effectively positive transformants.

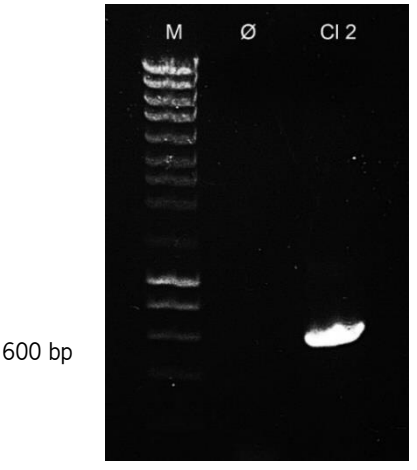

Figure 21: DNA agarose gel of the amplified *hCTR1* gene obtained by a confirmation PCR, from the pmCherry-CTR1 extracted from positive transformants. "M" lane: molecular weight marker (NZYDNA Ladder III). "Ø" lane: negative control (PCR reaction without template). Lane 2: *hCTR1* amplification (573 bp + 16 bp from

primers) using primers FW_CTR1 and RV_mCherry_CTR1. Cl: clone. With this methodology, it came to conclusion that colony Cl 2 is effectively a positive transformant.

After obtaining these positive results, one clone was selected for plasmid extraction and the DNA sent for sequencing confirmation. Successfully, pCTR1-mCherry and pmCherry-CTR1 sequences were confirmed.

IV.2.2. Construction of pCTR2-mCherry, pCTR2-AcGFP and pAcGFP-CTR2

Firstly, to develop the constructs pCTR2-mCherry, pCTR2-AcGFP and pAcGFP-CTR2, the sequence of *hCTR2* gene was amplified from pEYFP-CTR2. The *hCTR2* (432 bp) gene was amplified from pEYFP-CTR2 with primers FW_CTR2 and RV_CTR2_mCherry/AcGFP for the insertion in pmCherry-N1 and pAcGFP-N1. Whereas for the insertion in pAcGFP-C1, *hCTR2* (432 bp) gene was amplified from pEYFP-CTR2 using the primers FW_CTR2 and RV_AcGFP_CTR2. The size of the PCR products was analyzed by DNA gel electrophoresis, and images acquired using an UV transilluminator (VWR) (Figure 22). After confirmation of the size of the PCR products, both inserts and vectors were digested with *Bgl*II and *Hind*III and subsequently ligated. The plasmid generated by ligation was transformed in competent *E. coli* XL1 Blue competent cells with the resulting construct and plated in LB medium with kanamycin 50 μg/mL. The cloning strategy followed is schematized in Figure 23.

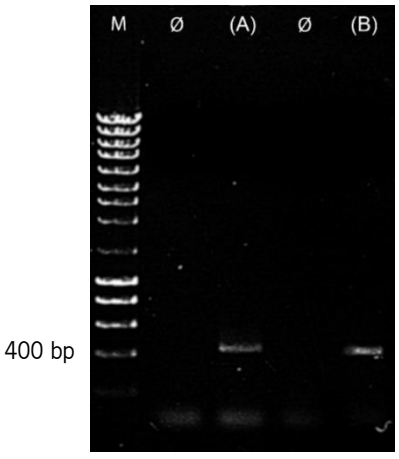

Figure 22: DNA agarose gel of the amplified *hCTR2* fragment obtained by PCR amplification from pEYFP-CTR2, using specific primers to clone in pmCherry-N1, pAcGFP-N1 or pmCherry-C1. "M" lane: molecular weight marker (NZYDNA Ladder III). "Ø" lanes: negative controls for the respective PCR reaction relative to the lane on

the right (PCR reaction without template). (A) lane: *hCTR2* gene amplified (432 bp + 16 bp from primers) from pEYFP-CTR2, using primers FW_CTR2 and RV_CTR2_mCherry/AcGFP, specific for cloning in pmCherry-N1 or pAcGFP-N1. (B) lane: *hCTR2* amplified (432 bp + 16 bp from primers) from pEYFP-CTR2, using primers FW_CTR2 and RV_AcGFP_CTR2, specific for cloning in pmCherry-C1.

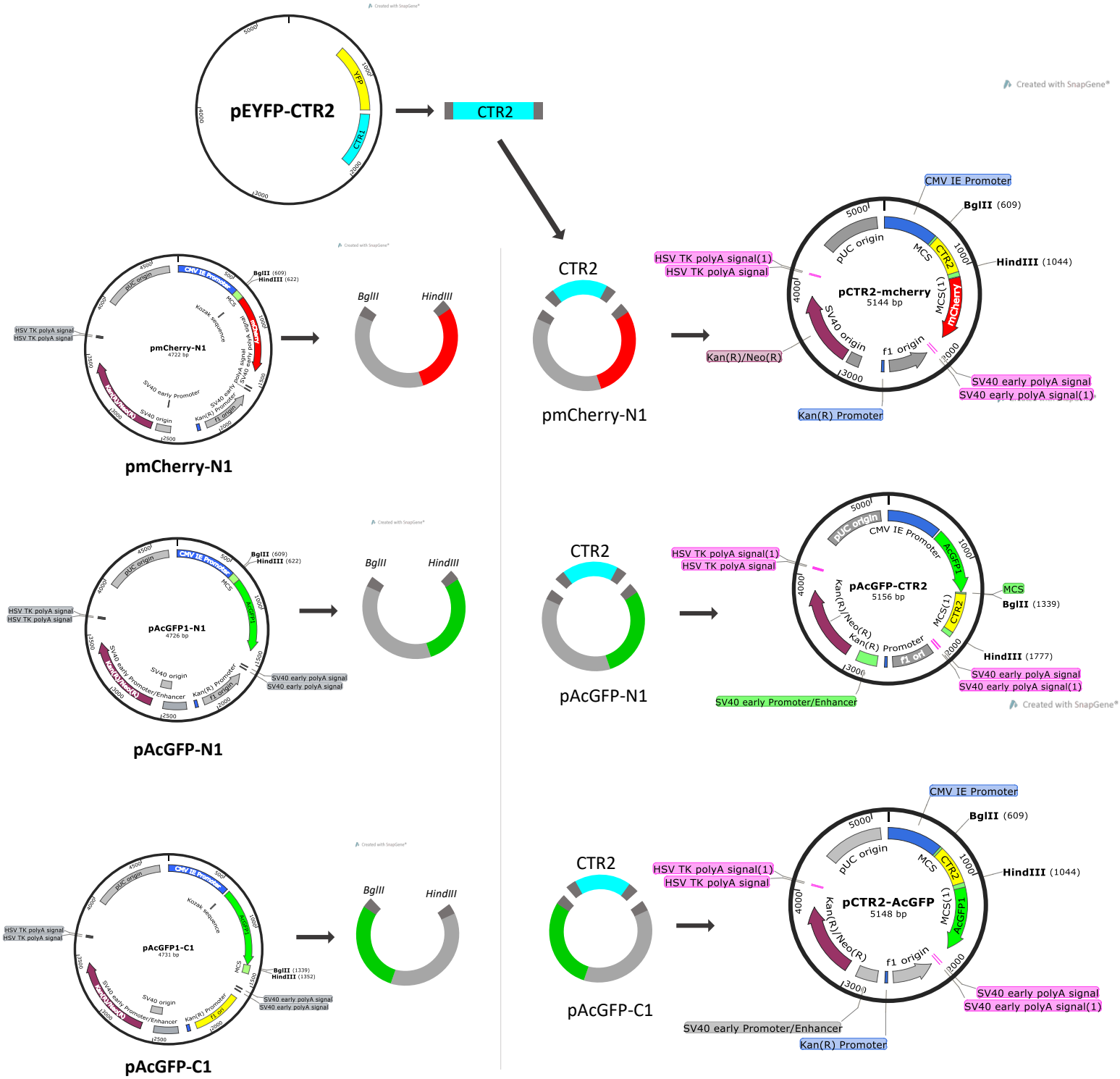

Figure 23 : Schematic representation of the cloning strategy followed for the construction of the pCTR1-mCherry and pmCherry-CTR1. CTR2 was amplified from pEYFP-CTR2, and digested, as pmCherry-N1, pAcGFP-N1

and pAcGFP-C1, with *Bgl*II and *Hind*III. pmCherry-N1, pAcGFP-N1 and pAcGFP-C1 were ligated with CTR2, giving rise to pCTR2-mCherry, pCTR2-AcGFP or pAcGFP-CTR2, respectively. CTR2: Copper transporter 2.

As seen in Figure 24, fourteen possible positive transformants of pCTR2-mCherry were tested by colony PCR, through the amplification of *hCTR2* (432 bp). Ten clones tested positive for the presence of *hCTR2* (Cl 2, 3, 5, 6, 7, 10, 11, 12, 13 and 14).

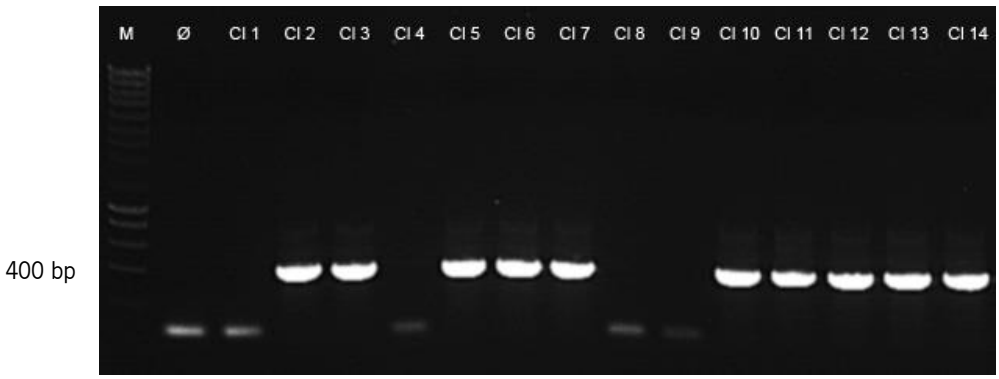

Figure 24: DNA agarose gel of the amplified *hCTR2* fragment obtained by PCR colony from pCTR2-mCherry. "M" lane: molecular weight marker (NZYDNA Ladder III). "Ø" lane: negative control (PCR reaction without template). Lanes Cl 1 to Cl 14: *hCTR2* amplification (432 bp + 16 bp from primers) using primers FW_CTR2 and RV_CTR2_mCherry/AcGFP. With this methodology, it came to conclusion that the positive transformants with pCTR2-mCherry were Cl 2, Cl 3, Cl 5, Cl 6, Cl 7, Cl 10, Cl 11, Cl 12, Cl 13 and Cl 14. Cl: clone.

For the pCTR2-AcGFP construction only four potentially positive transformants were tested by colony PCR, from which two tested positive by *hCTR2* (432 bp) amplification (Cl 1 and 4) (Figure 25).

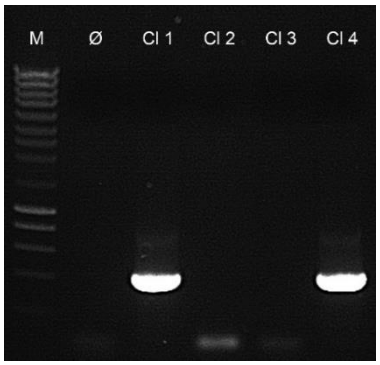

Figure 25: DNA agarose gel of the amplified *hCTR2* fragment obtained by PCR colony from pCTR2-AcGFP. "M" lane: molecular weight marker (NZYDNA Ladder III). "Ø" lane: negative control (PCR reaction without template). Lanes Cl 1 to Cl 4: *hCTR2* amplification (432 bp + 16 bp from primers) using primers FW_CTR2 and RV_CTR2_mCherry/AcGFP. With this methodology, it came to conclusion that the positive transformants with pCTR2-AcGFP were Cl 1 and Cl 4. Cl: clone.

Finally, for the pAcGFP-CTR2 construction six possible positive transformants were tested by colony PCR, and as seen in Figure 26 only clone 5 tested positive.

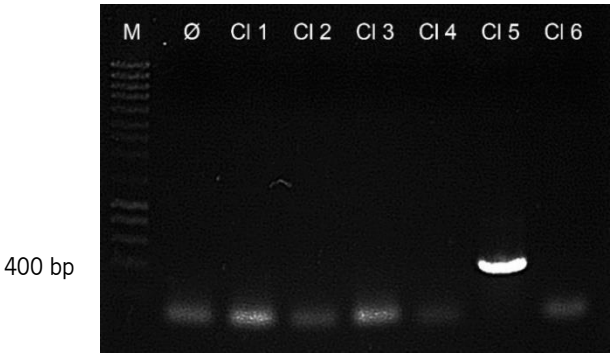

Figure 26: DNA agarose gel of the amplified *hCTR2* fragment obtained by PCR colony from pAcGFP-CTR2. "M" lane: molecular weight marker (NZYDNA Ladder III). "Ø" lane: negative control (PCR reaction without template). Lane Cl 1 to Cl 14: *hCTR2* amplification (432 bp + 16 bp from primers) using primers FW_CTR2 and RV_AcGFP_CTR2. With this methodology, it came to conclusion that the only positive transformant with pAcGFP-CTR2 was the Cl 5. Cl: clone.

For further confirmation of the effective cloning strategy, 1 or 2 positive colonies were selected, and their plasmid extracted. Finally, a confirmation PCR was performed, using specific primers to amplify

hCTR2 (432 bp) and the PCR products analyzed by DNA gel electrophoresis. All of the tested clones were positive for the respective construction (Figure 27, Figure 28 and Figure 29).

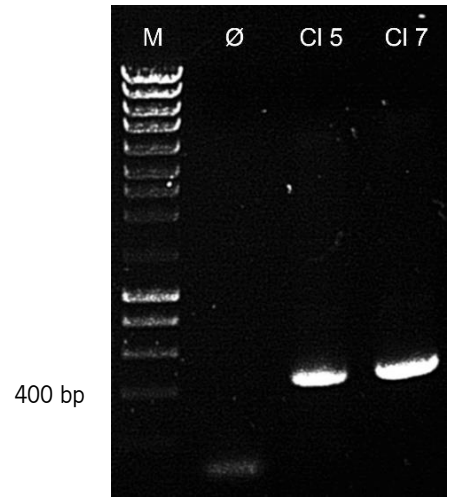

Figure 27: DNA agarose gel of the amplified *hCTR2* gene obtained by a confirmation PCR, from the pCTR2-mCherry extracted from positive transformants. "M" lane: molecular weight marker (NZYDNA Ladder III). "Ø" lane: negative control (PCR reaction without template). Lanes Cl 5 and Cl 7: *hCTR2* amplification (432 bp + 16 bp from primers) using primers FW_CTR2 and RV_CTR2_mCherry/AcGFP. With this methodology, it came to conclusion that colonies Cl 5 and Cl 7 are effectively positive transformants. Cl: clone.

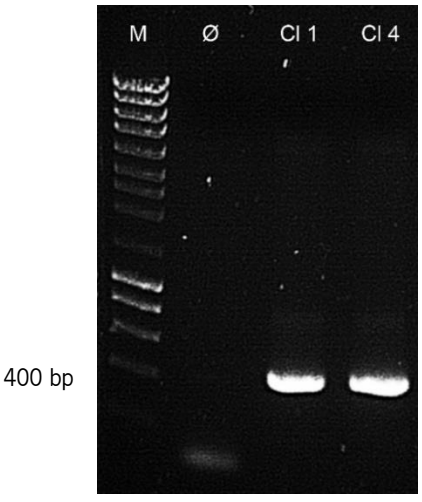

Figure 28: DNA agarose gel of the amplified *hCTR2* gene obtained by a confirmation PCR, from the pCTR2-AcGFP extracted from positive transformants. "M" lane: molecular weight marker (NZYDNA Ladder III). "Ø" lane: negative control (PCR reaction without template). Lanes Cl 1 and Cl 4: *hCTR2* amplification (432 bp + 16 bp from

primers) using primers FW_CTR2 and RV_CTR2_mCherry/AcGFP. With this methodology, it came to conclusion that colonies Cl 1 and Cl 4 are effectively positive transformants. Cl: clone.

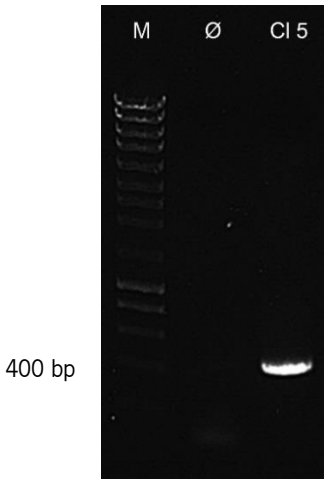

Figure 29: DNA agarose gel of the amplified *hCTR2* gene obtained by a confirmation PCR, from the pAcGFP-CTR2 extracted from positive transformants. "M" lane: molecular weight marker (NZYDNA Ladder III). "Ø" lane: negative control (PCR reaction without template). Lane Cl 5: *hCTR2* amplification (432 bp + 16 bp from primers) using primers FW_CTR2 and RV_AcGFP_CTR2. With this methodology, it came to conclusion that the colony Cl 5 is effectively a positive transformant. Cl: clone.

After obtaining these positive results, one clone was selected for plasmid extraction and the DNA sent for sequencing confirmation. Successfully, pCTR2-mCherry, pCTR2-AcGFP and pCTR2-AcGFP sequences were confirmed.

CHAPTER V

DISCUSSION AND FUTURE PERSPECTIVES

V. DISCUSSION AND FUTURE PERSPECTIVES

V.I. Intracellular Trafficking and Expression analysis of MCT4, and cellular metabolic response to glucose stimuli in the PC-3 and TM4 cell lines

The MCT4 transporter is essential both in cancer and in spermatogenesis, due to its main role in exporting monocarboxylic acids, namely lactate (Felmlee et al., 2020; San-Millán & Brooks, 2017). In this work we evaluated the expression and trafficking of MCT4 upon different metabolic conditions, particularly in response to glucose concentrations. This is a relevant study considering the lack of reports regarding MCT localization and expression upon glucose variations, both in cancer and Sertoli cells. Based on data from the World Health Organization, the selected concentrations were 0 mM and 2 mM (hypoglycemic conditions), 5.5 mM (physiological concentration of glucose) and 20 mM (hyperglycemic condition – diabetes indicator) (World Health Organization, 2021).

Initially, we transfected TM4 and PC-3 cell lines with the plasmid pMCT4-mCherry to analyze by direct fluorescence the expression and cellular localization of MCT4. It is important to notice that the encoded gene is the human MCT4 and that TM4 is a mouse cell line. However, MCT4 is still expressed in these conditions since the vector used was pmCherry-N1, which is a mammalian expression vector, containing the CMV IE Promoter (cytomegalovirus immediate early promoter). Other studies revealed the possibility of studying human genes and proteins in mouse cells (Kulesh & Oshima, 1988; Reardon et al., 1986), and even the "humanisation" of the mouse genome is being explored, through targeted replacement of mouse genomic regions with orthologous human sequences (Zhu et al., 2019). These studies reinforce the viability and scientific strength of our study.

Firstly, the optimal transfection conditions were determined (see section IV.1.1.), and the transfection was carried out as described in section III.3. Since the medium values for highest transfection efficiency are of only 33.93 ± 3.580 %, it would have been of interest to perform Fluorescence-activated Cell Sorting (FACS), so that we could have obtained a more homogeneous pool of transfected cells for the following experiences, even with a short work window, considering it is a transient transfection. We tested the possibility to select transfected cells with a blocker of polypeptide synthesis - G418 (geneticin) - as the expression vector used, pmCherry-N1, contained a neomycin resistance gene from Tn5, which encodes for aminoglycoside-3'-phosphotransferase, and provides transfected cells resistance to this antibiotic. Either the higher concentrations of geneticin led to the total death of cells (transfected and not

transfected), or although there was a good selection, the transfected cells were not able to proliferate. The selected cells were few and too far apart in the culture well, which does not promote cell proliferation in a timely manner that allowed for the maintenance of the plasmid, since it is transiently transfected instead of incorporated into the genome. Therefore, the plasmid is lost before transfected cells could grow enough to endure the treatments that would follow. The alternative protocol using FACS would allow a quicker establishment of a larger homogenous pool of transfected cells and perhaps would give the possibility for a wider net of treatments at test.

The results obtained in PC-3 cells are in accordance with what was expected since in physiological or hyperglycemic glucose concentrations, in highly glycolytic cells, the glycolytic metabolism would be maintain or enhanced, respectively, leading to higher lactate production and export rates. Therefore, MCT4 localization in the PM would be fundamental to export the produced lactate. Low concentrations of glucose, or even none, would lead to a decrease in the produced lactate levels, and consequently, MCT4 would no longer be as much necessary at the PM as in physiological glucose concentration, as observed in the PC-3 cell line. However, it does not happen in Sertoli cells, demonstrating to have the same localization in the PM in every glucose treatment performed, possibly due to its primordial function of providing nutritional support – lactate – to developing germ cells (Oliveira et al., 2015). Furthermore, Sertoli cells do not display the plasticity known to cancer cells when facing variable conditions. Although we can see internalization of MCT4, it remains unclear if it enters the endocytic pathway for delivery to lysosomes for degradation, or if it is internalized for later recycling to the PM. Therefore, it would be of interest to analyze through co-localization with a lysosomal marker, as LAMP-1 (Alessandrini et al., 2017), or even using a compound that would inhibit this recycling process, as monensin, that inhibits the transport of macromolecules from the Golgi complex to the PM (Fan et al., 2016). In a study conducted by Li et al., 2020, for the trafficking study of GLUT1, a tandem fluorescent tracing system was implemented in live cells, through the use of a plasmid that translates in a protein with both mCherry and EGFP fluorescence (Z. Y. Li et al., 2020). Their findings were based on the difference in pH resistance of mCherry (is resistance to acidic pH) and EGFP (is quenched by acidic pH), altogether with endosomal and lysosomal markers. Giving that in early endosomes pH values are of 6.8-6.1 and in late endosomes they range from 6.0-4.8, a difference in red and green (Z. Y. Li et al., 2020) fluorescence (yellow though overlapping) provides reliable intel on transporter trafficking. Hence, it would be at interest to develop a similar plasmid for MCT4, with both mCherry and GFP, for a more detailed study of its PM and endolysosomal trafficking system.

We confirmed MCT4 expression in the non-transfected PC-3 and TM4 cell lines, and came to conclusion that MCT4 protein expression is not significantly altered, in both cell lines, in response to all the glucose stimuli. Since pMCT4-mCherry is composed of a constitutive promoter – CMV promoter – MCT4 gene transcription is not regulated by its own promoter. Therefore, an expression study at the transcriptional level, through real-time qPCR (quantitative PCR), would allow us to better understand the fool dynamic of MCT4 in response to glucose levels, in both cancer and Sertoli cells.

Altogether, since PC-3 showed internalization of MCT4 in response to a hypoglycemic condition, it was expected that there would be a significantly higher export of lactate in TM4 cells relatively to PC-3 cells. Nevertheless, we verify that it does not occur. As expected, the stimuli of increased glucose concentrations led also to increase lactate export levels, in both cell lines. Interestingly, PC-3 cells consume significantly more glucose than TM4 cells in response to the same treatments, and a consequent significantly higher lactate efflux. These results suggest that there might be an important player in the PC-3 cell line involved in lactate export, to overcome the effects of MCT4's internalization in lactate export. The monocarboxylate transporter 1 – MCT1 – might be the protein in action, being already described as a main exporter of lactate in cancer cells (reviewed in C. Pinheiro et al., 2012). Therefore, it would be important to ascertain the protein expression profile of MCT1 in response to the glucose stimuli described above, as well as to evaluate its intracellular trafficking in response to the same stimuli. Moreover, the development of a plasmid containing MCT1 fused with GFP would give the possibility for a co-transfection study with pMCT4-mCherry. This would allow for the simultaneous assessment of cellular trafficking of MCT1 and MCT4, in order to better understand their dynamics in both cell types, especially in the PC-3 cell line. Nevertheless, MCT4 is not entirely internalized, and the remaining protein localized in the PM may be sufficient to maintain lactate export in the hypoglycemic treatment. Moreover, higher lactate export and glucose consumption levels in the PC-3 cell line indicate that this cell line has a faster glucose metabolism, leading them to produce more lactate than TM4. Even though MCT4 protein expression is not increased, its activity might be, supporting the continuous and increased efflux of lactate from PC-3 cells.

To notice, one molecule of glucose can give origin to two molecules of pyruvate, which through the activity of lactate dehydrogenase are converted into two molecules of lactate (Odet et al., 2008). However, if quantitatively analyzed, the ratio of glucose consumption and lactate export is 1:1, indicating that 3 carbons are being lost from the glycolytic pathway, in the metabolism of both TM4 and PC-3 cells. Cancer cells rely on glycolysis as its main metabolic pathway, however, there is emerging evidence of tumor

heterogeneity. In this case, some cells use the excess lactate produced as fuel for mitochondrial oxidative phosphorylation (Sonveaux et al., 2008; Vander Heiden et al., 2009). Once again, an analysis via the Seahorse Analyzer would allow for an advance and detailed study of ATP production in cancer cells. With this information, we could unveil if the remaining carbons are entering the TCA cycle, augmenting ATP production or if they are just supporting cell growth and proliferation. Furthermore, we would be able to analyze the effects of glucose in these metabolic pathways.

Upon the results obtained in this work, it is crucial to further disclose the molecular mechanisms involved in the MCT4 internalization from the PM, as well as analyze MCT4 expression at the transcriptional level, and how its modulation affects both cancer and Sertoli cells' metabolism.

V.II. Biomolecular tools for future studies of hCTR1 and hCTR2 expression and intracellular trafficking

The roles of copper in cells' function and homeostasis have long been known, ranging from acting as a fundamental co-factor for several enzymes (McCord & Fridovich, 1969; Vander Wende & Wainio, 1960), to its involvement in hemoglobin formation, carbohydrate metabolism, or even in the antioxidant defense mechanism (Iakovidis et al., 2011). This essential metal ion has been linked to pathological phenotypes and their development and aggressiveness, from which cancer progression is a very important example (Blockhuys & Wittung-Stafshede, 2017; Brady et al., 2014; Kagan & Li, 2003). Copper imbalance and expression dysregulation of its transporters – CTR1 and CTR2 – showed to negatively impact the primordial process of spermatogenesis (Ghaffari & Richburg, 2019; H. Guo et al., 2021), elucidating the importance of emerging anti-cancer treatments directed to CTRs.

Ishida et al., 2013, suggested that the lack of copper in the extracellular milieu may lead to increased glycolysis (Ishida et al., 2013). Using the novel biomolecular tools developed in this work, namely, pCTR1-mCherry, pmCherry-CTR1, and pAcGFP-CTR2, we can study the trafficking modulation of hCTR1 and hCTR2 in response to different copper concentrations. Considering copper's roles in both cancer progression and spermatogenesis (H. Guo et al., 2021; Gupta & Lutsenko, 2009), these studies should be conducted on the PC-3 and TM4 cell lines, or if possible in human non-immortalized Sertoli cells. Moreover, there are few studies focused on the interplay between CTRs and MCTs, both in

carcinogenesis and spermatogenesis. Therefore, the development of these biomolecular tools will allow to explore these potential relations and interactions.

Since lactate efflux and consumption are influenced by copper bioavailability, as aforementioned in section I.5., MCT4 trafficking should be evaluated simultaneously. For that, co-transfection strategy, with one of the developed plasmids encoding CTR1 and GFP, should be performed, since the available plasmid containing MCT4 results in MCT4 fused with mCherry.

Furthermore, the analysis of ATP production through a Seahorse Analyzer, with different copper levels, would be of great interest due to its vital role in mitochondrial respiration (Ishida et al., 2013). Through the use of this advanced analyzer, it would be possible to quantify the rate of ATP production from glycolysis and mitochondria simultaneously. In addition, a complete analysis integrating both glucose and copper variations would allow for proper metabolic analysis and comparison of the two distinct cell types at study. This would complement the work presented, due to the known correlation between copper and glucose metabolism (Luo et al., 2012). Altogether with an ^{1}H-NMR analysis, we could evaluate copper's influence in CTR1, MCT4 and cellular metabolism. Considering the literature, low to no copper in the medium should lead to an increase of the glycolytic pathway (Ishida et al., 2013; Luo et al., 2012; Yuk et al., 2014), an augmented production and export of lactate, together with the placement of MCT4 in the PM.

Copper homeostasis is also of great importance for further fundamental studies. It has already been demonstrated that the knockout of *CTR2* in mice increases tissue and cellular copper levels, retaining Cu in endosomal or lysosomal compartments (Öhrvik et al., 2013). Moreover, CTR2 plays a fundamental role in the biogenesis of a CTR1 truncated form, either by the recruitment of a protease or through the stabilization of this truncated form against degradation. This truncated form of CTR1 lacks the copper-binding ectodomain that confers full-length CTR1 its high-affinity for copper acquisition and has been linked to the mobilization of copper from endosomes (Öhrvik et al., 2013; Öhrvik & Thiele, 2014). However, the mobilization of copper from endosomes and lysosomes is still fairly unknown, being unclear if CTR2 and truncated CTR1 form a complex, or if they act as individual proteins. To answer that question, and use the developed plasmids in this work, it would be interesting to perform a co-localization study through a co-transfection strategy with two of the developed plasmids, for example, pCTR1-mCherry and pCTR2-AcGFP. Nevertheless, to truly understand if these molecules interact, and not just co-localize, the Fluorescence Resonance Energy Transfer (FRET) technique should be used. FRET is a powerful technique with superior temporal (nanosecond) and spatial (angstrom) resolution, used for molecular

interaction studies in living cells. This approach is distance-dependent and relies on the non-radiative energy transference from a donor fluorophore in an excited electronic state to an acceptor fluorophore through intermolecular long-range dipole-dipole interactions. As a result, the donor molecule fluorescence extinguishes and the acceptor molecule is excited (Sekar & Periasamy, 2003).

Due to its sensitive range of activity of less than 10 nm, FRET is a reliable technique to report protein interactions. In large protein complexes, labeled components might be too far for FRET reaction to take place, resulting in a false-negative result. As seen in Figure 4 (CTRs constructs in the membrane), CTRs display their N- and C- terminals on opposite sides of the membrane, therefore the chosen plasmids should have the fluorescent tag in the same terminal, to ensure the best biologically meaningful results possible.

Succinctly, the developed constructs are valuable molecular tools, essential for a deeper study of CTR1 and CTR2 expression, endocytic trafficking and interaction. Indeed, studies focused on these transporters, as well as in their interplay with MCTs in carcinogenesis versus spermatogenesis are lacking, and these newly developed constructions are valuable assets for future research.

CHAPTER VI

REFERENCES

VI. REFERENCES

Akinloye, O., Abbiyesuku, F. . M., Oguntibeju, O. O., Arowojolu, A. O., & Truter, E. J. (2011). The impact of blood and seminal plasma zinc and copper concentrations on spermogram and hormonal changes in infertile Nigerian men. *Reproductive Biology*, *11*(2), 83–98. https://doi.org/10.1016/s1642-431x(12)60047-3

Alessandrini, F., Pezzè, L., & Ciribilli, Y. (2017). LAMPs: Shedding light on cancer biology. *Seminars in Oncology*, *44*(4), 239–253. https://doi.org/10.1053/j.seminoncol.2017.10.013

Alves, M. G., Martins, A. D., Cavaco, J. E., Socorro, S., & Oliveira, P. F. (2013). Diabetes , insulin-mediated glucose metabolism and Sertoli / blood-testis barrier function. *Tissue Barriers*, *1*(2). https://doi.org/10.4161/tisb.23992

Alves, M. G., Martins, A. D., Rato, L., Moreira, P. I., Socorro, S., & Oliveira, P. F. (2013). Molecular mechanisms beyond glucose transport in diabetes-related male infertility. *BBA - Molecular Basis of Disease*, *1832*(5), 626–635. https://doi.org/10.1016/j.bbadis.2013.01.011

Aydemir, B., Kiziler, A. R., Onaran, I., Alici, B., Ozkara, H., & Akyolcu, M. C. (2006). Impact of Cu and Fe concentrations on oxidative damage in male infertility. *Biological Trace Element Research*, *112*(3), 193–203. https://doi.org/10.1385/BTER:112:3:193

Baker, A. M., Bird, D., Lang, G., Cox, T. R., & Erler, J. T. (2013). Lysyl oxidase enzymatic function increases stiffness to drive colorectal cancer progression through FAK. *Oncogene*, *32*(14), 1863–1868. https://doi.org/10.1038/onc.2012.202

Bernardino, R. L., D'Souza, W. N., Rato, L., Rothstein, J. L., Dias, T. R., Chui, D., Wannberg, S., Alves, M. G., & Oliveira, P. F. (2019). Knockout of MCT1 results in total absence of spermatozoa, sex hormones dysregulation, and morphological alterations in the testicular tissue. *Cell and Tissue Research*, *378*(2), 333–339. https://doi.org/10.1007/s00441-019-03028-4

Bertinato, J., Swist, E., Plouffe, L. J., Brooks, S. P. J., & L'Abbé, M. R. (2008). Ctr2 is partially localized to the plasma membrane and stimulates copper uptake in COS-7 cells. *Biochemical Journal*, *409*(3), 731–740. https://doi.org/10.1042/BJ20071025

Blockhuys, S., & Wittung-Stafshede, P. (2017). Roles of copper-binding proteins in breast cancer. In *International Journal of Molecular Sciences* (Vol. 18, Issue 4, pp. 1–10). https://doi.org/10.3390/ijms18040871

Boidot, R., Vegran, F., Meulle, A., Le Breton, A., Dessy, C., Sonveaux, P., Lizard-Nacol, S., & Feron, O. (2012). Regulation of monocarboxylate transporter MCT1 expression by p53 mediates inward and outward lactate fluxes in tumors. *Cancer Research*, *72*(4), 939–948. https://doi.org/10.1158/0008-5472.CAN-11-2474

Bonen, A. (2001). The expression of lactate transporters (MCT1 and MCT4) in heart and muscle. *European Journal of Applied Physiology*, *86*(1), 6–11. https://doi.org/10.1007/s004210100516

Boussouar, F., & Benahmed, M. (2004). Lactate and energy metabolism in male germ cells. *Trends in Endocrinology and Metabolism*, *15*(7), 345–350. https://doi.org/10.1016/j.tem.2004.07.003

Brady, D., Crowe, M., Turski, M., Hobbs, A., Yao, X., Chaikuad, A., Knapp, S., Xiao, K., Campbell, S., Thiele, D., & Counter, C. (2014). Copper is required for oncogenic BRAF signaling and tumorigenesis. *Nature*, *509*(7501), 492–496. https://doi.org/10.1038/nature13180

Brauchi, S., Rauch, M. C., Alfaro, I. E., Cea, C., Concha, I. I., Benos, D. J., & Reyes, J. G. (2005). Kinetics, molecular basis, and differentiation of L-lactate transport in spermatogenic cells. *American Journal of Physiology - Cell Physiology*, *288*(3), 523–534. https://doi.org/10.1152/ajpcell.00448.2003

Chan, A., Wong, F., & Arumanayagam, M. (1993). Serum ultrafiltrable copper, total copper and caeruloplasmin concentrations in gynaecological carcinomas. *Annals of Clinical Biochemistry*, *30*(6), 545–549. https://doi.org/10.1177/000456329303000603

Chen, H. H. W., Yanc, J., Chenc, W., Kuod, M. T., Laib, Y., Laie, W., Liu, H., & Su, W. (2012). Predictive and prognostic value of human copper transporter 1 (hCtr1) in patients with stage III non-small-cell lung cancer receiving first-line platinum-based doublet chemotherapy. *Lung Cancer*, *75*(2), 228–234. https://doi.org/10.1016/j.lungcan.2011.06.011

Christofk, H. R., Vander Heiden, M. G., Harris, M. H., Ramanathan, A., Gerszten, R. E., Wei, R., Fleming, M. D.,

Schreiber, S. L., & Cantley, L. C. (2008). The M2 splice isoform of pyruvate kinase is important for cancer metabolism and tumour growth. *Nature*, *452*(7184), 230–233. https://doi.org/10.1038/nature06734

Dancis, A., Yuan, D. S., Haile, D., Askwith, C., Eide, D., Moehle, C., Kaplan, J., & Klausner, R. D. (1994). Molecular characterization of a copper transport protein in S. cerevisiae: An unexpected role for copper in iron transport. *Cell*, *76*(2), 393–402. https://doi.org/10.1016/0092-8674(94)90345-X

Das, S. K., & Ray, K. (2006). Wilson's disease: An update. *Nature Clinical Practice Neurology*, *2*(9), 482–493. https://doi.org/10.1038/ncpneuro0291

De Feo, C. J., Aller, S. G., Siluvai, G. S., Blackburn, N. J., & Unger, V. M. (2009). Three-dimensional structure of the human copper transporter hCTR1. *Proceedings of the National Academy of Sciences of the United States of America*, *106*(11), 4237–4242. https://doi.org/10.1073/pnas.0810286106

Denoyer, D., Masaldan, S., La Fontaine, S., & Cater, M. A. (2015). Targeting copper in cancer therapy: "Copper That Cancer." *Metallomics*, *7*(11), 1459–1476. https://doi.org/10.1039/c5mt00149h

Dias, T. R., Martins, A. D., Reis, V. P., Socorro, S., Silva, B. M., Alves, M. G., & Oliveira, P. F. (2013). Glucose Transport and Metabolism in Sertoli Cell: Relevance for Male Fertility. *Current Chemical Biology*, *7*(3), 282–293. https://doi.org/10.2174/22127968079991311281255l0

Diez, M., Arroyo, M., Cerdàn, D. J., Munoz, M., Martin, M. A., & Balibrea, J. L. (1989). Serum and Tissue Trace Metal Levels in Lung Cancer. *Oncology*, *46*(4), 230–234. https://doi.org/10.1159/000226722

Eichner, R., Heider, M., Fernández-Sáiz, V., Van Bebber, F., Garz, A. K., Lemeer, S., Rudelius, M., Targosz, B. S., Jacobs, L., Knorn, A. M., Slawska, J., Platzbecker, U., Germing, U., Langer, C., Knop, S., Einsele, H., Peschel, C., Haass, C., Keller, U., … Bassermann, F. (2016). Immunomodulatory drugs disrupt the cereblon-CD147-MCT1 axis to exert antitumor activity and teratogenicity. *Nature Medicine*, *22*(7), 735–743. https://doi.org/10.1038/nm.4128

Eisses, J. F., & Kaplan, J. H. (2002). Molecular characterization of hCTR1, the human copper uptake protein. *The Journal of Biological Chemistry*, *277*(32), 29162–29171. https://doi.org/10.1074/jbc.M203652200

Elstrom, R. L., Bauer, D. E., Buzzai, M., Karnauskas, R., Harris, M. H., Plas, D. R., Zhuang, H., Cinalli, R. M., Alavi, A., Rudin, C. M., & Thompson, C. B. (2004). Akt stimulates aerobic glycolysis in cancer cells. *Cancer Research*, *64*(11), 3892–3899. https://doi.org/10.1158/0008-5472.CAN-03-2904

Erfanizadeh, M., Noorafshan, A., Naseh, M., & Karbalay-Doust, S. (2021). The effects of copper sulfate on the structure and function of the rat cerebellum: A stereological and behavioral study. *IBRO Neuroscience Reports*, *15*(11), 119–127. https://doi.org/10.1016/j.ibneur.2021.09.001

Fan, W., Xia, D., Zhu, Q., Hu, L., & Gan, Y. (2016). Intracellular transport of nanocarriers across the intestinal epithelium. *Drug Discovery Today*, *21*(5), 856–863. https://doi.org/10.1016/j.drudis.2016.04.007

Felmlee, M. A., Jones, R. S., Rodriguez-Cruz, V., Follman, K. E., & Morris, M. E. (2020). Monocarboxylate transporters (SLC16): Function, regulation, and role in health and disease. *Pharmacological Reviews*, *72*(2), 466–485. https://doi.org/10.1124/pr.119.018762

Fisel, P., Schaeffeler, E., & Schwab, M. (2018). Clinical and Functional Relevance of the Monocarboxylate Transporter Family in Disease Pathophysiology and Drug Therapy. *Clinical and Translational Science*, *11*(4), 352–364. https://doi.org/10.1111/cts.12551

Galardo, M. N., Riera, M. F., Pellizzari, E. H., Cigorraga, S. B., & Meroni, S. B. (2007). The AMP-activated protein kinase activator, 5-aminoimidazole-4-carboxamide-1-b-D-ribonucleoside, regulates lactate production in rat Sertoli cells. *Journal of Molecular Endocrinology*, *39*(4), 279–288. https://doi.org/10.1677/JME-07-0054

Gatenby, R. A., & Gillies, R. J. (2004). Why do cancers have high aerobic glycolysis? *Nature Reviews Cancer*, *4*(11), 891–899. https://doi.org/10.1038/nrc1478

Ghaffari, R., & Richburg, J. H. (2019). Mice with a Sertoli cell-specific knockout of the: Ctr1 gene exhibit a reduced sensitivity to cisplatin-induced testicular germ cell apoptosis. *Toxicology Research*, *8*(6), 972–978. https://doi.org/10.1039/c9tx00142e

Gottschalk, S., Anderson, N., Hainz, C., Eckhardt, S. G., & Serkova, N. J. (2004). Imatinib (STI571)-mediated changes in glucose metabolism in human leukemia BCR-ABL-positive cells. *Clinical Cancer Research*, *10*(19), 6661–6668. https://doi.org/10.1158/1078-0432.CCR-04-0039

Grootegoed, J. A., & Den Boer, P. J. (1989). Energy metabolism in spermatids: a review. In *Cellular and*

Molecular Events in Spermiogenesis (Hamilton, D.W. and Waites, G.H.M. eds) (pp. 135–159). Cambridge University Press.

Grubman, A., & White, A. R. (2014). Copper as a key regulator of cell signalling pathways. *Expert Reviews in Molecular Medicine*, *16*, 1–27. https://doi.org/10.1017/erm.2014.11

Guo, H., Ouyang, Y., Wang, J., Cui, H., Deng, H., Zhong, X., Jian, Z., Liu, H., Fang, J., Zuo, Z., Wang, X., Zhao, L., Geng, Y., Ouyang, P., & Tang, H. (2021). Cu-induced spermatogenesis disease is related to oxidative stress-mediated germ cell apoptosis and DNA damage. *Journal of Hazardous Materials*, *416*, 1-14. https://doi.org/10.1016/j.jhazmat.2021.125903

Guo, Y., Smith, K., Lee, J., Thiele, D. J., & Petris, M. J. (2004). Identification of Methionine-rich Clusters That Regulate Copper-stimulated Endocytosis of the Human Ctr1 Copper Transporter. *Journal of Biological Chemistry*, *279*(17), 17428–17433. https://doi.org/10.1074/jbc.M401493200

Guo, Y., Smith, K., & Petris, M. J. (2004). Cisplatin stabilizes a multimeric complex of the human Ctr1 copper transporter: Requirement for the extracellular methionine-rich clusters. *Journal of Biological Chemistry*, *279*(45), 46393–46399. https://doi.org/10.1074/jbc.M407777200

Gupta, A., & Lutsenko, S. (2009). Human copper transporters: mechanism, role in human diseases and therapeutic potential. *Future Medicinal Chemistry*, *1*(6), 1125–1142. https://doi.org/10.4155/fmc.09.84

Gupte, A., & Mumper, R. J. (2009). Elevated copper and oxidative stress in cancer cells as a target for cancer treatment. *Cancer Treatment Reviews*, *35*(1), 32–46. https://doi.org/10.1016/j.ctrv.2008.07.004

Habbib, F. K., Dembinski, T. C., & Stitch, R. S. (1980). The zinc and copper content of blood leucocytes and plasma from patients with benign and malignant prostates. *Clinica Chimica Acta*, *104*(3), 329–335. https://doi.org/10.1016/0009-8981(80)90390-3

Halestrap, A. P. (2009). Monocarboxylate transporter 1. *UCSD Nature Molecule Pages*. https://doi.org/10.1038/mp.a001490.01

Halestrap, A. P. (2013). The SLC16 gene family-Structure, role and regulation in health and disease. *Molecular Aspects of Medicine*, *34*(2–3), 337–349. https://doi.org/10.1016/j.mam.2012.05.003

Halestrap, A. P., & Meredith, D. (2004). The SLC16 gene family - From monocarboxylate transporters (MCTs) to aromatic amino acid transporters and beyond. *Pflugers Archiv European Journal of Physiology*, *447*(5), 619–628. https://doi.org/10.1007/s00424-003-1067-2

Halestrap, A. P., & Price, N. T. (1999). The proton-linked monocarboxylate transporter (MCT) family: structure, function and regulation. *Biochemical Journal*, *343*(2), 281–299. https://doi.org/10.1042/0264-6021:3430281

Halestrap, A. P., & Wilson, M. C. (2012). The monocarboxylate transporter family-Role and regulation. *IUBMB Life*, *64*(2), 109–119. https://doi.org/10.1002/iub.572

Hassett, R., & Kosman, D. J. (1995). Evidence for Cu(II) reduction as a component of copper uptake by Saccharomyces cerevisiae. In *Journal of Biological Chemistry* (Vol. 270, Issue 1, pp. 128–134). https://doi.org/10.1074/jbc.270.1.128

Holzer, A. K., Samimi, G., Katano, K., Naerdemann, W., Lin, X., Safaei, R., & Howell, S. B. (2004). The copper influx transporter human copper transport protein 1 regulates the uptake of cisplatin in human ovarian carcinoma cells. *Molecular Pharmacology*, *66*(4), 817–823. https://doi.org/10.1124/mol.104.001198

Iakovidis, I., Delimaris, I., & Piperakis, S. M. (2011). Copper and Its Complexes in Medicine: A Biochemical Approach. *Molecular Biology International*, *2011*, 1–13. https://doi.org/10.4061/2011/594529

Ishida, S., Andreux, P., Poitry-Yamate, C., Auwerx, J., & Hanahan, D. (2013). Bioavailable copper modulates oxidative phosphorylation and growth of tumors. *Proceedings of the National Academy of Sciences of the United States of America*, *110*(48), 19507–19512. https://doi.org/10.1073/pnas.1318431110

Ishida, S., Lee, J., Thiele, D. J., & Herskowitz, I. (2002). Uptake of the anticancer drug cisplatin mediated by the copper transporter Ctr1 in yeast and mammals. *Proceedings of the National Academy of Sciences of the United States of America*, *99*(22), 14298–14302. https://doi.org/10.1073/pnas.162491399

Kagan, H. M., & Li, W. (2003). Lysyl oxidase: Properties, specificity, and biological roles inside and outside of the cell. *Journal of Cellular Biochemistry*, *88*(4), 660–672. https://doi.org/10.1002/jcb.10413

Kim, Y., Choi, J. W., Lee, J. H., & Kim, Y. S. (2015). Expression of lactate/H+ symporters MCT1 and MCT4 and

their chaperone CD147 predicts tumor progression in clear cell renal cell carcinoma: Immunohistochemical and the Cancer Genome Atlas data analyses. *Human Pathology*, *46*(1), 104–112. https://doi.org/10.1016/j.humpath.2014.09.013

Kirk, P., Wilson, M. C., Heddle, C., Brown, M. H., Barclay, A. N., & Halestrap, A. P. (2000). CD147 is tightly associated with lactate transporters MCT1 and MCT4 and facilitates their cell surface expression. *EMBO Journal*, *19*(15), 3896–3904. https://doi.org/10.1093/emboj/19.15.3896

Koukourakis, M. I., Giatromanolaki, A., Harris, A. L., & Sivridis, E. (2006). Comparison of metabolic pathways between cancer cells and stromal cells in colorectal carcinomas: A metabolic survival role for tumor-associated stroma. *Cancer Research*, *66*(2), 632–637. https://doi.org/10.1158/0008-5472.CAN-05-3260

Kulesh, D. A., & Oshima, R. G. (1988). Cloning of the human keratin 18 gene and its expression in nonepithelial mouse cells. *Molecular and Cellular Biology*, *8*(4), 1540–1550. https://doi.org/10.1128/mcb.8.4.1540-1550.1988

Kuo, H. W., Chen, S. F., Wu, C. C., Chen, D. R., & Lee, J. H. (2002). Serum and tissue trace elements in patients with breast cancer in Taiwan. *Biological Trace Element Research*, *89*(1), 1–11. https://doi.org/10.1385/BTER:89:1:1

Kuo, Y., Gybina, A. A., Pyatskowit, J. W., Gitschier, J., & Prohaska, J. R. (2006). Copper Transport Protein (Ctr1) Levels in Mice Are Tissue Specific and Dependent on Copper Status. *The Journal of Nutrition*, *136*(1), 21–26. https://doi.org/10.1093/jn/136.1.21

Lee, J., Prohaska, J. R., & Thiele, D. J. (2001). Essential role for mammalian copper transporter Ctr1 in copper homeostasis and embryonic development. *Proceedings of the National Academy of Sciences of the United States of America*, *98*(12), 6842–6847. https://doi.org/10.1073/pnas.111058698

Lee, Y. Y., Choi, C. H., Do, I. G., Song, S. Y., Lee, W., Park, H. S., Song, T. J., Kim, M. K., Kim, T. J., Lee, J. W., Bae, D. S., & Kim, B. G. (2011). Prognostic value of the copper transporters, CTR1 and CTR2, in patients with ovarian carcinoma receiving platinum-based chemotherapy. *Gynecologic Oncology*, *122*(2), 361–365. https://doi.org/10.1016/j.ygyno.2011.04.025

Li, Y. (2020). Copper homeostasis: Emerging target for cancer treatment. *IUBMB Life*, *72*(9), 1900–1908. https://doi.org/10.1002/iub.2341

Li, Y., Chen, H., Liao, J., Chen, K., Javed, M. T., Qiao, N., Zeng, Q., Liu, B., Yi, J., Tang, Z., & Li, Y. (2021). Long-term copper exposure promotes apoptosis and autophagy by inducing oxidative stress in pig testis. *Environmental Science and Pollution Research*, *28*(39), 55140–55153. https://doi.org/10.1007/s11356-021-14853-y

Li, Z. Y., Shi, Y. L., Liang, G. X., Yang, J., Zhuang, S. K., Lin, J. B., Ghodbane, A., Tam, M. S., Liang, Z. J., Zha, Z. G., & Zhang, H. T. (2020). Visualization of GLUT1 Trafficking in Live Cancer Cells by the Use of a Dual-Fluorescence Reporter. *ACS Omega*, *5*(26), 15911–15921. https://doi.org/10.1021/acsomega.0c01054

Liang, Z. D., Tsai, W. B., Lee, M. Y., Savaraj, N., & Kuo, M. T. (2012). Specificity protein 1 (Sp1) oscillation is involved in copper homeostasis maintenance by regulating human high-affinity copper transporter 1 expression. *Molecular Pharmacology*, *81*(3), 455–464. https://doi.org/10.1124/mol.111.076422

Lim, K. S., Lim, K. J., Price, A. C., Orr, B. A., Eberhart, C. G., & Bar, E. E. (2014). Inhibition of monocarboxylate transporter-4 depletes stem-like glioblastoma cells and inhibits HIF transcriptional response in a lactate-independent manner. *Oncogene*, *33*(35), 4433–4441. https://doi.org/10.1038/onc.2013.390

Liu, J. Y., Yang, X., Sun, X. D., Zhuang, C. C., Xu, F. B., & Li, Y. F. (2016). Suppressive Effects of Copper Sulfate Accumulation on the Spermatogenesis of Rats. *Biological Trace Element Research*, *174*(2), 356–361. https://doi.org/10.1007/s12011-016-0710-7

Luo, J., Vijayasankaran, N., Autsen, J., Santuray, R., Hudson, T., Amanullah, A., & Li, F. (2012). Comparative metabolite analysis to understand lactate metabolism shift in Chinese hamster ovary cell culture process. *Biotechnology and Bioengineering*, *109*(1), 146–156. https://doi.org/10.1002/bit.23291

Lyubimov, A. V., Smith, J. A., Rousselle, S. D., Mercieca, M. D., Tomaszewski, J. E., Smith, A. C., & Levine, B. S. (2004). The effects of tetrathiomolybdate (TTM, NSC-714598) and copper supplementation on fertility and early embryonic development in rats. *Reproductive Toxicology*, *19*(2), 223–233.

https://doi.org/10.1016/j.reprotox.2004.07.006

Mandal, T., Kar, S., Maji, S., Sen, S., & Gupta, A. (2020). Structural and Functional Diversity Among the Members of CTR, the Membrane Copper Transporter Family. *The Journal of Membrane Biology*, *253*(5), 459–468. https://doi.org/10.1007/s00232-020-00139-w

Maryon, E. B., Molloy, S. A., & Kaplan, J. H. (2007). O-linked glycosylation at threonine 27 protects the copper transporter hCTR1 from proteolytic cleavage in mammalian cells. *Journal of Biological Chemistry*, *282*(28), 20376–20387. https://doi.org/10.1074/jbc.M701806200

Mather, J. P. (1980). Establishment and characterization of two distinct mouse testicular epithelial cell lines. *Biology of Reproduction*, *23*(1), 243–252. https://doi.org/10.1095/biolreprod23.1.243

McCord, J. M., & Fridovich, I. (1969). Superoxide dismutase. An enzymic function for erythrocuprein (hemocuprein). *Journal of Biological Chemistry*, *244*(22), 6049–6055.

Morris, M. E., & Felmlee, M. A. (2008). Overview of the proton-coupled MCT (SLC16A) family of transporters: Characterization, function and role in the transport of the drug of abuse γ-Hydroxybutyric acid. *AAPS Journal*, *10*(2), 311–321. https://doi.org/10.1208/s12248-008-9035-6

Noble, R. A., Bell, N., Blair, H., Sikka, A., Thomas, H., Phillips, N., Nakjang, S., Miwa, S., Crossland, R., Rand, V., Televantou, D., Long, A., Keun, H. C., Bacon, C. M., Bomken, S., Critchlow, S. E., & Wedge, S. R. (2017). Inhibition of monocarboxyate transporter 1 by AZD3965 as a novel therapeutic approach for diffuse large B-cell lymphoma and burkitt lymphoma. *Haematologica*, *102*(7), 1247–1257. https://doi.org/10.3324/haematol.2016.163030

Nolop, K. B., Rhodes, C. G., Brudin, L. H., Beaney, R. P., Krausz, T., Jones, T., & Hughes, J. M. B. (1987). Glucose utilization in vivo by human pulmonary neoplasms. *Cancer*, *60*(11), 2682–2689. https://doi.org/10.1002/1097-0142(19871201)60:11<2682::AID-CNCR2820601118>3.0.CO;2-H

Nose, Y., Kim, B. E., & Thiele, D. J. (2006). Ctr1 drives intestinal copper absorption and is essential for growth, iron metabolism, and neonatal cardiac function. *Cell Metabolism*, *4*(3), 235–244. https://doi.org/10.1016/j.cmet.2006.08.009

Odet, F., Duan, C., Willis, W. D., Goulding, E. H., Kung, A., Eddy, E. M., & Goldberg, E. (2008). Expression of the Gene for Mouse Lactate Dehydrogenase C (Ldhc) Is Required for Male Fertility. *Biology of Reproduction*, *79*(1), 26–34. https://doi.org/10.1095/biolreprod.108.068353

Öhrvik, H., Nose, Y., Wood, L. K., Kim, B. E., Gleber, S. C., & Ralle, M.Thiele, D. J. (2013). Ctr2 regulates biogenesis of a cleaved form of mammalian Ctr1 metal transporter lacking the copper- and cisplatin-binding ecto-domain. *Proceedings of the National Academy of Sciences of the United States of America*, *110*(46), E4279–E4288. https://doi.org/10.1073/pnas.1311749110

Öhrvik, H., & Thiele, D. J. (2014). How copper traverses cellular membranes through the mammalian copper transporter 1, Ctr1. *Annals of the New York Academy of Sciences*, *1314*, 32–41. https://doi.org/10.1111/nyas.12371

Öhrvik, H., & Thiele, D. J. (2015). The Role of Ctr1 and Ctr2 in Mammalian Copper Homeostasis and Platinum-based Chemotherapy. *Journal of Trace Elements in Medicine and Biology*, *31*, 178–182. https://doi.org/doi.org/10.1016/j.jtemb.2014.03.006

Oliveira, P. F., Martins, A. D., Moreira, A. C., Cheng, C. Y., & Alves, M. G. (2015). The Warburg Effect Revisited-Lesson from the Sertoli Cell. *Medicinal Research Reviews*, *35*(1), 126–151. https://doi.org/10.1002/med.21325

Ord, J. J., Streeter, E. H., Roberts, I. S. D., Cranston, D., & Harris, A. L. (2005). Comparison of hypoxia transcriptome in vitro with in vivo gene expression in human bladder cancer. *British Journal of Cancer*, *93*(3), 346–354. https://doi.org/10.1038/sj.bjc.6602666

Pellerin, L., & Magistretti, P. J. (2012). Sweet sixteen for ANLS. *Journal of Cerebral Blood Flow and Metabolism*, *32*(7), 1152–1166. https://doi.org/10.1038/jcbfm.2011.149

Pham, A. N., Xing, G., Miller, C. J., & Waite, T. D. (2013). Fenton-like copper redox chemistry revisited: Hydrogen peroxide and superoxide mediation of copper-catalyzed oxidant production. *Journal of Catalysis*, *301*, 54–64. https://doi.org/10.1016/j.jcat.2013.01.025

Pinheiro, C., Longatto-Filho, A., Azevedo-Silva, J., Casal, M., Schmitt, F. C., & Baltazar, F. (2012). Role of

monocarboxylate transporters in human cancers: State of the art. *Journal of Bioenergetics and Biomembranes*, *44*(1), 127–139. https://doi.org/10.1007/s10863-012-9428-1

Pinheiro, C., Longatto-Filho, A., Scapulatempo, C., Ferreira, L., Martins, S., Pellerin, L., Rodrigues, M., Alves, V. A. F., Schmitt, F., & Baltazar, F. (2008). Increased expression of monocarboxylate transporters 1, 2, and 4 in colorectal carcinomas. *Virchows Archiv*, *452*(2), 139–146. https://doi.org/10.1007/s00428-007-0558-5

Pinheiro, C., Reis, R. M., Ricardo, S., Longatto-Filho, A., Schmitt, F., & Baltazar, F. (2010). Expression of monocarboxylate transporters 1, 2, and 4 in human tumours and their association with CD147 and CD44. *Journal of Biomedicine and Biotechnology*, *2010*9, 1-7. https://doi.org/10.1155/2010/427694

Puig, S., Lee, J., Lau, M., & Thiele, D. J. (2002). Biochemical and genetic analyses of yeast and human high affinity copper transporters suggest a conserved mechanism for copper uptake. *Journal of Biological Chemistry*, *277*(29), 26021–26030. https://doi.org/10.1074/jbc.M202547200

Qian, Y., Khattak, S. F., Xing, Z., He, A., Kayne, P. S., Qian, N. X., Pan, S. H., & Li, Z. J. (2011). Cell culture and gene transcription effects of copper sulfate on Chinese hamster ovary cells. *Biotechnology Progress*, *27*(4), 1190–1194. https://doi.org/10.1002/btpr.630

Racker, E. (1972). Bioenergetics and the problem of tumor growth. *American Scientist*, *60*(1), 56–63.

Rato, L., Alves, M. G., Socorro, S., Carvalho, R. A., Cavaco, J. E., & Oliveira, P. F. (2012). Metabolic modulation induced by oestradiol and DHT in immature rat Sertoli cells cultured in vitro. *Bioscience Reports*, *32*(1), 61–69. https://doi.org/10.1042/BSR20110030

Reardon, C. A., Lau, Y. F., Paik, Y. K., Weisgraber, K. H., Mahley, R. W., & Taylor, J. M. (1986). Expression of the human apolipoprotein E gene in cultured mammalian cells. *Journal of Biological Chemistry*, *261*(21), 9858–9864. https://doi.org/10.1016/s0021-9258(18)67595-7

Rubino, J. T., Riggs-Gelasco, P., & Franz, K. J. (2010). Methionine motifs of copper transport proteins provide general and flexible thioether-only binding sites for Cu(I) and Ag(I). *Journal of Biological Inorganic Chemistry*, *15*(7), 1033–1049. https://doi.org/10.1007/s00775-010-0663-9

San-Millán, I., & Brooks, G. A. (2017). Reexamining cancer metabolism: Lactate production for carcinogenesis could be the purpose and explanation of the Warburg Effect. *Carcinogenesis*, *38*(2), 119–133. https://doi.org/10.1093/carcin/bgw127

Schweigel-Röntgen, M. (2014). The Families of Zinc (SLC30 and SLC39) and Copper (SLC31) Transporters. In *Current Topics in Membranes* (Vol. 73). https://doi.org/10.1016/B978-0-12-800223-0.00009-8

Sekar, R. B., & Periasamy, A. (2003). Fluorescence resonance energy transfer (FRET) microscopy imaging of live cell protein localizations. *Journal of Cell Biology*, *160*(5), 629–633. https://doi.org/10.1083/jcb.200210140

Shanbhag, V. C., Gudekar, N., Jasmer, K., Papageorgiou, C., Singh, K., & Petris, M. J. (2021). Copper metabolism as a unique vulnerability in cancer. *Biochimica et Biophysica Acta - Molecular Cell Research*, *1868*. https://doi.org/10.1016/j.bbamcr.2020.118893

Smolinski, L., Litwin, T., Redzia-Ogrodnik, B., Dziezyc, K., Kurkowska-Jastrzebska, I., & Czlonkowska, A. (2019). Brain volume is related to neurological impairment and to copper overload in Wilson's disease. *Neurological Sciences*, *40*(10), 2089–2095. https://doi.org/10.1007/s10072-019-03942-z

Sonveaux, P., Végran, F., Schroeder, T., Wergin, M. C., Verrax, J., Rabbani, Z. N., De Saedeleer, C. J., Kennedy, K. M., Diepart, C., Jordan, B. F., Kelley, M. J., Gallez, B., Wahl, M. L., Feron, O., & Dewhirst, M. W. (2008). Targeting lactate-fueled respiration selectively kills hypoxic tumor cells in mice. *Journal of Clinical Investigation*, *118*(12), 3930–3942. https://doi.org/10.1172/JCI36843

Su, L., Mruk, D. D., & Cheng, C. Y. (2016). Drug transporters, the blood–testis barrier, and spermatogenesis. *Physiology & Behavior*, *208*(3), 207–223. https://doi.org/10.1677/JOE-10-0363.Drug

Tsigelny, I. F., Sharikov, Y., Greenberg, J. P., Miller, M. A., Kouznetsova, V. L., Larson, C. A., & Howell, S. B. (2012). An All-Atom Model of the Structure of Human Copper Transporter 1. *Cell Biochemistry and Biophysics*, *63*(3), 223–234. https://doi.org/10.1007/s12013-012-9358-x

Turski, M. L., Brady, D. C., Kim, H. J., Kim, B., Nose, Y., Counter, C. M., Winge, D. R., & Thiele, D. J. (2012). A Novel Role for Copper in Ras/Mitogen-Activated Protein Kinase Signaling. *Molecular and Cellular Biology*,

32(7), 1284–1295. https://doi.org/10.1128/mcb.05722-11

Tvrda, E., Peer, R., Sikka, S. C., & Agarwal, A. (2015). Iron and copper in male reproduction: a double-edged sword. *Journal of Assisted Reproduction and Genetics*, *32*(1), 3–16. https://doi.org/10.1007/s10815-014-0344-7

Ullah, M. S., Davies, A. J., & Halestrap, A. P. (2006). The plasma membrane lactate transporter MCT4, but not MCT1, is up-regulated by hypoxia through a HIF-1α-dependent mechanism. *Journal of Biological Chemistry*, *281*(14), 9030–9037. https://doi.org/10.1074/jbc.M511397200

Van Den Berghe, P. V. E., Folmer, D. E., Malingré, H. E. M., Van Beurden, E., Klomp, A. E. M., Van De Sluis, B., Merkx, M., Berger, R., & Klomp, L. W. J. (2007). Human copper transporter 2 is localized in late endosomes and lysosomes and facilitates cellular copper uptake. *Biochemical Journal*, *407*(1), 49–59. https://doi.org/10.1042/BJ20070705

Van Den Berghe, P. V. E., & Klomp, L. W. J. (2010). Posttranslational regulation of copper transporters. *Journal of Biological Inorganic Chemistry*, *15*(1), 37–46. https://doi.org/10.1007/s00775-009-0592-7

Van Niekerk, F. E., & Van Niekerk, C. H. (1989). The influence of experimentally induced copper deficiency on the fertility of rams. I. Semen parameters and peripheral plasma androgen concentration. *Journal of the South African Veterinary Association*, *60*(1), 28–31.

Vander Heiden, M. G., Cantley, L., & Thompson, C. (2009). Understanding the Warburg Effect: The Metabolic Requirements of Cell Proliferation. *Science*, *324*(5930), 1029–1033. https://doi.org/10.1126/science.1160809

Vander Wende, C., & Wainio, W. W. (1960). The state of the copper in cytochrome c oxidase. *The Journal of Biological Chemistry*, *235*(3), 11–13.

Voli, F., Valli, E., Lerra, L., Kimpton, K., Saletta, F., Giorgi, F. M., Mercatelli, D., Rouaen, J. R. C., Shen, S., Murray, J. E., Ahmed-Cox, A., Cirillo, G., Mayoh, C., Beavis, P. A., Haber, M., Trapani, J. A., Kavallaris, M., & Vittorio, O. (2020). Intratumoral copper modulates PD-L1 expression and influences tumor immune evasion. *Cancer Research*, *80*(19), 4129–4144. https://doi.org/10.1158/0008-5472.CAN-20-0471

Walters, D. K., Arendt, B. K., & Jelinek, D. F. (2013). CD147 regulates the expression of MCT1 and lactate export in multiple myeloma cells. *Cell Cycle*, *12*(19), 3175–3183. https://doi.org/10.4161/cc.26193

Wang, H., Wen, L., Yuan, Q., Sun, M., Niu, M., & He, Z. (2016). Establishment and applications of male germ cell and Sertoli cell lines. *Reproduction*, *152*(2), R31–R40. https://doi.org/10.1530/REP-15-0546

Warburg, O., Posener, K., & Negelein, E. (1924). Über den Stoffwechsel der Carcinomzelle. In *Klin Wochenschr Berl* (Vol. 4, pp. 310–343).

Warburg, O., Wind, F., & Negelein, E. (1927). The metabolism of tumors in the body. *Journal of General Physiology*, *8*(6), 519–530. https://doi.org/10.1085/jgp.8.6.519

Wee, N. K. Y., Weinstein, D. C., Fraser, S. T., & Assinder, S. J. (2013). The mammalian copper transporters CTR1 and CTR2 and their roles in development and disease. *International Journal of Biochemistry and Cell Biology*, *45*(5), 960–963. https://doi.org/10.1016/j.biocel.2013.01.018

Weinhouse, S. (1956). On Respiratory Impairment in Cancer Cells. *Science*, *124*(3215), 267–269. https://doi.org/10.1126/science.124.3215.267

Wenger, R. H., & Katschinski, M. (2005). The hypoxic testis and post-meiotic expression of PAS domain proteins. *Seminars in Cell & Developmental Biology*, *16*(4–5), 547–553. https://doi.org/10.1016/j.semcdb.2005.03.008

World Health Organization. (2021). *Mean fasting blood glucose*. https://www.who.int/data/gho/indicator-metadata-registry/imr-details/2380

Xu, J., Brosseau, J. P. P., & Shi, H. (2020). Targeted degradation of immune checkpoint proteins: emerging strategies for cancer immunotherapy. *Oncogene*, *39*(48), 7106–7113. https://doi.org/10.1038/s41388-020-01491-w

Yuk, I. H., Zhang, J. D., Ebeling, M., Berrera, M., Gomez, N., Werz, S., Meiringer, C., Shao, Z., Swanberg, J. C., Lee, K. H., Luo, J., & Szperalski, B. (2014). Effects of copper on CHO cells: Insights from gene expression analyses. *Biotechnology Progress*, *30*(2), 429–442. https://doi.org/10.1002/btpr.1868

Zhou, B., & Gitschier, J. (1997). hCTR1: A human gene for copper uptake identified by complementation in

yeast. *Proceedings of the National Academy of Sciences of the United States of America*, *94*(14), 7481–7486. https://doi.org/10.1073/pnas.94.14.7481

Zhu, F., Nair, R. R., Fisher, E. M. C., & Cunningham, T. J. (2019). Humanising the mouse genome piece by piece. *Nature Communications*, *10*(1), 1–13. https://doi.org/10.1038/s41467-019-09716-7

CHAPTER VII

APPENDIX

VII. APPENDIX

VII. Appendix A: Circular map of pMCT4-mCherry

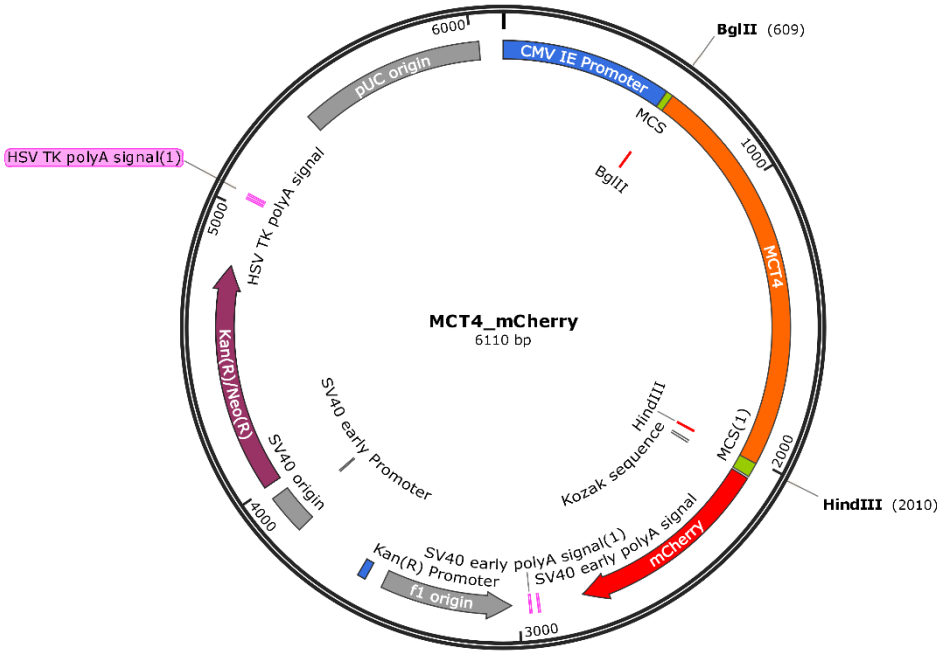

Figure 30: Circular map of pMCT4-mCherry. The relevant features are highlighted, such as CMV IE Promoter (human cytomegalovirus-immediate early promoter), CTR1 (human *CTR1* sequence), MCS (Multiple Cloning Site), restriction sites for *Bgl*II and *Hind*III enzymes, SV40 origin (SV40 origin of replication induces replication within mammalian cells), Kan(R)/Neo(R) (this feature confers resistance to kanamycin or neomycin) and pUC origin (plasmid origin of replication). This map was constructed using SnapGene version 3.1.1.

VII. Appendix B: Protocol for making XL-1 Blue competent cells

Day 1:

1. Streak out frozen glycerol stock of XL-1 Blue cells onto a Luria-Bertani broth plate (without addition of antibiotics since these cells do not contain a plasmid). Leave the bacterial cells to grow on plate overnight at 37 °C.

2. Autoclave:

- 1 L Transformation Buffer (TB) solution, with pH adjusted to 6.7
- 1 L Super Optimum Broth (SB)
- 1 L of 100 mM $CaCl_2$
- 1 L of 100 mM $MgCl_2$
- 100 mL of 85 mM $CaCl_2$ with 15 % glycerol v/v
- 4 centrifuge bottles and caps
- microfuge tubes
- 1x 1 L Schott bottle
- 1x 1000 mL glass beaker
- 1x 1000 mL volumetric bottle

Note:

- Use clean glassware with no detergent residue. Clean glassware with a solution with 70 % EtOH and let it dry. Glassware can also be autoclaved with some water to achieve the same result. It is best to set aside glassware for competent cell preparation that is not washed with detergent.

- TB solution to 50 mL sterile falcons and store at 4 °C.

3. After the autoclave, cool the SOB media to room temperature and add 5 mL of the sterile solutions of $MgCl_2$ 2 M and 5 mL of sterile $MgSO_4$ 2 M.

4. Chill overnight at 4 °C:

- 100 mM $CaCl_2$
- 100 mM $MgCl_2$
- 85 mM $CaCl_2$ with 15 % glycerol v/v

- 1 L TB solution autoclaved, with pH adjusted to 6.7

Day 2 (early in the morning):

1. Pick some of the *E. coli* colonies (2-3 mm in diameter) from the plate previously incubated overnight, and inoculate them in 20 mL of SOB medium, in a 50 mL falcon, and incubate at 37 °C, 200 rpm for 6 h – 8 h.

2. At the end of the day, inoculate three 2 L flasks with 250 mL of SOB medium with this starter culture (store the remaining SOB for DO dilutions and blanks).

3. Transfer 10 ml of starter culture into the first flask, 4 mL to the second flask and the third receives 2 mL. Incubate the three flasks overnight at 18 °C, 200 rpm.

Day 3:

1. The following morning read the OD_{640} and continue to monitor the OD every 45 min.

2. When the OD of one of the cultures reaches 0.55, transfer the culture vessel to an ice-water bath for 10 min. Discard the other two cultures.

3. Split the culture to 4 x 50 ml falcons (discard properly the remaining culture; only 200 ml of cultures will be used because our centrifuge only has place for 4 falcons).

4. Harvest the cells by centrifugation at 2,500 x g (i.e. 3727 rpm in the Eppendorf 5804R) for 10 min at 4 °C. Decant the supernatant and remove any drops of medium by pipetting them carefully.

5. Add 16 ml of ice-cold TB to each falcon and resuspend each pellet gently by swirling. After resuspending the cells, transfer the content of one falcon to another falcon in order to have only 2 falcons at the end.

6. Harvest the cells by centrifugation at 2500 x g (i.e. 3727 rpm in the Eppendorf 5804R) for 10 min at 4 °C. Decant the supernatant and remove any drops of medium by pipetting them carefully.

7. Add 8 mL of ice-cold TB solution to each falcon and resuspend gently by swirling.

8. Add 0.6 mL of DMSO (aliquots stored in the fridge) to final concentration of 7 %. Mix gently by swirling and incubate on ice for 10 min.

9. Dispense the cell suspension in 200 µl aliquots and immediately flash-freeze by immersion in liquid nitrogen. Store frozen cells at -80 °C.

VII. Appendix C: Plasmid predicted nucleotide sequences

The predicted DNA sequences of the five plasmid constructions made (pCTR1-mCherry, pmCherry-CTR1, pAcGFP-CTR2, pCTR2-AcGFP and pCTR2-mCherry) and the respective horizontal maps (Figure 31, Figure 32, Figure 33, Figure 34 and Figure 35) are represented bellow. The nucleotide sequence highlighted in yellow corresponds to the DNA sequence of *hCTR1* or *hCTR2*, depending on the plasmid construction presented. The nucleotide sequence in red corresponds to the *mCherry* DNA sequence, and in green is highlighted the *AcGFP* nucleotide sequence.

1. pCTR1-mCherry

TAGTTATTAATAGTAATCAATTACGGGGTCATTAGTTCATAGCCCATATATGGAGTTCCGCGTTACATAACTTACGG
TAAATGGCCCGCCTGGCTGACCGCCCAACGACCCCCGCCCATTGACGTCAATAATGACGTATGTTCCCATAGTAACGCC
AATAGGGACTTTCCATTGACGTCAATGGGTGGAGTATTTACGGTAAACTGCCCACTTGGCAGTACATCAAGTGTATCATAT
GCCAAGTACGCCCCCTATTGACGTCAATGACGGTAAATGGCCCGCCTGGCATTATGCCCAGTACATGACCTTATGGGACT
TTCCTACTTGGCAGTACATCTACGTATTAGTCATCGCTATTACCATGGTGATGCGGTTTTGGCAGTACATCAATGGGCGTG
GATAGCGGTTTGACTCACGGGGATTTCCAAGTCTCCACCCCATTGACGTCAATGGGAGTTTGTTTTGGCACCAAAATCAAC
GGGACTTTCCAAAATGTCGTAACAACTCCGCCCCATTGACGCAAATGGGCGGTAGGCGTGTACGGTGGGAGGTCTATATA
AGCAGAGCTGGTTTAGTGAACCGTCAGATCCGCTAGCGCTACCGGACTCAGATCTATGGATCATTCCCACCATATGGGGA
TGAGCTATATGGACTCCAACAGTACCATGCAACCTTCTCACCATCACCCAACCACTTCAGCCTCACACTCCCATGGTGGA
GGAGACAGCAGCATGATGATGATGCCTATGACCTTCTACTTTGGCTTTAAGAATGTGGAACTACTGTTTTCCGGTTTGGTG
ATCAATACAGCTGGAGAAATGGCTGGAGCTTTTGTGGCAGTGTTTTTACTAGCAATGTTCTATGAAGGACTCAAGATAGCC
CGAGAGAGCCTGCTGCGTAAGTCACAAGTCAGCATTCGCTACAATTCCATGCCTGTCCCAGGACCAAATGGAACCATCCT
TATGGAGACACACAAAACTGTTGGGCAACAGATGCTGAGCTTTCCTCACCTCCTGCAAACAGTGCTGCACATCATCCAGG
TGGTCATAAGCTACTTCCTCATGCTCATCTTCATGACCTACAACGGGTACCTCTGCATTGCAGTAGCAGCAGGGGCCGGT
ACAGGATACTTCCTCTTCAGCTGGAAGAAGGCAGTGGTAGTGGATATCACAGAGCATTGCCATAAGCTTCGAATTCTGCAG
TCGACGGTACCGCGGGCCCGGGATCCACCGGTCGCCACCATGGTGAGCAAGGGCGAGGAGGATAACATGGCCATCATC
AAGGAGTTCATGCGCTTCAAGGTGCACATGGAGGGCTCCGTGAACGGCCACGAGTTCGAGATCGAGGGCGAGGGCGAGG
GCCGCCCCTACGAGGGCACCCAGACCGCCAAGCTGAAGGTGACCAAGGGTGGCCCCCTGCCCTTCGCCTGGGACATCC
TGTCCCCTCAGTTCATGTACGGCTCCAAGGCCTACGTGAAGCACCCCGCCGACATCCCCGACTACTTGAAGCTGTCCTT
CCCCGAGGGCTTCAAGTGGGAGCGCGTGATGAACTTCGAGGACGGCGGCGTGGTGACCGTGACCCAGGACTCCTCCCT
GCAGGACGGCGAGTTCATCTACAAGGTGAAGCTGCGCGGCACCAACTTCCCCTCCGACGGCCCCGTAATGCAGAAGAAG
ACCATGGGCTGGGAGGCCTCCTCCGAGCGGATGTACCCCGAGGACGGCGCCCTGAAGGGCGAGATCAAGCAGAGGCTG

AAGCTGAAGGACGGCGGCCACTACGACGCTGAGGTCAAGACCACCTACAAGGCCAAGAAGCCCGTGCAGCTGCCCGGC
GCCTACAACGTCAACATCAAGTTGGACATCACCTCCCACAACGAGGACTACACCATCGTGGAACAGTACGAACGCGCCG
AGGGCCGCCACTCCACCGGCGGCATGGACGAGCTGTACAAGTAGCGGCCGCGACTCTAGATCATAATCAGCCATACCAC
ATTTGTAGAGGTTTTACTTGCTTTAAAAAACCTCCCACACCTCCCCCTGAACCTGAAACATAAAATGAATGCAATTGTTGTT
GTTAACTTGTTTATTGCAGCTTATAATGGTTACAAATAAAGCAATAGCATCACAAATTTCACAAATAAAGCATTTTTTTCACT
GCATTCTAGTTGTGGTTTGTCCAAACTCATCAATGTATCTTAAGGCGTAAATTGTAAGCGTTAATATTTTGTTAAAATTCGCG
TTAAATTTTTGTTAAATCAGCTCATTTTTTAACCAATAGGCCGAAATCGGCAAAATCCCTTATAAATCAAAAGAATAGACCGA
GATAGGGTTGAGTGTTGTTCCAGTTTGGAACAAGAGTCCACTATTAAAGAACGTGGACTCCAACGTCAAAGGGCGAAAAAC
CGTCTATCAGGGCGATGGCCCACTACGTGAACCATCACCCTAATCAAGTTTTTTGGGGTCGAGGTGCCGTAAAGCACTAA
ATCGGAACCCTAAAGGGAGCCCCCGATTTAGAGCTTGACGGGGAAAGCCGGCGAACGTGGCGAGAAAGGAAGGGAAGAA
AGCGAAAGGAGCGGGCGCTAGGGCGCTGGCAAGTGTAGCGGTCACGCTGCGCGTAACCACCACACCCGCCGCGCTTAA
TGCGCCGCTACAGGGCGCGTCAGGTGGCACTTTTCGGGGAAATGTGCGCGGAACCCCTATTTGTTTATTTTTCTAAATAC
ATTCAAATATGTATCCGCTCATGAGACAATAACCCTGATAAATGCTTCAATAATATTGAAAAAGGAAGAGTCCTGAGGCGGA
AAGAACCAGCTGTGGAATGTGTGTCAGTTAGGGTGTGGAAAGTCCCCAGGCTCCCCAGCAGGCAGAAGTATGCAAAGCAT
GCATCTCAATTAGTCAGCAACCAGGTGTGGAAAGTCCCCAGGCTCCCCAGCAGGCAGAAGTATGCAAAGCATGCATCTCA
ATTAGTCAGCAACCATAGTCCCGCCCCTAACTCCGCCCATCCCGCCCCTAACTCCGCCCAGTTCCGCCCATTCTCCGCC
CCATGGCTGACTAATTTTTTTTATTTATGCAGAGGCCGAGGCCGCCTCGGCCTCTGAGCTATTCCAGAAGTAGTGAGGAG
GCTTTTTTGGAGGCCTAGGCTTTTGCAAAGATCGATCAAGAGACAGGATGAGGATCGTTTCGCATGATTGAACAAGATGGA
TTGCACGCAGGTTCTCCGGCCGCTTGGGTGGAGAGGCTATTCGGCTATGACTGGGCACAACAGACAATCGGCTGCTCTG
ATGCCGCCGTGTTCCGGCTGTCAGCGCAGGGGCGCCCGGTTCTTTTTGTCAAGACCGACCTGTCCGGTGCCCTGAATGA
ACTGCAAGACGAGGCAGCGCGGCTATCGTGGCTGGCCACGACGGGCGTTCCTTGCGCAGCTGTGCTCGACGTTGTCACT
GAAGCGGGAAGGGACTGGCTGCTATTGGGCGAAGTGCCGGGGCAGGATCTCCTGTCATCTCACCTTGCTCCTGCCGAGA
AAGTATCCATCATGGCTGATGCAATGCGGCGGCTGCATACGCTTGATCCGGCTACCTGCCCATTCGACCACCAAGCGAAA
CATCGCATCGAGCGAGCACGTACTCGGATGGAAGCCGGTCTTGTCGATCAGGATGATCTGGACGAAGAGCATCAGGGGC
TCGCGCCAGCCGAACTGTTCGCCAGGCTCAAGGCGAGCATGCCCGACGGCGAGGATCTCGTCGTGACCCATGGCGATG
CCTGCTTGCCGAATATCATGGTGGAAAATGGCCGCTTTTCTGGATTCATCGACTGTGGCCGGCTGGGTGTGGCGGACCG
CTATCAGGACATAGCGTTGGCTACCCGTGATATTGCTGAAGAGCTTGGCGGCGAATGGGCTGACCGCTTCCTCGTGCTTT
ACGGTATCGCCGCTCCCGATTCGCAGCGCATCGCCTTCTATCGCCTTCTTGACGAGTTCTTCTGAGCGGGACTCTGGGG
TTCGAAATGACCGACCAAGCGACGCCCAACCTGCCATCACGAGATTTCGATTCCACCGCCGCCTTCTATGAAAGGTTGGG
CTTCGGAATCGTTTTCCGGGACGCCGGCTGGATGATCCTCCAGCGCGGGGATCTCATGCTGGAGTTCTTCGCCCACCCT
AGGGGGAGGCTAACTGAAACACGGAAGGAGACAATACCGGAAGGAACCCGCGCTATGACGGCAATAAAAAGACAGAATAA
AACGCACGGTGTTGGGTCGTTTGTTCATAAACGCGGGGTTCGGTCCCAGGGCTGGCACTCTGTCGATACCCCACCGAGA
CCCCATTGGGGCCAATACGCCCGCGTTTCTTCCTTTTCCCCACCCCACCCCCCAAGTTCGGGTGAAGGCCCAGGGCTCG
CAGCCAACGTCGGGGCGGCAGGCCCTGCCATAGCCTCAGGTTACTCATATATACTTTAGATTGATTTAAAACTTCATTTTT

AATTTAAAAGGATCTAGGTGAAGATCCTTTTTGATAATCTCATGACCAAAATCCCTTAACGTGAGTTTTCGTTCCACTGAGC
GTCAGACCCCGTAGAAAAGATCAAAGGATCTTCTTGAGATCCTTTTTTTCTGCGCGTAATCTGCTGCTTGCAAACAAAAAAA
CCACCGCTACCAGCGGTGGTTTGTTTGCCGGATCAAGAGCTACCAACTCTTTTTCCGAAGGTAACTGGCTTCAGCAGAGC
GCAGATACCAAATACTGTTCTTCTAGTGTAGCCGTAGTTAGGCCACCACTTCAAGAACTCTGTAGCACCGCCTACATACCT
CGCTCTGCTAATCCTGTTACCAGTGGCTGCTGCCAGTGGCGATAAGTCGTGTCTTACCGGGTTGGACTCAAGACGATAGT
TACCGGATAAGGCGCAGCGGTCGGGCTGAACGGGGGGTTCGTGCACACAGCCCAGCTTGGAGCGAACGACCTACACCG
AACTGAGATACCTACAGCGTGAGCTATGAGAAAGCGCCACGCTTCCCGAAGGGAGAAAGGCGGACAGGTATCCGGTAAG
CGGCAGGGTCGGAACAGGAGAGCGCACGAGGGAGCTTCCAGGGGGAAACGCCTGGTATCTTTATAGTCCTGTCGGGTTT
CGCCACCTCTGACTTGAGCGTCGATTTTTGTGATGCTCGTCAGGGGGGCGGAGCCTATGGAAAAACGCCAGCAACGCGG
CCTTTTTACGGTTCCTGGCCTTTTGCTGGCCTTTTGCTCACATGTTCTTTCCTGCGTTATCCCCTGATTCTGTGGATAACC
GTATTACCGCCATGCAT

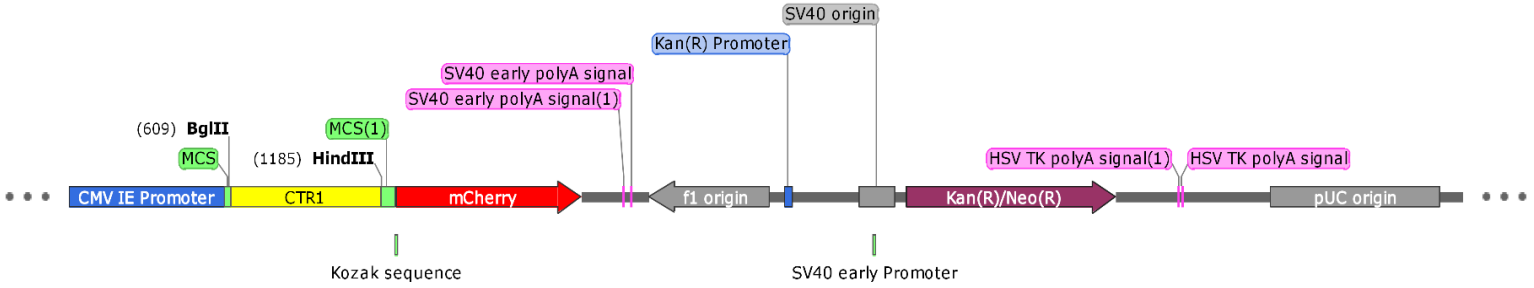

Figure 31: Horizontal map of pCTR1-mCherry. The relevant features are highlighted, such as CMV IE Promoter (human cytomegalovirus-immediate early promoter), CTR1 (human *CTR1* sequence), MCS (Multiple Cloning Site), restriction sites for *Bgl*II and *Hind*III enzymes, SV40 origin (SV40 origin of replication induces replication within mammalian cells), Kan(R)/Neo(R) (this feature confers resistance to kanamycin or neomycin) and pUC origin (plasmid origin of replication). This map was constructed using SnapGene version 3.1.1.

2. pmCherry-CTR1

TAGTTATTAATAGTAATCAATTACGGGGTCATTAGTTCATAGCCCATATATGGAGTTCCGCGTTACATAACTTACGG
TAAATGGCCCGCCTGGCTGACCGCCCAACGACCCCCGCCCATTGACGTCAATAATGACGTATGTTCCCATAGTAACGCC
AATAGGGACTTTCCATTGACGTCAATGGGTGGAGTATTTACGGTAAACTGCCCACTTGGCAGTACATCAAGTGTATCATAT
GCCAAGTACGCCCCCTATTGACGTCAATGACGGTAAATGGCCCGCCTGGCATTATGCCCAGTACATGACCTTATGGGACT
TTCCTACTTGGCAGTACATCTACGTATTAGTCATCGCTATTACCATGGTGATGCGGTTTTGGCAGTACATCAATGGGCGTG
GATAGCGGTTTGACTCACGGGGATTTCCAAGTCTCCACCCCATTGACGTCAATGGGAGTTTGTTTTGGCACCAAAATCAAC
GGGACTTTCCAAAATGTCGTAACAACTCCGCCCCATTGACGCAAATGGGCGGTAGGCGTGTACGGTGGGAGGTCTATATA
AGCAGAGCTGGTTTAGTGAACCGTCAGATCCGCTAGCGCTACCGGTCGCCACCATGGTGAGCAAGGGCGAGGAGGATAA
CATGGCCATCATCAAGGAGTTCATGCGCTTCAAGGTGCACATGGAGGGCTCCGTGAACGGCCACGAGTTCGAGATCGAG

GGCGAGGGCGAGGGCCGCCCCTACGAGGGCACCCAGACCGCCAAGCTGAAGGTGACCAAGGGTGGCCCCCTGCCCTT
CGCCTGGGACATCCTGTCCCCTCAGTTCATGTACGGCTCCAAGGCCTACGTGAAGCACCCCGCCGACATCCCCGACTAC
TTGAAGCTGTCCTTCCCCGAGGGCTTCAAGTGGGAGCGCGTGATGAACTTCGAGGACGGCGGCGTGGTGACCGTGACCC
AGGACTCCTCCCTGCAGGACGGCGAGTTCATCTACAAGGTGAAGCTGCGCGGCACCAACTTCCCCTCCGACGGCCCCGT
AATGCAGAAGAAGACCATGGGCTGGGAGGCCTCCTCCGAGCGGATGTACCCCGAGGACGGCGCCCTGAAGGGCGAGAT
CAAGCAGAGGCTGAAGCTGAAGGACGGCGGCCACTACGACGCTGAGGTCAAGACCACCTACAAGGCCAAGAAGCCCGT
GCAGCTGCCCGGCGCCTACAACGTCAACATCAAGTTGGACATCACCTCCCACAACGAGGACTACACCATCGTGGAACAG
TACGAACGCGCCGAGGGCCGCCACTCCACCGGCGGCATGGACGAGCTGTACAAGTCCGGACTCAGATCTATGGATCATT
CCCACCATATGGGGATGAGCTATATGGACTCCAACAGTACCATGCAACCTTCTCACCATCACCCAACCACTTCAGCCTCA
CACTCCCATGGTGGAGGAGACAGCAGCATGATGATGATGCCTATGACCTTCTACTTTGGCTTTAAGAATGTGGAACTACTG
TTTTCCGGTTTGGTGATCAATACAGCTGGAGAAATGGCTGGAGCTTTTGTGGCAGTGTTTTTACTAGCAATGTTCTATGAAG
GACTCAAGATAGCCCGAGAGAGCCTGCTGCGTAAGTCACAAGTCAGCATTCGCTACAATTCCATGCCTGTCCCAGGACCA
AATGGAACCATCCTTATGGAGACACACAAAACTGTTGGGCAACAGATGCTGAGCTTTCCTCACCTCCTGCAAACAGTGCT
GCACATCATCCAGGTGGTCATAAGCTACTTCCTCATGCTCATCTTCATGACCTACAACGGGTACCTCTGCATTGCAGTAGC
AGCAGGGGCCGGTACAGGATACTTCCTCTTCAGCTGGAAGAAGGCAGTGGTAGTGGATATCACAGAGCATTGCCATTGAA
AGCTTCGAATTCTGCAGTCGACGGTACCGCGGGCCCGGGATCCACCGGATCTAGATAACTGATCATAATCAGCCATACCA
CATTTGTAGAGGTTTTACTTGCTTTAAAAAACCTCCCACACCTCCCCCTGAACCTGAAACATAAAATGAATGCAATTGTTGT
TGTTAACTTGTTTATTGCAGCTTATAATGGTTACAAATAAAGCAATAGCATCACAAATTTCACAAATAAAGCATTTTTTTCACT
GCATTCTAGTTGTGGTTTGTCCAAACTCATCAATGTATCTTAACGCGTAAATTGTAAGCGTTAATATTTTGTTAAAATTCGCG
TTAAATTTTTGTTAAATCAGCTCATTTTTTAACCAATAGGCCGAAATCGGCAAAATCCCTTATAAATCAAAAGAATAGACCGA
GATAGGGTTGAGTGTTGTTCCAGTTTGGAACAAGAGTCCACTATTAAAGAACGTGGACTCCAACGTCAAAGGGCGAAAAAC
CGTCTATCAGGGCGATGGCCCACTACGTGAACCATCACCCTAATCAAGTTTTTTGGGGTCGAGGTGCCGTAAAGCACTAA
ATCGGAACCCTAAAGGGAGCCCCCGATTTAGAGCTTGACGGGGAAAGCCGGCGAACGTGGCGAGAAAGGAAGGGAAGAA
AGCGAAAGGAGCGGGCGCTAGGGCGCTGGCAAGTGTAGCGGTCACGCTGCGCGTAACCACCACACCCGCCGCGCTTAA
TGCGCCGCTACAGGGCGCGTCAGGTGGCACTTTTCGGGGAAATGTGCGCGGAACCCCTATTTGTTTATTTTTCTAAATAC
ATTCAAATATGTATCCGCTCATGAGACAATAACCCTGATAAATGCTTCAATAATATTGAAAAAGGAAGAGTCCTGAGGCGGA
AAGAACCAGCTGTGGAATGTGTGTCAGTTAGGGTGTGGAAAGTCCCCAGGCTCCCCAGCAGGCAGAAGTATGCAAAGCAT
GCATCTCAATTAGTCAGCAACCAGGTGTGGAAAGTCCCCAGGCTCCCCAGCAGGCAGAAGTATGCAAAGCATGCATCTCA
ATTAGTCAGCAACCATAGTCCCGCCCCTAACTCCGCCCATCCCGCCCCTAACTCCGCCCAGTTCCGCCCATTCTCCGCC
CCATGGCTGACTAATTTTTTTTATTTATGCAGAGGCCGAGGCCGCCTCGGCCTCTGAGCTATTCCAGAAGTAGTGAGGAG
GCTTTTTTGGAGGCCTAGGCTTTTGCAAAGATCGATCAAGAGACAGGATGAGGATCGTTTCGCATGATTGAACAAGATGGA
TTGCACGCAGGTTCTCCGGCCGCTTGGGTGGAGAGGCTATTCGGCTATGACTGGGCACAACAGACAATCGGCTGCTCTG
ATGCCGCCGTGTTCCGGCTGTCAGCGCAGGGGCGCCCGGTTCTTTTTGTCAAGACCGACCTGTCCGGTGCCCTGAATGA
ACTGCAAGACGAGGCAGCGCGGCTATCGTGGCTGGCCACGACGGGCGTTCCTTGCGCAGCTGTGCTCGACGTTGTCACT

GAAGCGGGAAGGGACTGGCTGCTATTGGGCGAAGTGCCGGGGCAGGATCTCCTGTCATCTCACCTTGCTCCTGCCGAGA
AAGTATCCATCATGGCTGATGCAATGCGGCGGCTGCATACGCTTGATCCGGCTACCTGCCCATTCGACCACCAAGCGAAA
CATCGCATCGAGCGAGCACGTACTCGGATGGAAGCCGGTCTTGTCGATCAGGATGATCTGGACGAAGAGCATCAGGGGC
TCGCGCCAGCCGAACTGTTCGCCAGGCTCAAGGCGAGCATGCCCGACGGCGAGGATCTCGTCGTGACCCATGGCGATG
CCTGCTTGCCGAATATCATGGTGGAAAATGGCCGCTTTTCTGGATTCATCGACTGTGGCCGGCTGGGTGTGGCGGACCG
CTATCAGGACATAGCGTTGGCTACCCGTGATATTGCTGAAGAGCTTGGCGGCGAATGGGCTGACCGCTTCCTCGTGCTTT
ACGGTATCGCCGCTCCCGATTCGCAGCGCATCGCCTTCTATCGCCTTCTTGACGAGTTCTTCTGAGCGGGACTCTGGGG
TTCGAAATGACCGACCAAGCGACGCCCAACCTGCCATCACGAGATTTCGATTCCACCGCCGCCTTCTATGAAAGGTTGGG
CTTCGGAATCGTTTTCCGGGACGCCGGCTGGATGATCCTCCAGCGCGGGGATCTCATGCTGGAGTTCTTCGCCCACCCT
AGGGGGAGGCTAACTGAAACACGGAAGGAGACAATACCGGAAGGAACCCGCGCTATGACGGCAATAAAAAGACAGAATAA
AACGCACGGTGTTGGGTCGTTTGTTCATAAACGCGGGGTTCGGTCCCAGGGCTGGCACTCTGTCGATACCCCACCGAGA
CCCCATTGGGGCCAATACGCCCGCGTTTCTTCCTTTTCCCCACCCCACCCCCCAAGTTCGGGTGAAGGCCCAGGGCTCG
CAGCCAACGTCGGGGCGGCAGGCCCTGCCATAGCCTCAGGTTACTCATATATACTTTAGATTGATTTAAAACTTCATTTTT
AATTTAAAAGGATCTAGGTGAAGATCCTTTTTGATAATCTCATGACCAAAATCCCTTAACGTGAGTTTTCGTTCCACTGAGC
GTCAGACCCCGTAGAAAAGATCAAAGGATCTTCTTGAGATCCTTTTTTTCTGCGCGTAATCTGCTGCTTGCAAACAAAAAAA
CCACCGCTACCAGCGGTGGTTTGTTTGCCGGATCAAGAGCTACCAACTCTTTTTCCGAAGGTAACTGGCTTCAGCAGAGC
GCAGATACCAAATACTGTTCTTCTAGTGTAGCCGTAGTTAGGCCACCACTTCAAGAACTCTGTAGCACCGCCTACATACCT
CGCTCTGCTAATCCTGTTACCAGTGGCTGCTGCCAGTGGCGATAAGTCGTGTCTTACCGGGTTGGACTCAAGACGATAGT
TACCGGATAAGGCGCAGCGGTCGGGCTGAACGGGGGGTTCGTGCACACAGCCCAGCTTGGAGCGAACGACCTACACCG
AACTGAGATACCTACAGCGTGAGCTATGAGAAAGCGCCACGCTTCCCGAAGGGAGAAAGGCGGACAGGTATCCGGTAAG
CGGCAGGGTCGGAACAGGAGAGCGCACGAGGGAGCTTCCAGGGGGAAACGCCTGGTATCTTTATAGTCCTGTCGGGTTT
CGCCACCTCTGACTTGAGCGTCGATTTTTGTGATGCTCGTCAGGGGGGCGGAGCCTATGGAAAAACGCCAGCAACGCGG
CCTTTTTACGGTTCCTGGCCTTTTGCTGGCCTTTTGCTCACATGTTCTTTCCTGCGTTATCCCCTGATTCTGTGGATAACC
GTATTACCGCCATGCAT

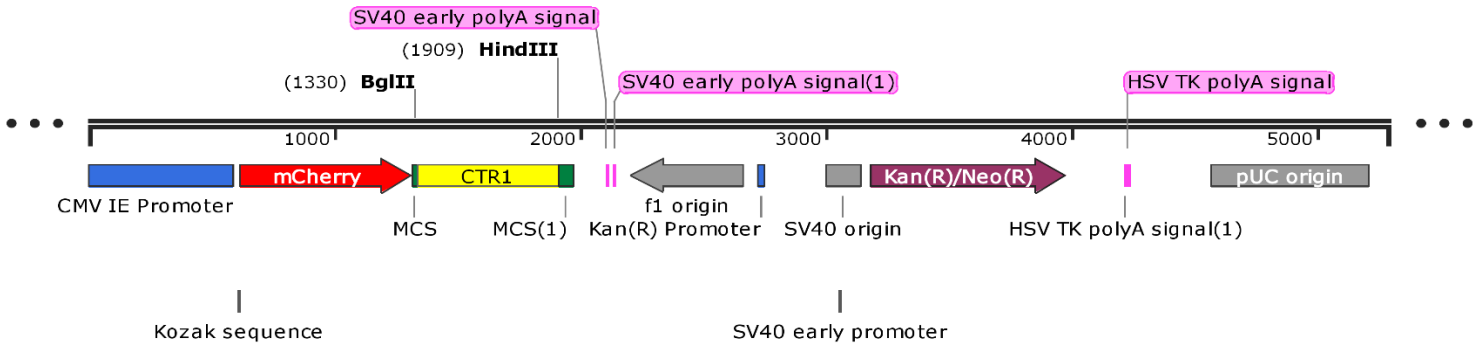

Figure 32: Horizontal map of pmCherry-CTR1. The relevant features are highlighted, such as CMV IE Promoter (human cytomegalovirus-immediate early promoter), CTR1 (human *CTR1* sequence), MCS (Multiple

Cloning Site), restriction sites for *Bgl*II and *Hind*III enzymes, SV40 origin (SV40 origin of replication induces replication within mammalian cells), Kan(R)/Neo(R) (this feature confers resistance to kanamycin or neomycin) and pUC origin (plasmid origin of replication). This map was constructed using SnapGene version 3.1.1.

3. pCTR2-mCherry

TAGTTATTAATAGTAATCAATTACGGGGTCATTAGTTCATAGCCCATATATGGAGTTCCGCGTTACATAACTTACGG
TAAATGGCCCGCCTGGCTGACCGCCCAACGACCCCCGCCCATTGACGTCAATAATGACGTATGTTCCCATAGTAACGCC
AATAGGGACTTTCCATTGACGTCAATGGGTGGAGTATTTACGGTAAACTGCCCACTTGGCAGTACATCAAGTGTATCATAT
GCCAAGTACGCCCCCTATTGACGTCAATGACGGTAAATGGCCCGCCTGGCATTATGCCCAGTACATGACCTTATGGGACT
TTCCTACTTGGCAGTACATCTACGTATTAGTCATCGCTATTACCATGGTGATGCGGTTTTGGCAGTACATCAATGGGCGTG
GATAGCGGTTTGACTCACGGGGATTTCCAAGTCTCCACCCCATTGACGTCAATGGGAGTTTGTTTTGGCACCAAAATCAAC
GGGACTTTCCAAAATGTCGTAACAACTCCGCCCCATTGACGCAAATGGGCGGTAGGCGTGTACGGTGGGAGGTCTATATA
AGCAGAGCTGGTTTAGTGAACCGTCAGATCCGCTAGCGCTACCGGACTCAGATCTATGGCGATGCATTTCATCTTCTCAG
ATACAGCGGTGCTTCTGTTTGATTTCTGGAGTGTCCACAGTCCTGCTGGCATGGCCCTTTCGGTGTTGGTGCTCCTGCTT
CTGGCTGTACTGTATGAAGGCATCAAGGTTGGCAAAGCCAAGCTGCTCAACCAGGTACTGGTGAACCTGCCAACCTCCAT
CAGCCAGCAGACCATCGCAGAGACAGACGGGGACTCTGCAGGCTCAGATTCATTCCCTGTTGGCAGAACCCACCACAGG
TGGTATTTGTGTCACTTTGGCCAGTCTCTAATCCATGTCATCCAGGTGGTCATCGGCTACTTCATCATGCTGGCCGTAATG
TCCTACAACACCTGGATTTTCCTTGGTGTGGTCTTGGGCTCTGCTGTGGGCTACTACCTAGCTTACCCACTTCTCAGCACA
GCTAAGCTTCGAATTCTGCAGTCGACGGTACCGCGGGCCCGGGATCCACCGGTCGCCACCATGGTGAGCAAGGGCGAG
GAGGATAACATGGCCATCATCAAGGAGTTCATGCGCTTCAAGGTGCACATGGAGGGCTCCGTGAACGGCCACGAGTTCG
AGATCGAGGGCGAGGGCGAGGGCCGCCCCTACGAGGGCACCCAGACCGCCAAGCTGAAGGTGACCAAGGGTGGCCCC
CTGCCCTTCGCCTGGGACATCCTGTCCCCTCAGTTCATGTACGGCTCCAAGGCCTACGTGAAGCACCCCGCCGACATCC
CCGACTACTTGAAGCTGTCCTTCCCCGAGGGCTTCAAGTGGGAGCGCGTGATGAACTTCGAGGACGGCGGCGTGGTGAC
CGTGACCCAGGACTCCTCCCTGCAGGACGGCGAGTTCATCTACAAGGTGAAGCTGCGCGGCACCAACTTCCCCTCCGAC
GGCCCCGTAATGCAGAAGAAGACCATGGGCTGGGAGGCCTCCTCCGAGCGGATGTACCCCGAGGACGGCGCCCTGAAG
GGCGAGATCAAGCAGAGGCTGAAGCTGAAGGACGGCGGCCACTACGACGCTGAGGTCAAGACCACCTACAAGGCCAAGA
AGCCCGTGCAGCTGCCCGGCGCCTACAACGTCAACATCAAGTTGGACATCACCTCCCACAACGAGGACTACACCATCGT
GGAACAGTACGAACGCGCCGAGGGCCGCCACTCCACCGGCGGCATGGACGAGCTGTACAAGTAGCGGCCGCGACTCTA
GATCATAATCAGCCATACCACATTTGTAGAGGTTTTACTTGCTTTAAAAAACCTCCCACACCTCCCCCTGAACCTGAAACA
TAAAATGAATGCAATTGTTGTTGTTAACTTGTTTATTGCAGCTTATAATGGTTACAAATAAAGCAATAGCATCACAAATTTCA
CAAATAAAGCATTTTTTTCACTGCATTCTAGTTGTGGTTTGTCCAAACTCATCAATGTATCTTAAGGCGTAAATTGTAAGCGT
TAATATTTTGTTAAAATTCGCGTTAAATTTTTGTTAAATCAGCTCATTTTTTAACCAATAGGCCGAAATCGGCAAAATCCCTT
ATAAATCAAAAGAATAGACCGAGATAGGGTTGAGTGTTGTTCCAGTTTGGAACAAGAGTCCACTATTAAAGAACGTGGACT

CCAACGTCAAAGGGCGAAAAACCGTCTATCAGGGCGATGGCCCACTACGTGAACCATCACCCTAATCAAGTTTTTTGGGG
TCGAGGTGCCGTAAAGCACTAAATCGGAACCCTAAAGGGAGCCCCCGATTTAGAGCTTGACGGGGAAAGCCGGCGAACG
TGGCGAGAAAGGAAGGGAAGAAAGCGAAAGGAGCGGGCGCTAGGGCGCTGGCAAGTGTAGCGGTCACGCTGCGCGTAA
CCACCACACCCGCCGCGCTTAATGCGCCGCTACAGGGCGCGTCAGGTGGCACTTTTCGGGGAAATGTGCGCGGAACCC
CTATTTGTTTATTTTTCTAAATACATTCAAATATGTATCCGCTCATGAGACAATAACCCTGATAAATGCTTCAATAATATTGAA
AAAGGAAGAGTCCTGAGGCGGAAAGAACCAGCTGTGGAATGTGTGTCAGTTAGGGTGTGGAAAGTCCCCAGGCTCCCCA
GCAGGCAGAAGTATGCAAAGCATGCATCTCAATTAGTCAGCAACCAGGTGTGGAAAGTCCCCAGGCTCCCCAGCAGGCA
GAAGTATGCAAAGCATGCATCTCAATTAGTCAGCAACCATAGTCCCGCCCCTAACTCCGCCCATCCCGCCCCTAACTCCG
CCCAGTTCCGCCCATTCTCCGCCCCATGGCTGACTAATTTTTTTTATTTATGCAGAGGCCGAGGCCGCCTCGGCCTCTGA
GCTATTCCAGAAGTAGTGAGGAGGCTTTTTTGGAGGCCTAGGCTTTTGCAAAGATCGATCAAGAGACAGGATGAGGATCGT
TTCGCATGATTGAACAAGATGGATTGCACGCAGGTTCTCCGGCCGCTTGGGTGGAGAGGCTATTCGGCTATGACTGGGCA
CAACAGACAATCGGCTGCTCTGATGCCGCCGTGTTCCGGCTGTCAGCGCAGGGGCGCCCGGTTCTTTTTGTCAAGACCG
ACCTGTCCGGTGCCCTGAATGAACTGCAAGACGAGGCAGCGCGGCTATCGTGGCTGGCCACGACGGGCGTTCCTTGCG
CAGCTGTGCTCGACGTTGTCACTGAAGCGGGAAGGGACTGGCTGCTATTGGGCGAAGTGCCGGGGCAGGATCTCCTGTC
ATCTCACCTTGCTCCTGCCGAGAAAGTATCCATCATGGCTGATGCAATGCGGCGGCTGCATACGCTTGATCCGGCTACCT
GCCCATTCGACCACCAAGCGAAACATCGCATCGAGCGAGCACGTACTCGGATGGAAGCCGGTCTTGTCGATCAGGATGA
TCTGGACGAAGAGCATCAGGGGCTCGCGCCAGCCGAACTGTTCGCCAGGCTCAAGGCGAGCATGCCCGACGGCGAGGA
TCTCGTCGTGACCCATGGCGATGCCTGCTTGCCGAATATCATGGTGGAAAATGGCCGCTTTTCTGGATTCATCGACTGTG
GCCGGCTGGGTGTGGCGGACCGCTATCAGGACATAGCGTTGGCTACCCGTGATATTGCTGAAGAGCTTGGCGGCGAATG
GGCTGACCGCTTCCTCGTGCTTTACGGTATCGCCGCTCCCGATTCGCAGCGCATCGCCTTCTATCGCCTTCTTGACGAGT
TCTTCTGAGCGGGACTCTGGGGTTCGAAATGACCGACCAAGCGACGCCCAACCTGCCATCACGAGATTTCGATTCCACC
GCCGCCTTCTATGAAAGGTTGGGCTTCGGAATCGTTTTCCGGGACGCCGGCTGGATGATCCTCCAGCGCGGGGATCTCA
TGCTGGAGTTCTTCGCCCACCCTAGGGGGAGGCTAACTGAAACACGGAAGGAGACAATACCGGAAGGAACCCGCGCTAT
GACGGCAATAAAAAGACAGAATAAAACGCACGGTGTTGGGTCGTTTGTTCATAAACGCGGGGTTCGGTCCCAGGGCTGGC
ACTCTGTCGATACCCCACCGAGACCCCATTGGGGCCAATACGCCCGCGTTTCTTCCTTTTCCCCACCCCACCCCCCAAG
TTCGGGTGAAGGCCCAGGGCTCGCAGCCAACGTCGGGGCGGCAGGCCCTGCCATAGCCTCAGGTTACTCATATATACTT
TAGATTGATTTAAAACTTCATTTTTAATTTAAAAGGATCTAGGTGAAGATCCTTTTTGATAATCTCATGACCAAAATCCCTTAA
CGTGAGTTTTCGTTCCACTGAGCGTCAGACCCCGTAGAAAAGATCAAAGGATCTTCTTGAGATCCTTTTTTTCTGCGCGTA
ATCTGCTGCTTGCAAACAAAAAAACCACCGCTACCAGCGGTGGTTTGTTTGCCGGATCAAGAGCTACCAACTCTTTTTCCG
AAGGTAACTGGCTTCAGCAGAGCGCAGATACCAAATACTGTTCTTCTAGTGTAGCCGTAGTTAGGCCACCACTTCAAGAAC
TCTGTAGCACCGCCTACATACCTCGCTCTGCTAATCCTGTTACCAGTGGCTGCTGCCAGTGGCGATAAGTCGTGTCTTAC
CGGGTTGGACTCAAGACGATAGTTACCGGATAAGGCGCAGCGGTCGGGCTGAACGGGGGGTTCGTGCACACAGCCCAG
CTTGGAGCGAACGACCTACACCGAACTGAGATACCTACAGCGTGAGCTATGAGAAAGCGCCACGCTTCCCGAAGGGAGA
AAGGCGGACAGGTATCCGGTAAGCGGCAGGGTCGGAACAGGAGAGCGCACGAGGGAGCTTCCAGGGGGAAACGCCTGG

TATCTTTATAGTCCTGTCGGGTTTCGCCACCTCTGACTTGAGCGTCGATTTTTGTGATGCTCGTCAGGGGGGCGGAGCCT
ATGGAAAAACGCCAGCAACGCGGCCTTTTTACGGTTCCTGGCCTTTTGCTGGCCTTTTGCTCACATGTTCTTTCCTGCGTT
ATCCCCTGATTCTGTGGATAACCGTATTACCGCCATGCAT

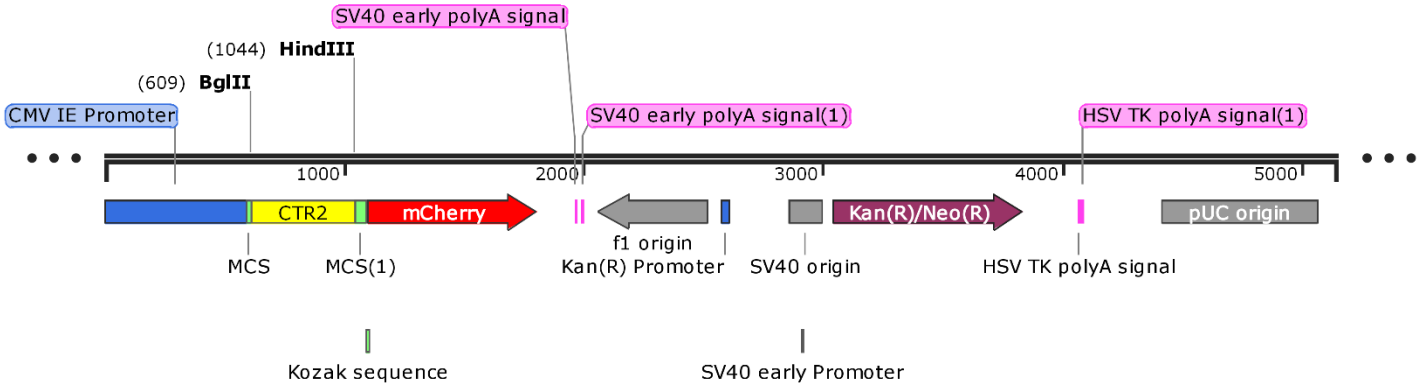

Figure 33: Horizontal map of pCTR2-mCherry. The relevant features are highlighted, such as CMV IE Promoter (human cytomegalovirus-immediate early promoter), CTR2 (human *CTR2* sequence), MCS (Multiple Cloning Site), restriction sites for *Bgl*II and *Hind*III enzymes, SV40 origin (SV40 origin of replication induces replication within mammalian cells), Kan(R)/Neo(R) (this feature confers resistance to kanamycin or neomycin) and pUC origin (plasmid origin of replication). This map was constructed using SnapGene version 3.1.1.

4. pCTR2-AcGFP

TAGTTATTAATAGTAATCAATTACGGGGTCATTAGTTCATAGCCCATATATGGAGTTCCGCGTTACATAACTTACGG
TAAATGGCCCGCCTGGCTGACCGCCCAACGACCCCCGCCCATTGACGTCAATAATGACGTATGTTCCCATAGTAACGCC
AATAGGGACTTTCCATTGACGTCAATGGGTGGAGTATTTACGGTAAACTGCCCACTTGGCAGTACATCAAGTGTATCATAT
GCCAAGTACGCCCCCTATTGACGTCAATGACGGTAAATGGCCCGCCTGGCATTATGCCCAGTACATGACCTTATGGGACT
TTCCTACTTGGCAGTACATCTACGTATTAGTCATCGCTATTACCATGGTGATGCGGTTTTGGCAGTACATCAATGGGCGTG
GATAGCGGTTTGACTCACGGGGATTTCCAAGTCTCCACCCCATTGACGTCAATGGGAGTTTGTTTTGGCACCAAAATCAAC
GGGACTTTCCAAAATGTCGTAACAACTCCGCCCCATTGACGCAAATGGGCGGTAGGCGTGTACGGTGGGAGGTCTATATA
AGCAGAGCTGGTTTAGTGAACCGTCAGATCCGCTAGCGCTACCGGACTCAGATCTATGGCGATGCATTTCATCTTCTCAG
ATACAGCGGTGCTTCTGTTTGATTTCTGGAGTGTCCACAGTCCTGCTGGCATGGCCCTTTCGGTGTTGGTGCTCCTGCTT
CTGGCTGTACTGTATGAAGGCATCAAGGTTGGCAAAGCCAAGCTGCTCAACCAGGTACTGGTGAACCTGCCAACCTCCAT
CAGCCAGCAGACCATCGCAGAGACAGACGGGGACTCTGCAGGCTCAGATTCATTCCCTGTTGGCAGAACCCACCACAGG
TGGTATTTGTGTCACTTTGGCCAGTCTCTAATCCATGTCATCCAGGTGGTCATCGGCTACTTCATCATGCTGGCCGTAATG
TCCTACAACACCTGGATTTTCCTTGGTGTGGTCTTGGGCTCTGCTGTGGGCTACTACCTAGCTTACCCACTTCTCAGCACA
GCTAAGCTTCGAATTCTGCAGTCGACGGTACCGCGGGCCCGGGATCCACCGGTCATGGTGAGCAAGGGCGCCGAGCTGT
TCACCGGCATCGTGCCCATCCTGATCGAGCTGAATGGCGATGTGAATGGCCACAAGTTCAGCGTGAGCGGCGAGGGCGA

GGGCGATGCCACCTACGGCAAGCTGACCCTGAAGTTCATCTGCACCACCGGCAAGCTGCCTGTGCCCTGGCCCACCCT
GGTGACCACCCTGAGCTACGGCGTGCAGTGCTTCTCACGCTACCCCGATCACATGAAGCAGCACGACTTCTTCAAGAGC
GCCATGCCTGAGGGCTACATCCAGGAGCGCACCATCTTCTTCGAGGATGACGGCAACTACAAGTCGCGCGCCGAGGTGA
AGTTCGAGGGCGATACCCTGGTGAATCGCATCGAGCTGACCGGCACCGATTTCAAGGAGGATGGCAACATCCTGGGCAA
TAAGATGGAGTACAACTACAACGCCCACAATGTGTACATCATGACCGACAAGGCCAAGAATGGCATCAAGGTGAACTTCAA
GATCCGCCACAACATCGAGGATGGCAGCGTGCAGCTGGCCGACCACTACCAGCAGAATACCCCCATCGGCGATGGCCC
TGTGCTGCTGCCCGATAACCACTACCTGTCCACCCAGAGCGCCCTGTCCAAGGACCCCAACGAGAAGCGCGATCACATG
ATCTACTTCGGCTTCGTGACCGCCGCCGCCATCACCCACGGCATGGATGAGCTGTACAAGTGAGCGGCCGCGACTCTAG
ATCATAATCAGCCATACCACATTTGTAGAGGTTTTACTTGCTTTAAAAAACCTCCCACACCTCCCCCTGAACCTGAAACATA
AAATGAATGCAATTGTTGTTGTTAACTTGTTTATTGCAGCTTATAATGGTTACAAATAAAGCAATAGCATCACAAATTTCACA
AATAAAGCATTTTTTTCACTGCATTCTAGTTGTGGTTTGTCCAAACTCATCAATGTATCTTAAGGCGTAAATTGTAAGCGTTA
ATATTTTGTTAAAATTCGCGTTAAATTTTTGTTAAATCAGCTCATTTTTTAACCAATAGGCCGAAATCGGCAAAATCCCTTAT
AAATCAAAAGAATAGACCGAGATAGGGTTGAGTGTTGTTCCAGTTTGGAACAAGAGTCCACTATTAAAGAACGTGGACTCC
AACGTCAAAGGGCGAAAAACCGTCTATCAGGGCGATGGCCCACTACGTGAACCATCACCCTAATCAAGTTTTTTGGGGTC
GAGGTGCCGTAAAGCACTAAATCGGAACCCTAAAGGGAGCCCCCGATTTAGAGCTTGACGGGGAAAGCCGGCGAACGTG
GCGAGAAAGGAAGGGAAGAAAGCGAAAGGAGCGGGCGCTAGGGCGCTGGCAAGTGTAGCGGTCACGCTGCGCGTAACC
ACCACACCCGCCGCGCTTAATGCGCCGCTACAGGGCGCGTCAGGTGGCACTTTTCGGGGAAATGTGCGCGGAACCCCT
ATTTGTTTATTTTTCTAAATACATTCAAATATGTATCCGCTCATGAGACAATAACCCTGATAAATGCTTCAATAATATTGAAAA
AGGAAGAGTCCTGAGGCGGAAAGAACCAGCTGTGGAATGTGTGTCAGTTAGGGTGTGGAAAGTCCCCAGGCTCCCCAGC
AGGCAGAAGTATGCAAAGCATGCATCTCAATTAGTCAGCAACCAGGTGTGGAAAGTCCCCAGGCTCCCCAGCAGGCAGAA
GTATGCAAAGCATGCATCTCAATTAGTCAGCAACCATAGTCCCGCCCCTAACTCCGCCCATCCCGCCCCTAACTCCGCC
CAGTTCCGCCCATTCTCCGCCCCATGGCTGACTAATTTTTTTTATTTATGCAGAGGCCGAGGCCGCCTCGGCCTCTGAGC
TATTCCAGAAGTAGTGAGGAGGCTTTTTTGGAGGCCTAGGCTTTTGCAAAGATCGATCAAGAGACAGGATGAGGATCGTTT
CGCATGATTGAACAAGATGGATTGCACGCAGGTTCTCCGGCCGCTTGGGTGGAGAGGCTATTCGGCTATGACTGGGCACA
ACAGACAATCGGCTGCTCTGATGCCGCCGTGTTCCGGCTGTCAGCGCAGGGGCGCCCGGTTCTTTTTGTCAAGACCGAC
CTGTCCGGTGCCCTGAATGAACTGCAAGACGAGGCAGCGCGGCTATCGTGGCTGGCCACGACGGGCGTTCCTTGCGCA
GCTGTGCTCGACGTTGTCACTGAAGCGGGAAGGGACTGGCTGCTATTGGGCGAAGTGCCGGGGCAGGATCTCCTGTCAT
CTCACCTTGCTCCTGCCGAGAAAGTATCCATCATGGCTGATGCAATGCGGCGGCTGCATACGCTTGATCCGGCTACCTGC
CCATTCGACCACCAAGCGAAACATCGCATCGAGCGAGCACGTACTCGGATGGAAGCCGGTCTTGTCGATCAGGATGATCT
GGACGAAGAGCATCAGGGGCTCGCGCCAGCCGAACTGTTCGCCAGGCTCAAGGCGAGCATGCCCGACGGCGAGGATCT
CGTCGTGACCCATGGCGATGCCTGCTTGCCGAATATCATGGTGGAAAATGGCCGCTTTTCTGGATTCATCGACTGTGGCC
GGCTGGGTGTGGCGGACCGCTATCAGGACATAGCGTTGGCTACCCGTGATATTGCTGAAGAGCTTGGCGGCGAATGGGC
TGACCGCTTCCTCGTGCTTTACGGTATCGCCGCTCCCGATTCGCAGCGCATCGCCTTCTATCGCCTTCTTGACGAGTTCT
TCTGAGCGGGACTCTGGGGTTCGAAATGACCGACCAAGCGACGCCCAACCTGCCATCACGAGATTTCGATTCCACCGCC

GCCTTCTATGAAAGGTTGGGCTTCGGAATCGTTTTCCGGGACGCCGGCTGGATGATCCTCCAGCGCGGGGATCTCATGC
TGGAGTTCTTCGCCCACCCTAGGGGGAGGCTAACTGAAACACGGAAGGAGACAATACCGGAAGGAACCCGCGCTATGAC
GGCAATAAAAAGACAGAATAAAACGCACGGTGTTGGGTCGTTTGTTCATAAACGCGGGGTTCGGTCCCAGGGCTGGCACT
CTGTCGATACCCCACCGAGACCCCATTGGGGCCAATACGCCCGCGTTTCTTCCTTTTCCCCACCCCACCCCCCAAGTTC
GGGTGAAGGCCCAGGGCTCGCAGCCAACGTCGGGGCGGCAGGCCCTGCCATAGCCTCAGGTTACTCATATATACTTTAG
ATTGATTTAAAACTTCATTTTTAATTTAAAAGGATCTAGGTGAAGATCCTTTTTGATAATCTCATGACCAAAATCCCTTAACG
TGAGTTTTCGTTCCACTGAGCGTCAGACCCCGTAGAAAAGATCAAAGGATCTTCTTGAGATCCTTTTTTTCTGCGCGTAAT
CTGCTGCTTGCAAACAAAAAAACCACCGCTACCAGCGGTGGTTTGTTTGCCGGATCAAGAGCTACCAACTCTTTTTCCGAA
GGTAACTGGCTTCAGCAGAGCGCAGATACCAAATACTGTTCTTCTAGTGTAGCCGTAGTTAGGCCACCACTTCAAGAACTC
TGTAGCACCGCCTACATACCTCGCTCTGCTAATCCTGTTACCAGTGGCTGCTGCCAGTGGCGATAAGTCGTGTCTTACCG
GGTTGGACTCAAGACGATAGTTACCGGATAAGGCGCAGCGGTCGGGCTGAACGGGGGGTTCGTGCACACAGCCCAGCTT
GGAGCGAACGACCTACACCGAACTGAGATACCTACAGCGTGAGCTATGAGAAAGCGCCACGCTTCCCGAAGGGAGAAAG
GCGGACAGGTATCCGGTAAGCGGCAGGGTCGGAACAGGAGAGCGCACGAGGGAGCTTCCAGGGGGAAACGCCTGGTAT
CTTTATAGTCCTGTCGGGTTTCGCCACCTCTGACTTGAGCGTCGATTTTTGTGATGCTCGTCAGGGGGGCGGAGCCTATG
GAAAAACGCCAGCAACGCGGCCTTTTTACGGTTCCTGGCCTTTTGCTGGCCTTTTGCTCACATGTTCTTTCCTGCGTTATC
CCCTGATTCTGTGGATAACCGTATTACCGCCATGCAT

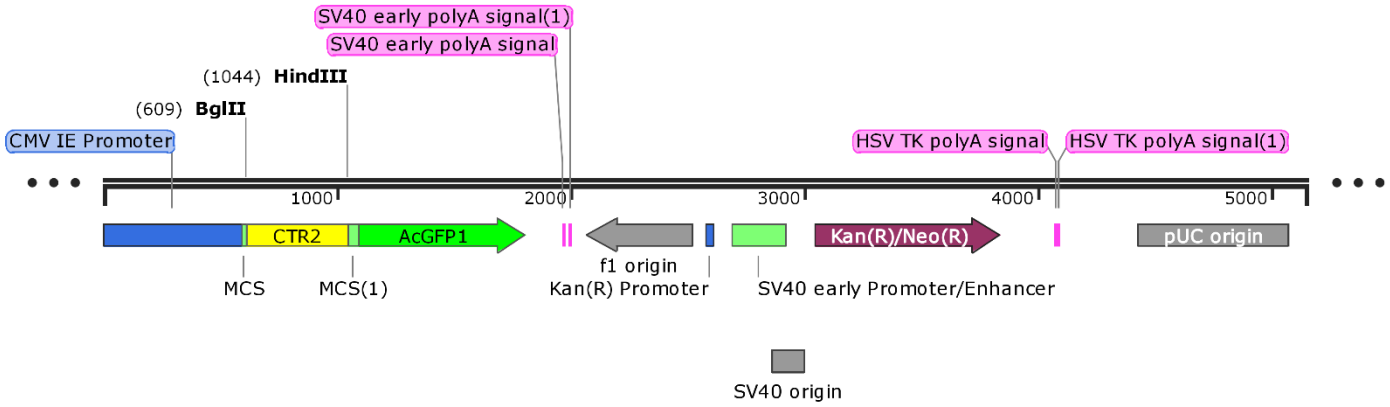

Figure 34: Horizontal map of pCTR2-AcGFP. The relevant features are highlighted, such as CMV IE Promoter (human cytomegalovirus-immediate early promoter), CTR2 (human *CTR2* sequence), MCS (Multiple Cloning Site), restriction sites for *Bgl*II and *Hind*III enzymes, SV40 origin (SV40 origin of replication induces replication within mammalian cells), Kan(R)/Neo(R) (this feature confers resistance to kanamycin or neomycin) and pUC origin (plasmid origin of replication). This map was constructed using SnapGene version 3.1.1.

5. pAcGFP-CTR2

TAGTTATTAATAGTAATCAATTACGGGGTCATTAGTTCATAGCCCATATATGGAGTTCCGCGTTACATAACTTACGG
TAAATGGCCCGCCTGGCTGACCGCCCAACGACCCCCGCCCATTGACGTCAATAATGACGTATGTTCCCATAGTAACGCC
AATAGGGACTTTCCATTGACGTCAATGGGTGGAGTATTTACGGTAAACTGCCCACTTGGCAGTACATCAAGTGTATCATAT
GCCAAGTACGCCCCCTATTGACGTCAATGACGGTAAATGGCCCGCCTGGCATTATGCCCAGTACATGACCTTATGGGACT
TTCCTACTTGGCAGTACATCTACGTATTAGTCATCGCTATTACCATGGTGATGCGGTTTTGGCAGTACATCAATGGGCGTG
GATAGCGGTTTGACTCACGGGGATTTCCAAGTCTCCACCCCATTGACGTCAATGGGAGTTTGTTTTGGCACCAAAATCAAC
GGGACTTTCCAAAATGTCGTAACAACTCCGCCCCATTGACGCAAATGGGCGGTAGGCGTGTACGGTGGGAGGTCTATATA
AGCAGAGCTGGTTTAGTGAACCGTCAGATCCGCTAGCGCTACCGGTCGCCACCATGGTGAGCAAGGGCGCCGAGCTGTT
CACCGGCATCGTGCCCATCCTGATCGAGCTGAATGGCGATGTGAATGGCCACAAGTTCAGCGTGAGCGGCGAGGGCGAG
GGCGATGCCACCTACGGCAAGCTGACCCTGAAGTTCATCTGCACCACCGGCAAGCTGCCTGTGCCCTGGCCCACCCTG
GTGACCACCCTGAGCTACGGCGTGCAGTGCTTCTCACGCTACCCCGATCACATGAAGCAGCACGACTTCTTCAAGAGCG
CCATGCCTGAGGGCTACATCCAGGAGCGCACCATCTTCTTCGAGGATGACGGCAACTACAAGTCGCGCGCCGAGGTGAA
GTTCGAGGGCGATACCCTGGTGAATCGCATCGAGCTGACCGGCACCGATTTCAAGGAGGATGGCAACATCCTGGGCAAT
AAGATGGAGTACAACTACAACGCCCACAATGTGTACATCATGACCGACAAGGCCAAGAATGGCATCAAGGTGAACTTCAA
GATCCGCCACAACATCGAGGATGGCAGCGTGCAGCTGGCCGACCACTACCAGCAGAATACCCCCATCGGCGATGGCCC
TGTGCTGCTGCCCGATAACCACTACCTGTCCACCCAGAGCGCCCTGTCCAAGGACCCCAACGAGAAGCGCGATCACATG
ATCTACTTCGGCTTCGTGACCGCCGCCGCCATCACCCACGGCATGGATGAGCTGTACAAGTCCGGACTCAGATCTATGG
CGATGCATTTCATCTTCTCAGATACAGCGGTGCTTCTGTTTGATTTCTGGAGTGTCCACAGTCCTGCTGGCATGGCCCTTT
CGGTGTTGGTGCTCCTGCTTCTGGCTGTACTGTATGAAGGCATCAAGGTTGGCAAAGCCAAGCTGCTCAACCAGGTACTG
GTGAACCTGCCAACCTCCATCAGCCAGCAGACCATCGCAGAGACAGACGGGGACTCTGCAGGCTCAGATTCATTCCCTG
TTGGCAGAACCCACCACAGGTGGTATTTGTGTCACTTTGGCCAGTCTCTAATCCATGTCATCCAGGTGGTCATCGGCTACT
TCATCATGCTGGCCGTAATGTCCTACAACACCTGGATTTTCCTTGGTGTGGTCTTGGGCTCTGCTGTGGGCTACTACCTAG
CTTACCCACTTCTCAGCACAGCTTAGAAGCTTCGAATTCTGCAGTCGACGGTACCGCGGGCCCGGGATCCACCGGATCT
AGATAACTGATCATAATCAGCCATACCACATTTGTAGAGGTTTTACTTGCTTTAAAAAACCTCCCACACCTCCCCCTGAAC
CTGAAACATAAAATGAATGCAATTGTTGTTGTTAACTTGTTTATTGCAGCTTATAATGGTTACAAATAAAGCAATAGCATCAC
AAATTTCACAAATAAAGCATTTTTTTCACTGCATTCTAGTTGTGGTTTGTCCAAACTCATCAATGTATCTTAACGCGTAAATT
GTAAGCGTTAATATTTTGTTAAAATTCGCGTTAAATTTTTGTTAAATCAGCTCATTTTTTAACCAATAGGCCGAAATCGGCAA
AATCCCTTATAAATCAAAAGAATAGACCGAGATAGGGTTGAGTGTTGTTCCAGTTTGGAACAAGAGTCCACTATTAAAGAAC
GTGGACTCCAACGTCAAAGGGCGAAAAACCGTCTATCAGGGCGATGGCCCACTACGTGAACCATCACCCTAATCAAGTTT
TTTGGGGTCGAGGTGCCGTAAAGCACTAAATCGGAACCCTAAAGGGAGCCCCCGATTTAGAGCTTGACGGGGAAAGCCG
GCGAACGTGGCGAGAAAGGAAGGGAAGAAAGCGAAAGGAGCGGGCGCTAGGGCGCTGGCAAGTGTAGCGGTCACGCTG
CGCGTAACCACCACACCCGCCGCGCTTAATGCGCCGCTACAGGGCGCGTCAGGTGGCACTTTTCGGGGAAATGTGCGC
GGAACCCCTATTTGTTTATTTTTCTAAATACATTCAAATATGTATCCGCTCATGAGACAATAACCCTGATAAATGCTTCAATA

ATATTGAAAAAGGAAGAGTCCTGAGGCGGAAAGAACCAGCTGTGGAATGTGTGTCAGTTAGGGTGTGGAAAGTCCCCAGG
CTCCCCAGCAGGCAGAAGTATGCAAAGCATGCATCTCAATTAGTCAGCAACCAGGTGTGGAAAGTCCCCAGGCTCCCCA
GCAGGCAGAAGTATGCAAAGCATGCATCTCAATTAGTCAGCAACCATAGTCCCGCCCCTAACTCCGCCCATCCCGCCCC
TAACTCCGCCCAGTTCCGCCCATTCTCCGCCCCATGGCTGACTAATTTTTTTTATTTATGCAGAGGCCGAGGCCGCCTCG
GCCTCTGAGCTATTCCAGAAGTAGTGAGGAGGCTTTTTTGGAGGCCTAGGCTTTTGCAAAGATCGATCAAGAGACAGGATG
AGGATCGTTTCGCATGATTGAACAAGATGGATTGCACGCAGGTTCTCCGGCCGCTTGGGTGGAGAGGCTATTCGGCTATG
ACTGGGCACAACAGACAATCGGCTGCTCTGATGCCGCCGTGTTCCGGCTGTCAGCGCAGGGGCGCCCGGTTCTTTTTGT
CAAGACCGACCTGTCCGGTGCCCTGAATGAACTGCAAGACGAGGCAGCGCGGCTATCGTGGCTGGCCACGACGGGCGT
TCCTTGCGCAGCTGTGCTCGACGTTGTCACTGAAGCGGGAAGGGACTGGCTGCTATTGGGCGAAGTGCCGGGGCAGGAT
CTCCTGTCATCTCACCTTGCTCCTGCCGAGAAAGTATCCATCATGGCTGATGCAATGCGGCGGCTGCATACGCTTGATCC
GGCTACCTGCCCATTCGACCACCAAGCGAAACATCGCATCGAGCGAGCACGTACTCGGATGGAAGCCGGTCTTGTCGAT
CAGGATGATCTGGACGAAGAGCATCAGGGGCTCGCGCCAGCCGAACTGTTCGCCAGGCTCAAGGCGAGCATGCCCGAC
GGCGAGGATCTCGTCGTGACCCATGGCGATGCCTGCTTGCCGAATATCATGGTGGAAAATGGCCGCTTTTCTGGATTCAT
CGACTGTGGCCGGCTGGGTGTGGCGGACCGCTATCAGGACATAGCGTTGGCTACCCGTGATATTGCTGAAGAGCTTGGC
GGCGAATGGGCTGACCGCTTCCTCGTGCTTTACGGTATCGCCGCTCCCGATTCGCAGCGCATCGCCTTCTATCGCCTTC
TTGACGAGTTCTTCTGAGCGGGACTCTGGGGTTCGAAATGACCGACCAAGCGACGCCCAACCTGCCATCACGAGATTTCG
ATTCCACCGCCGCCTTCTATGAAAGGTTGGGCTTCGGAATCGTTTTCCGGGACGCCGGCTGGATGATCCTCCAGCGCGG
GGATCTCATGCTGGAGTTCTTCGCCCACCCTAGGGGGAGGCTAACTGAAACACGGAAGGAGACAATACCGGAAGGAACC
CGCGCTATGACGGCAATAAAAAGACAGAATAAAACGCACGGTGTTGGGTCGTTTGTTCATAAACGCGGGGTTCGGTCCCA
GGGCTGGCACTCTGTCGATACCCCACCGAGACCCCATTGGGGCCAATACGCCCGCGTTTCTTCCTTTTCCCCACCCCAC
CCCCCAAGTTCGGGTGAAGGCCCAGGGCTCGCAGCCAACGTCGGGGCGGCAGGCCCTGCCATAGCCTCAGGTTACTCA
TATATACTTTAGATTGATTTAAAACTTCATTTTTAATTTAAAAGGATCTAGGTGAAGATCCTTTTTGATAATCTCATGACCAAA
ATCCCTTAACGTGAGTTTTCGTTCCACTGAGCGTCAGACCCCGTAGAAAAGATCAAAGGATCTTCTTGAGATCCTTTTTTTC
TGCGCGTAATCTGCTGCTTGCAAACAAAAAAACCACCGCTACCAGCGGTGGTTTGTTTGCCGGATCAAGAGCTACCAACT
CTTTTTCCGAAGGTAACTGGCTTCAGCAGAGCGCAGATACCAAATACTGTTCTTCTAGTGTAGCCGTAGTTAGGCCACCAC
TTCAAGAACTCTGTAGCACCGCCTACATACCTCGCTCTGCTAATCCTGTTACCAGTGGCTGCTGCCAGTGGCGATAAGTC
GTGTCTTACCGGGTTGGACTCAAGACGATAGTTACCGGATAAGGCGCAGCGGTCGGGCTGAACGGGGGGTTCGTGCACA
CAGCCCAGCTTGGAGCGAACGACCTACACCGAACTGAGATACCTACAGCGTGAGCTATGAGAAAGCGCCACGCTTCCCG
AAGGGAGAAAGGCGGACAGGTATCCGGTAAGCGGCAGGGTCGGAACAGGAGAGCGCACGAGGGAGCTTCCAGGGGGAA
ACGCCTGGTATCTTTATAGTCCTGTCGGGTTTCGCCACCTCTGACTTGAGCGTCGATTTTTGTGATGCTCGTCAGGGGGG
CGGAGCCTATGGAAAAACGCCAGCAACGCGGCCTTTTTACGGTTCCTGGCCTTTTGCTGGCCTTTTGCTCACATGTTCTTT
CCTGCGTTATCCCCTGATTCTGTGGATAACCGTATTACCGCCATGCAT

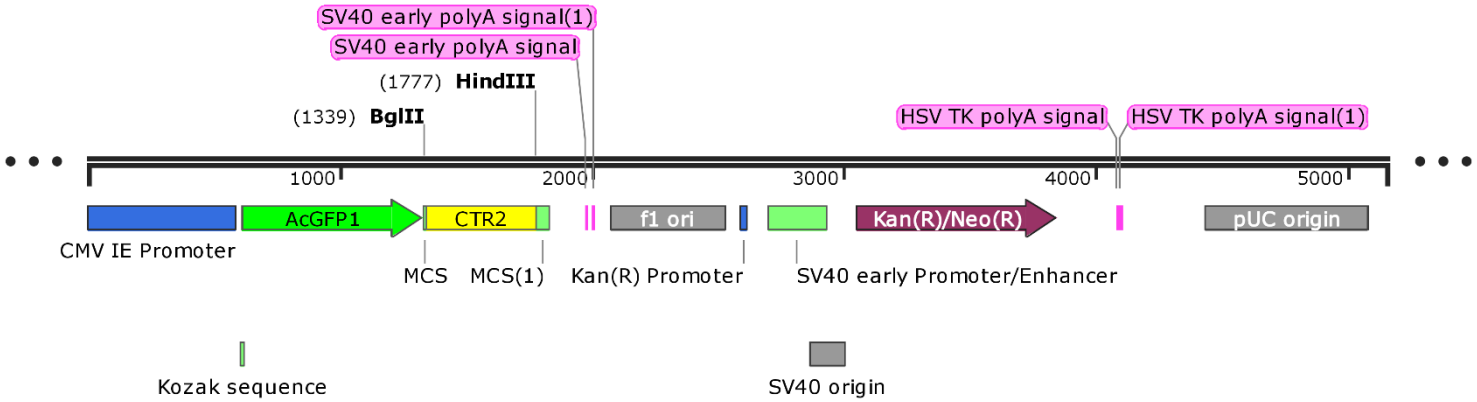

Figure 35: Horizontal map of pAcGFP-CTR2. The relevant features are highlighted, such as CMV IE Promoter (human cytomegalovirus-immediate early promoter), CTR2 (human *CTR2* sequence), MCS (Multiple Cloning Site), restriction sites for *Bgl*II and *Hind*III enzymes, SV40 origin (SV40 origin of replication induces replication within mammalian cells), Kan(R)/Neo(R) (this feature confers resistance to kanamycin or neomycin) and pUC origin (plasmid origin of replication). This map was constructed using SnapGene version 3.1.1.

VII. Appendix D: Sequencing results

To sequence the developed constructs, the plasmids were extracted and pre-mixed with specific primers and, finally, sent to Eurofins genomics. The six primers were designed following the strategy described in Figure 36. The constructs pCTR1-mCherry and pCTR2-mCherry were sequenced with Seq_FW_CMV and Seq_RV_CTR_mCherry. The construct pmCherry-CTR1 was sequenced with Seq_FW_mCherry_CTR and Seq_RV_TAG_CTR. The construct pCTR2-AcGFP was sequenced with Seq_FW_CMV and Seq_RV_CTR_GFP. The construct pAcGFP-CTR2 was sequenced with Seq_FW_GFP_CTR and Seq_RV_TAG_CTR. The first alignment results using the forward primers, and the second alignment corresponds to the sequencing results using the reverse primers (with correspondent reverse-complementary sequence).

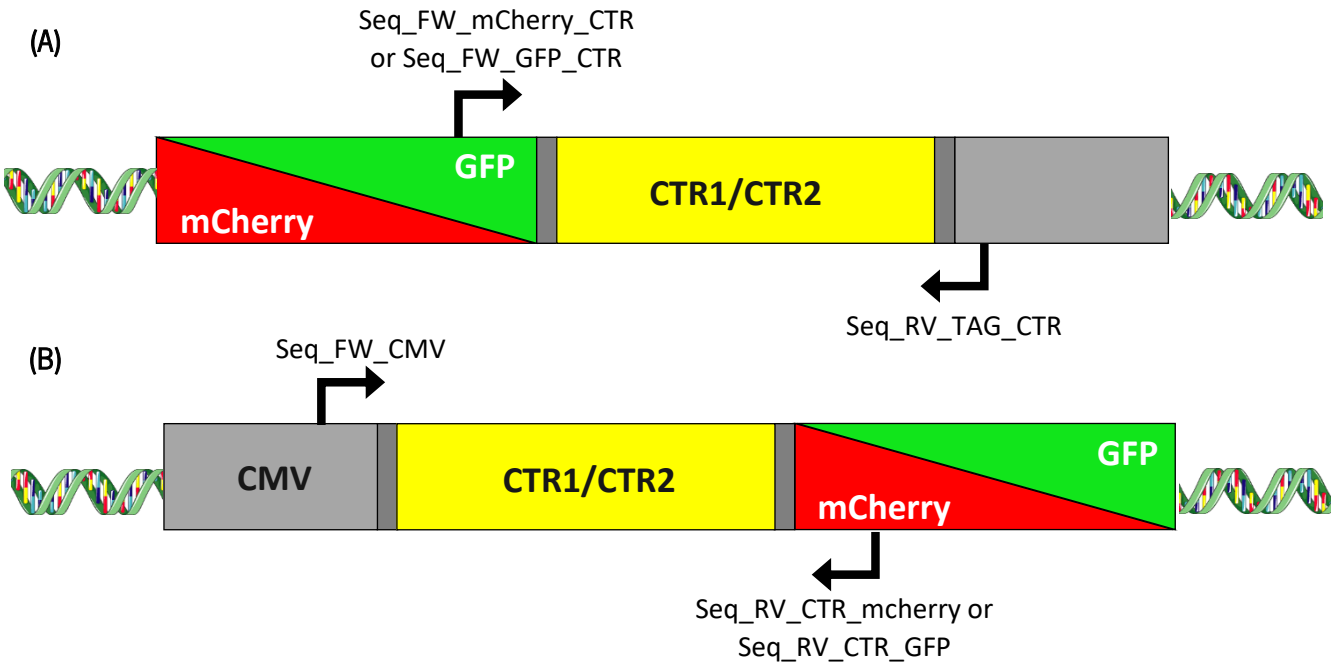

Figure 36: Schematic representation of the strategy for the design of the primers used for sequencing. All of the primers were designed considering the position in sequence of the tag. In Panel A are represented the primers used for sequencing pCTR1-mCherry, pCTR2-mCherry and pCTR2-AcGFP. In Panel B are represented the primers used for sequencing pmCherry-CTR1 and pAcGFP-CTR2.

1. pCTR1-mCherry

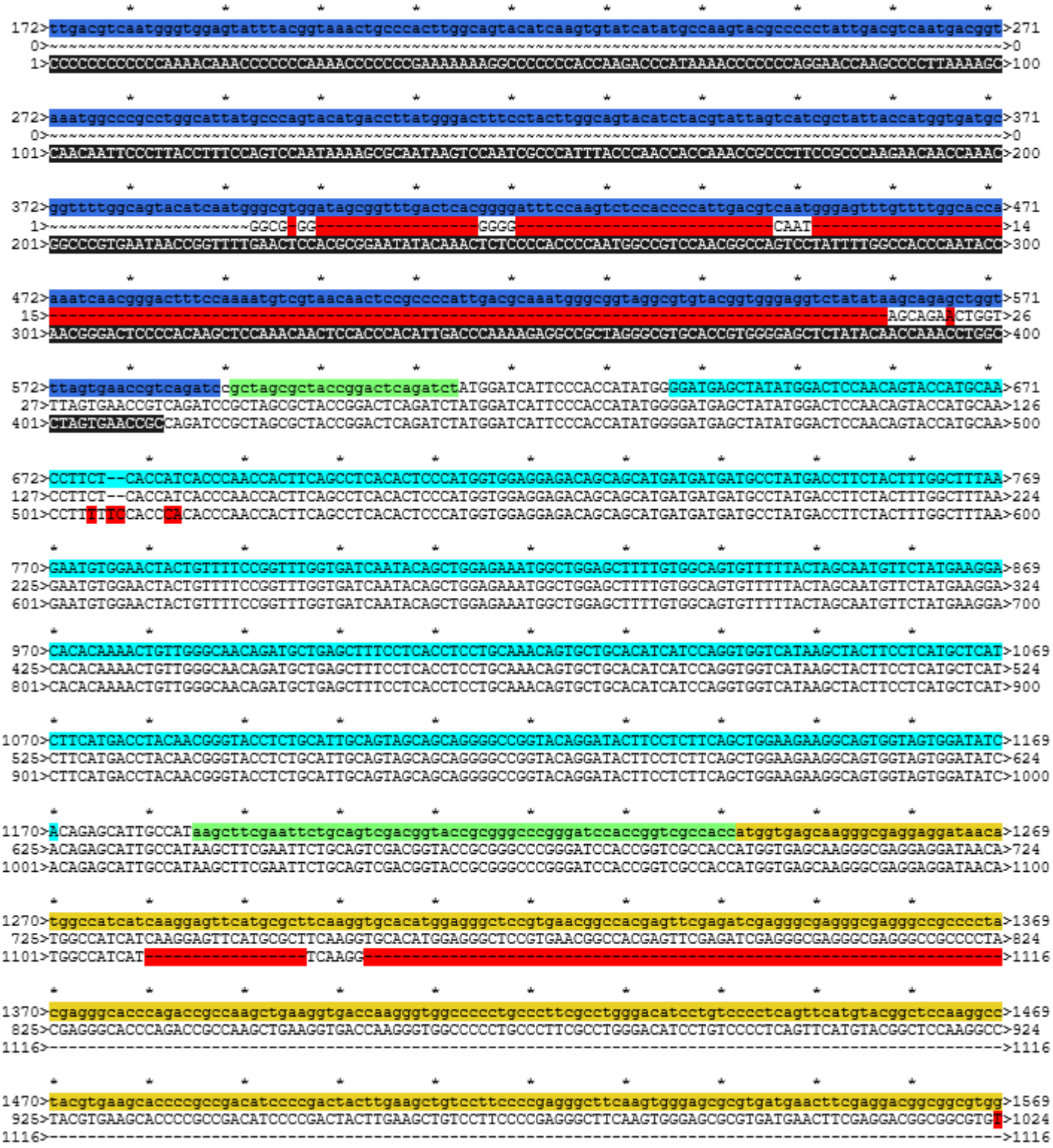

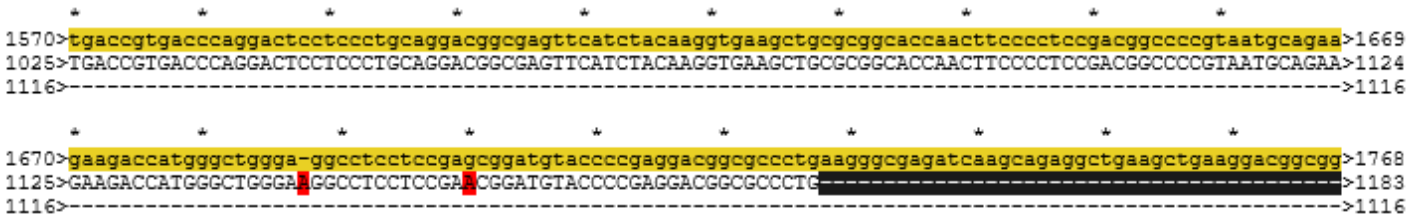

Figure 37: DNA Alignment of the pCTR1-mCherry predicted sequence with results obtained by sequencing of the pCTR1-mCherry plasmid using the Seq_FW_CMV and Seq_RV_CTR_mCherry. The alignment was performed using the ApE program (v2.0.61).

Through DNA alignment of the pCTR1-mCherry predicted sequence with the results obtained by sequencing of the pCTR1-mCherry plasmid using the Seq_FW_CMV and Seq_RV_CTR_mCherry, we can observe that the different mutations that appear in one sequence, are not present in the other. Therefore, it is expected that these mutations are sequencing errors.

2. pmCherry-CTR1

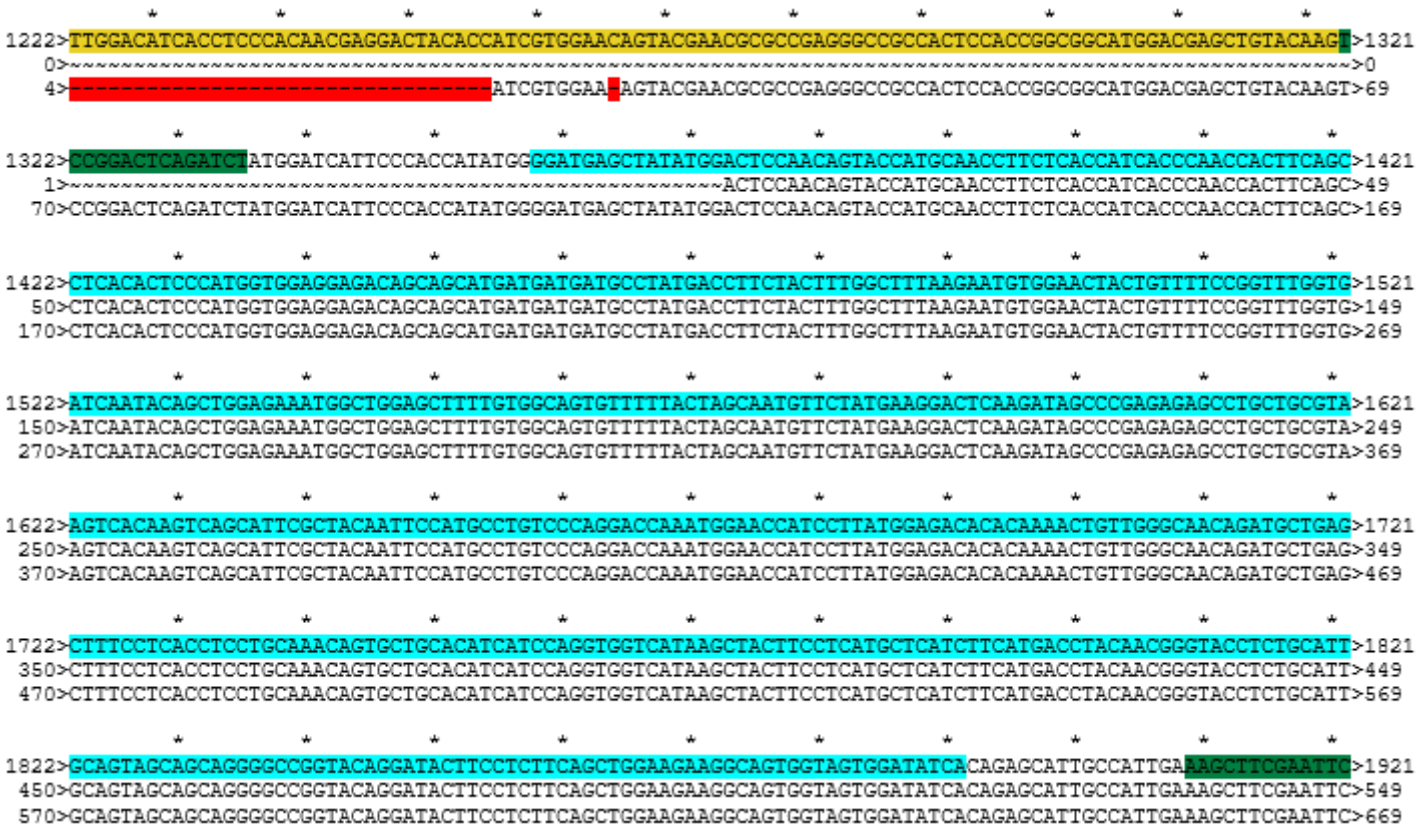

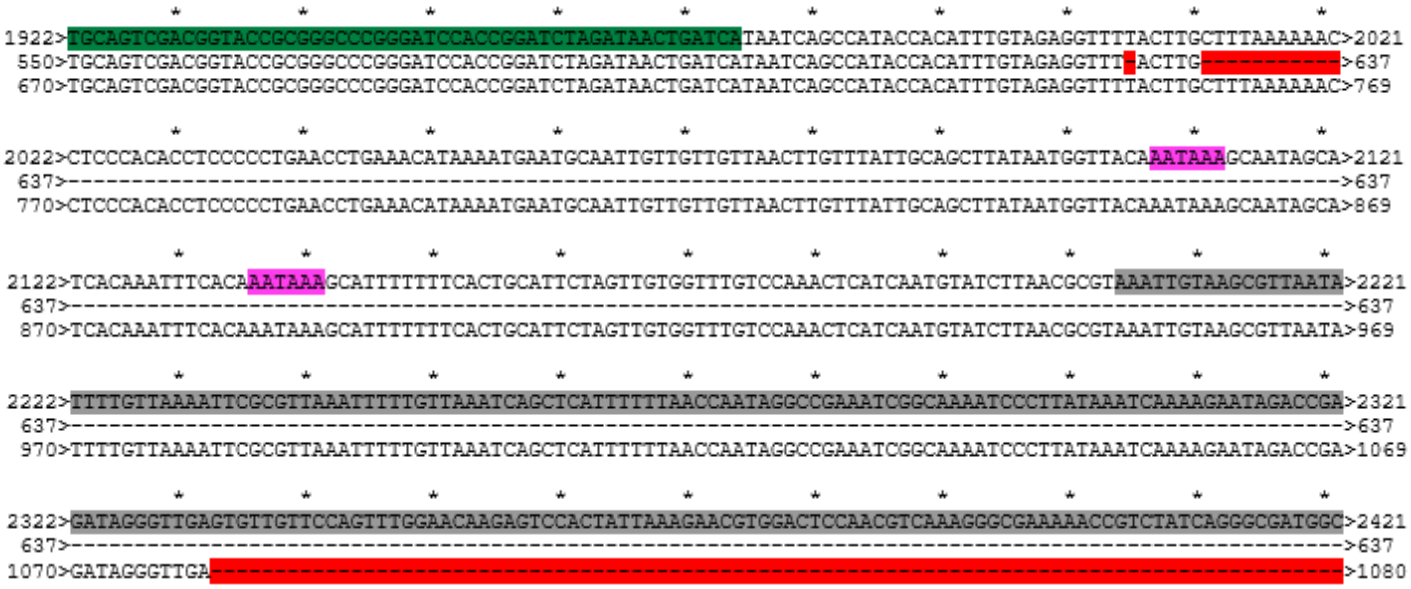

Figure 38: DNA Alignment of the pmCherry-CTR1 predicted sequence with results obtained by sequencing of the pmCherry-CTR1 plasmid using the Seq_FW_mCherry_CTR and Seq_RV_TAG_CTR. The alignment was performed using the ApE program (v2.0.61).

Through DNA alignment of the pmCherry-CTR1 predicted sequence with the results obtained by sequencing of the pmCherry-CTR1 plasmid using the Seq_FW_mCherry_CTR and Seq_RV_TAG_CTR, we can observe that there are no mutations observed. Only two nucleotide deletions are detected, in the end and beginning of the Seq_FW_mCherry_CTR sequence, which are probably result from sequencing errors, due to their sequence location.

3. pCTR2-mCherry

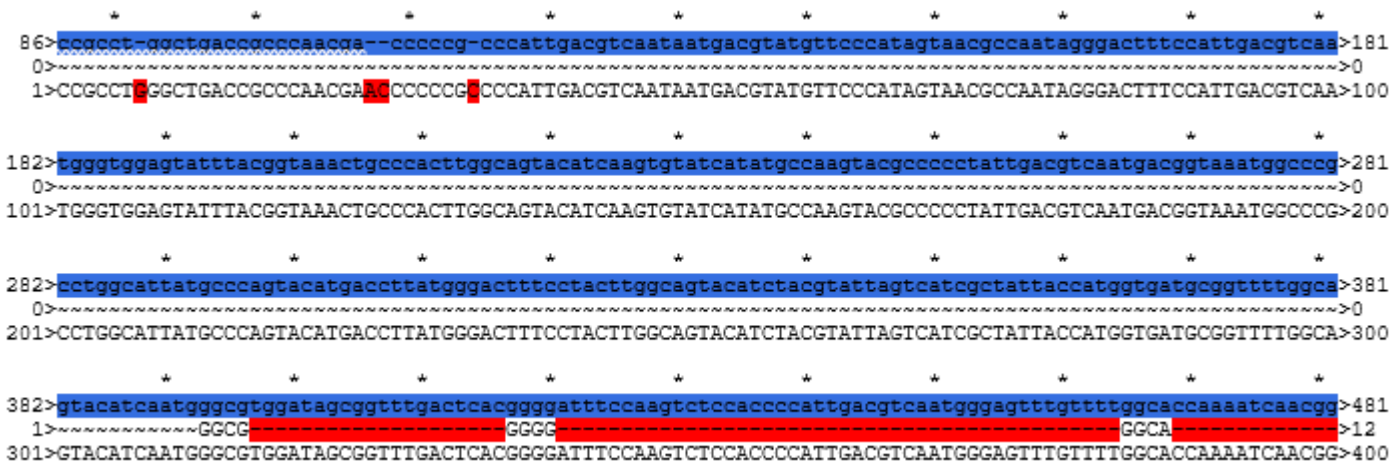

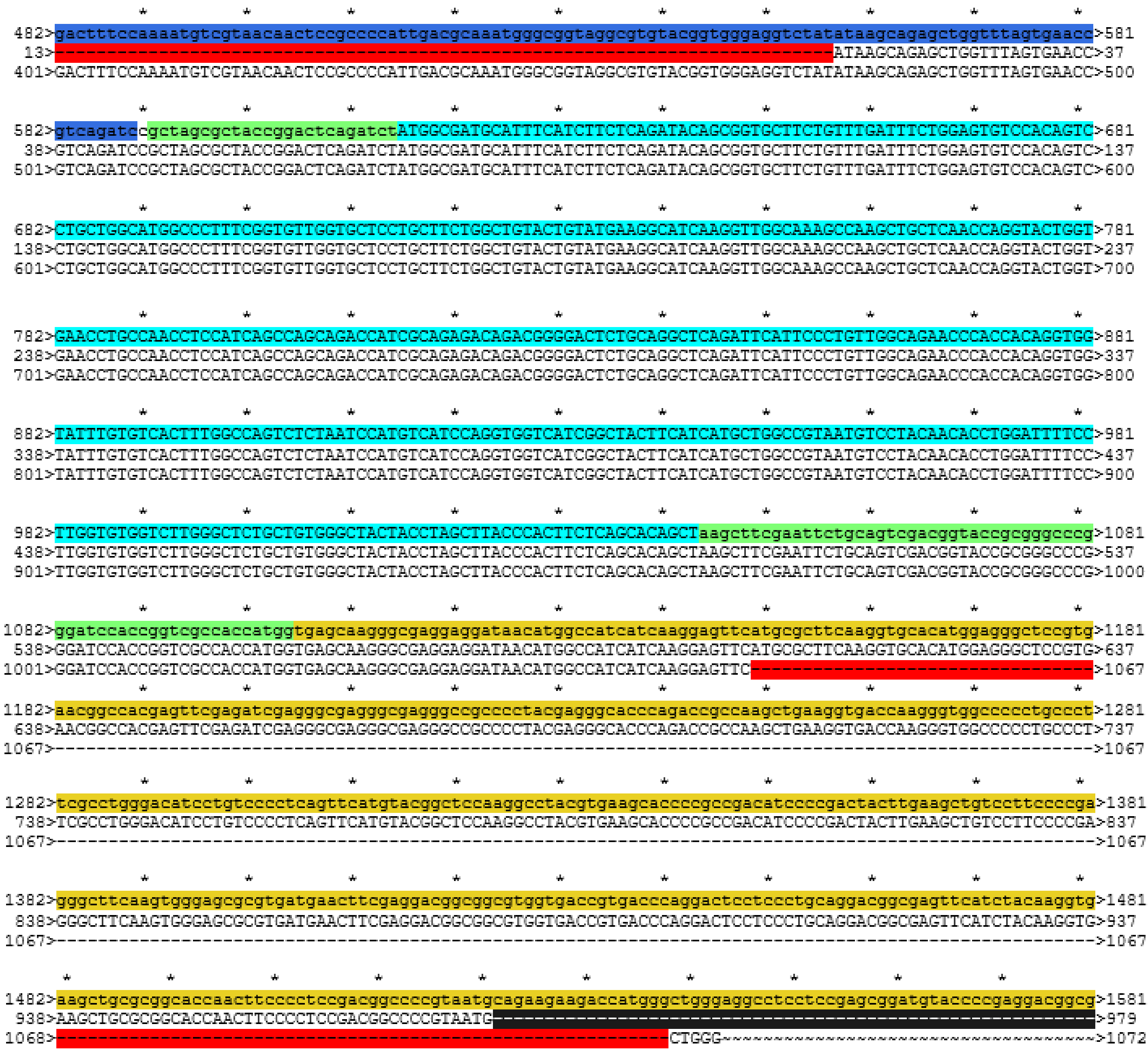

Figure 39: DNA Alignment of the pCTR2-mCherry predicted sequence with results obtained by sequencing of the pCTR2-mCherry plasmid using the Seq_FW_CMV and Seq_RV_CTR_mCherry. The alignment was performed using the ApE program (v2.0.61).

Through DNA alignment of the pCTR2-mCherry predicted sequence with the results obtained by sequencing of the pCTR2-mCherry plasmid using the Seq_FW_CMV and Seq_RV_CTR_mCherry, we can observe that there are no mutations observed in the *hCTR1* DNA sequence. However, the four insertions that still appear in the Seq_RV_CTR_mCherry sequence, do not affect the *hCTR2* gene sequence, and are present in the beginning of the sequence, likely being sequencing errors.

4. pCTR2-AcGFP

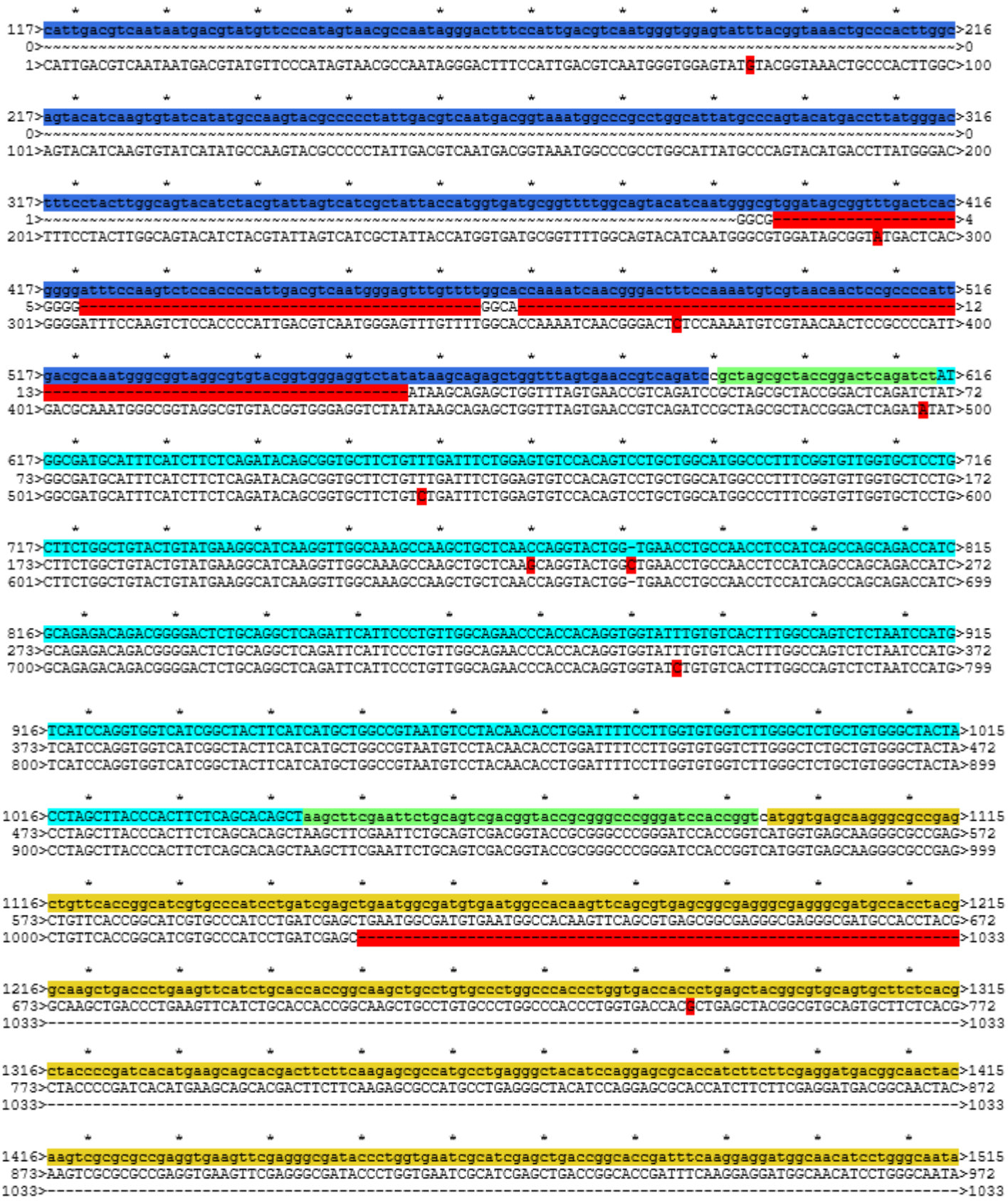

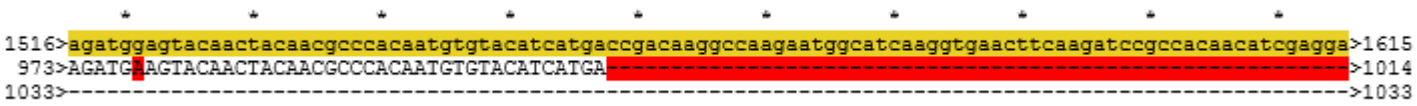

Figure 40: DNA Alignment of the pCTR2-AcGFP predicted sequence with results obtained by sequencing of the pCTR2-AcGFP plasmid using the Seq_FW_CMV and Seq_RV_CTR_AcGFP. The alignment was performed using the ApE program (v2.0.61).

Through DNA alignment of the pCTR2-AcGFP predicted sequence with the results obtained by sequencing of the pCTR2-AcGFP plasmid using the Seq_FW_CMV and Seq_RV_CTR_GFP, we can observe the different mutations in the *hCTR2* gene appear in one sequence, are not present in the other. Therefore, it is expected that these mutations are sequencing errors.

5. pAcGFP-CTR2

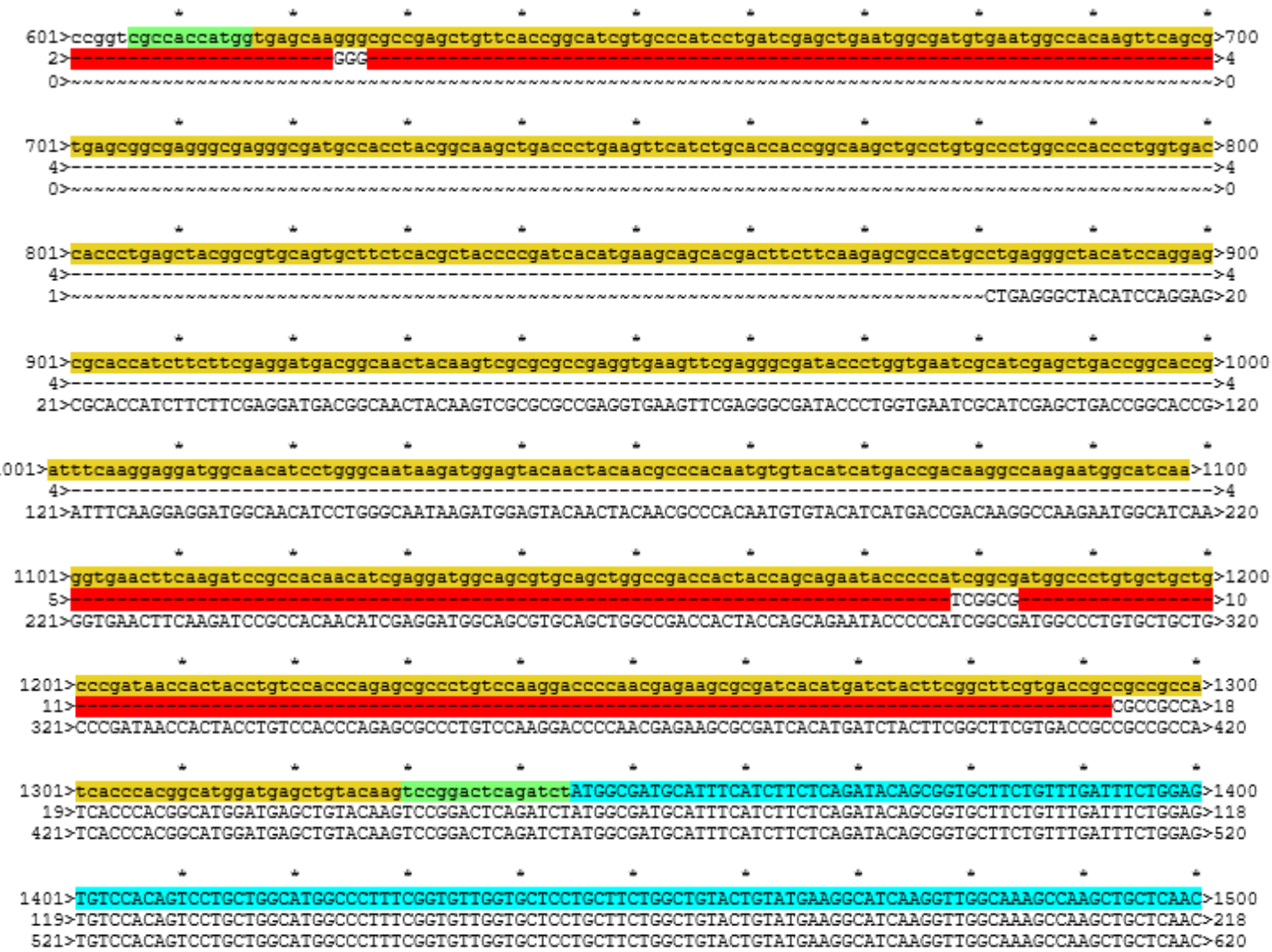

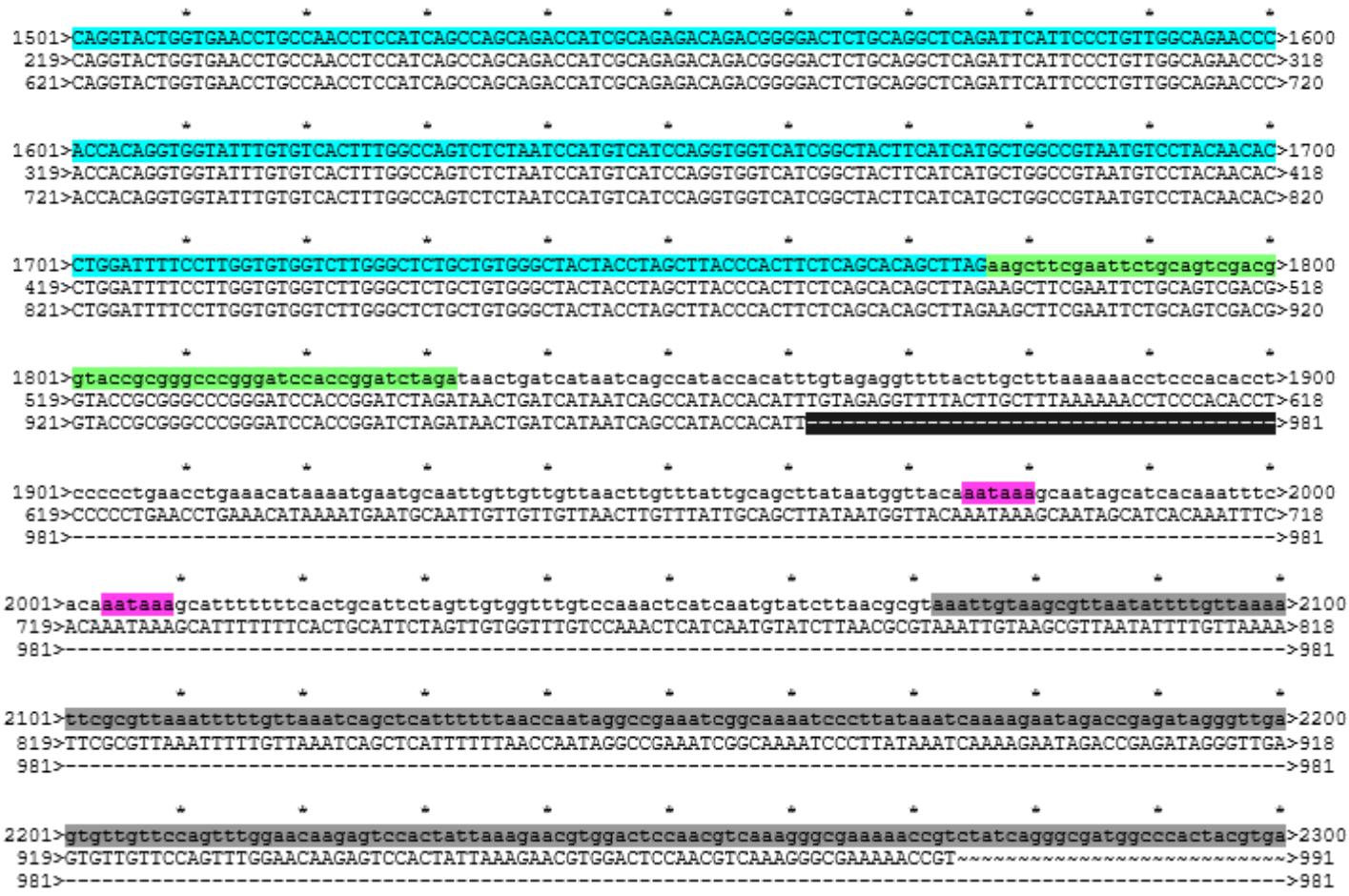

Figure 41: DNA Alignment of the pAcGFP-CTR2 predicted sequence with results obtained by sequencing of the pAcGFP-CTR2 plasmid using the Seq_FW_GFP_CTR and Seq_RV_TAG_CTR. The alignment was performed using the ApE program (v2.0.61).

Through DNA alignment of the pAcGFP-CTR2 predicted sequence with the results obtained by sequencing of the pAcGFP-CTR2 plasmid using the Seq_FW_GFP_CTR and Seq_RV_TAG_CTR, we can observe that there are no mutations present in any of the sequenced DNA sequences.

VII. Appendix E: Total protein transferred protein present in the previously activated polyvinylidene difluoride membranes

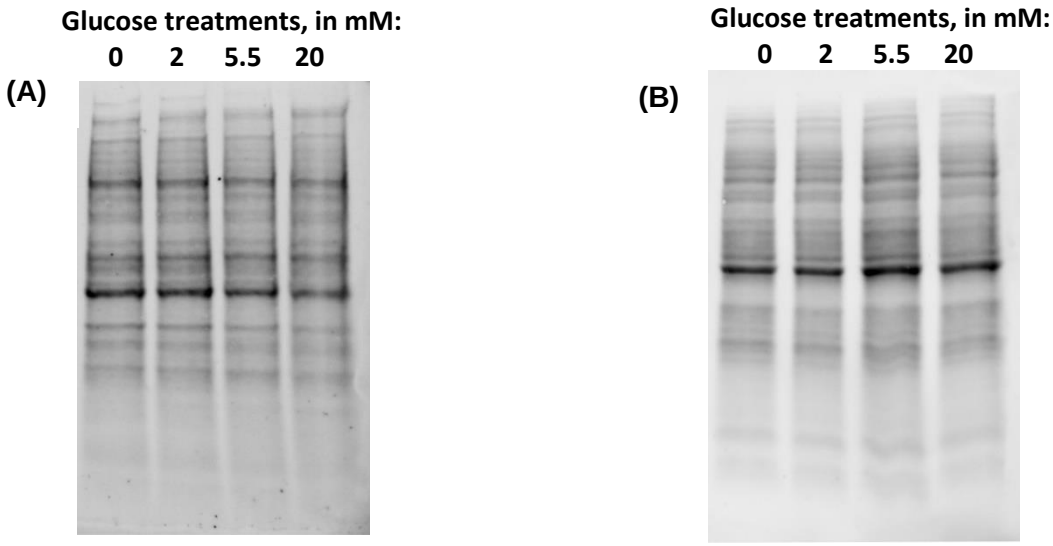

Figure 42: Representative images of total transferred protein extracted from PC-3 and TM4 cells after glucose treatments. Panel A shows a representative image of total transferred protein extracted from PC-3 cells, present in an activated polyvinylidene difluoride membrane. Panels B shows a representative image of total transferred protein extracted from TM4 cells, present in an activated polyvinylidene difluoride membrane. Both images were acquired using the Bio-Rad ChemiDoc XR, and calculated using the Image Lab Software.

VII. Appendix F: Measurement of acetate concentrations in the extracellular medium after TM4 cells were treated with distinct glucose concentrations for 24 h

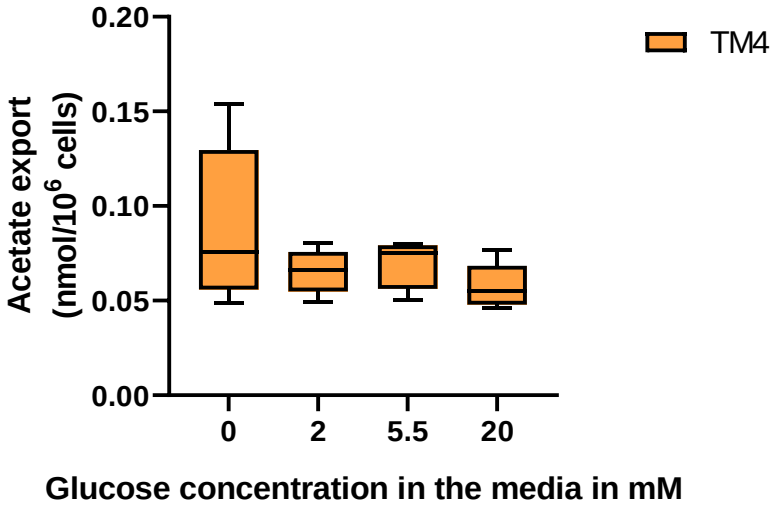

Figure 43: Measurement of acetate concentrations in the extracellular medium after a 24 h of treatment with distinct glucose concentrations in TM4 cells. The graphic represents the export of acetate after a 24 h treatment with DMEM-without glucose, non-supplemented, supplemented with 2 mM of glucose, 5.5 mM of glucose and 20 mM of glucose (n=6). The results are presented as Tukey's whisker boxes (median, 25th to 75th percentiles ± 5th to 95th percentile values).

VII. Appendix G: List of communications and prizes resultant from the work developed during the M.Sc. in Molecular Genetics

1. List of communications resultants from the work developed during the M.Sc. in Molecular Genetics:

Alves-Oliveira R., Barata-Antunes C., Natividade R., Alves R., Alves M.G., Oliveira P.F., Paiva S. Development of Biomolecular Tools for Expression and Trafficking Studies of The Human Copper Transporters. XIII Jornadas de Genética e Biotecnologia|III Jornadas Ibéricas de Genética y Biotecnología – UTAD/UL. 14-16 of April of 2021.

Alves-Oliveira R., Moreira B. P., Lopes D., Barata-Antunes C., Alves R., Sorkin A., Alves M.G., Paiva S., Oliveira P.F. Modulation of MCT4 trafficking by glucose levels – do Sertoli cells behave as cancer cells? I Reproductive Science & Fertility Virtual Summit. 26-27 July of 2021.

Alves-Oliveira R., Paiva S., Oliveira P.F., Expression and trafficking analysis of MCT4: do Sertoli cells behave as Cancer cells? I Encontro de Alunos do Mestrado em Genética Molecular. 5th November of 2021.

2. List of prizes resultants from the work developed during the M.Sc. in Molecular Genetics:

Honorable Mention Prize in the category of Human Genetics and Biotechnology, in the XIII Jornadas de Genética e Biotecnologia|III Jornadas Ibéricas de Genética y Biotecnología, with the Poster intitled "Development of Biomolecular Tools for Expression and Trafficking Studies of The Human Copper Transporters". Alves-Oliveira R., Barata-Antunes C., Natividade R., Alves R., Alves M.G., Oliveira P.F., Paiva S. 14-16 of April of 2021.